Presenilin deficiency leads to altered protein N-glycosylation and endo-lysosomal cholesterol accumulation

Doctoral thesis

to obtain a doctorate (PhD)

from the Faculty of Medicine

of the University of Bonn

Marietta Fabiano
from Catanzaro, Italy
2022

Written with authorization of

the Faculty of Medicine of the University of Bonn

First reviewer: Prof. Dr. Jochen Walter

Second reviewer: Prof. Dr. Jörg Höhfeld

Day of oral examination: 28.10.2022

From the Neurology Clinic

Director: Prof. Dr. Thomas Klockgether

Table of contents

List of abbreviations

AD	Alzheimer´s disease
Aβ	Amyloid β-peptide
ANOVA	Analysis of Variance
APP	Amyloid precursor protein
ARIA	Amyloid-related imaging abnormalities
BACE	Beta-site APP-cleaving enzyme 1
BSA	Bovine serum albumin
CDG	Congenital disorders of glycosylation
Cyp51	Lanosterol 14a-demethylase
DAPT	N-[N-(3,5-difluorophenacetyl)-L-alanyl]-S-phenylglycine t-butylester
DMEM	Dulbecco's Modi!ed Eagle's Medium
DTT	Dithiothreitol
ECL	Enhanced chemiluminescence
EOAD	Early-onset Alzheimer´s disease
ER	Endoplasmic reticulum
ERAD	ER-associated protein degradation
FAD	Familial AD
FCS	Fetal calf serum
FL	Full-length
HBSS	Hanks' Balanced Salt Solution
kDa	Kilodalton
KO	Knockout
LDL	Low-density lipoprotein
LDLR	Low-density lipoprotein receptor
MEF	Mouse embryonic fibroblasts
MES	2-(*N*-morpholino)ethanesulfonic acid
MOPS	3-(*N*-morpholino)propanesulfonic acid)
MRI	Magnetic resonance imaging
mRNA	Message RNA

MS	Mass spectrometry
NFT	Neurofibrillary tangles
NPC	Niemann–Pick´s disease type-C
OST	Oligosaccharyltransferase
PBS	Phosphate-buffered saline
PET	Positron emission tomography
PFA	Paraformaldehyde
PS1	Presenilin 1
PS2	Presenilin 2
RNA	Ribonucleic acid
SAD	Sporadic Alzheimer´s disease
SDS	Sodium dodecyl sulfate
SEM	Standard error of the mean
SREBP2	sterol regulatory element binding protein 2
TBS	Tris-buffered saline
TMD	Transmembrane domain
WT	Wild type

1. Introduction

1.1 Alzheimer´s disease.

In 1906, at the 37th Meeting of South-West German Psychiatrists, the German neurologist Alois Alzheimer presented the case study of a “peculiar severe disease process of the cerebral cortex” (Über einen eigenartigen, schweren Erkrankungsprozeβ der Hirnrinde). The respective patient was of a 51 years-old woman, Auguste Deter, today known as the first Alzheimer´s disease (AD) patient.

As main clinical symptoms, Alzheimer described a severe cognitive disturbance, disorientation, unpredictable behavior and aphasia. The post-mortem examination of the brain revealed a diffuse severe atrophy with degeneration of cortical nerve-cells characterized by presence of intracellular fibrils, deposition of aggregates disseminated throughout the whole cortex and many glia cells with “adipose saccules”. While the publication relative to this first case, in 1907, was only a short report (Alzheimer A., 1907a-b; Stelzmann et al., 1995), more histopathological details, including figures and drawings were published in 1911 together with a second case of Johann F. Hence. (Alzheimer A., 1911; (Alzheimer et al., 1991). Although in the absence of fibrils, presence of large and diffuse aggregates was described also in Johann F. case together with accumulation of “lipoid substances” in the ganglion cells, glial cells and the walls of the vessels of the cerebral cortex and the whole central nervous system.

To date, AD is the most common progressive and irreversible neurodegenerative disorder with high prevalence beyond the age of 65 and mean life expectancy of four to eight years after diagnosis. Approximately 44 million people are affected worldwide and the percentage of patients is expected to rise in the next years, owing to increasing life expectancy. Because of his huge prevalence, mortality, and high economic impact, due to the health care costs, AD became one of the most studied pathology (Alzheimer’s Association, 2019; Serge Gauthier et al., 2021).

During the years researchers defined the intracellular fibrils and extracellular aggregates, described by Alzheimer, as neurofibrillary tangles (NFTs) and senile plaques, respectively. The tangles are the results of hyperphosphorylated tau aggregation, a microtubule associated protein, while the plaques contain fibrillary forms of amyloid β-peptides (Aβ) that derive from the proteolytic processing of the amyloid precursor protein (APP) (Walter et al., 2001; Annaert and De Strooper, 2002). The concomitant presence of these two

phenomena is what define AD at the neuropathological level and distinguish it from other forms of dementia. In fact, although NFTs are one of the hallmarks of AD, they have been observed in several others diseases, defined as “primary tauopathies”, where tau pathology is the main neuropathological landmark (Chung et al., 2021).

Tau is poorly expressed in astrocytes and oligodendrocytes where its role is still not fully clarified (Gorath et al., 2001; Kovacs, 2015; Arendt et al., 2016). In neurons, tau is mainly localized to the axon where it regulates the microtubule assembly and dynamics, essential for maintaining neuronal integrity and axonal transport (Baas et al., 2016). In physiological conditions, tau undergoes several post-translational modifications including, phosphorylation, glycation, O-GlcNAcylation, methylation, SUMOylation, ubiquitylation, oxidation and truncation. Phosphorylation is the most common tau modification described and it is known that, through its regulation, tau promotes tubulin polymerization and stabilizes microtubules (Kadavath et al., 2015). An increase in tau phosphorylation reduces its affinity for microtubules, resulting in neuronal cytoskeleton destabilization, and leads also to tau accumulation and self-aggregation in insoluble filaments (Lee et al., 2001; Arendt et al., 2016). Hyperphosphorylation of tau occurs before the onset of NFTs (Iqbal and Grundke-Iqbal, 1991; Braak and Braak, 1995). In fact, NFTs mature through three defined levels known as pre-tangles, mature tangles and ghost tangles. While the first two refers to the formations of tangles intracellularly, the ghost tangles are remnants of mature tangles in the extracellular space once the neuron has died.

Tau aggregation is correlated to neurodegeneration (Noble et al., 2013; Iqbal et al., 2016). In fact, neuronal or glial deposition of tau characterizes an heterogenous group of neurodegenerative disorders grouped as “spectrum of tauopathy”.

In AD, depending on the distribution patter of NFTs in the patient´s brains, six neuropathological stages (Braak stages) have been described (Braak and Braak, 1991; Braak et al., 2006).

Although functional magnetic resonance imaging (MRI) and positron emission tomography (PET) *in vivo* brain imaging have been used in several studies to correlate tau pathology with Braak stages, the examination of postmortem brains remains the primary method to distinguish the spectrum of tauopathies and correlate it to different neurological disorders.

As mentioned above, the presence of Aβ plaques in the patient´s brain is another essential hallmark of AD. Aβ sequence spans parts of the membrane domain and adjacent ectodomain of APP, and it is released upon cleavage by β- and γ-secretase in the amyloidogenic pathway. Generation of the senile plaques can be due to a proteolytic abnormal processing of APP, with generation of Aβ species more prone to aggregate, or a decreased clearance of Aβ that, once accumulating, tend to form deposits. The “amyloid cascade hypothesis” supports the idea that Aβ plays a central and even causative role for AD (Hardy and Higgins, 1992; Karran et al., 2011). In particular, the accumulation and aggregation of Aβ into plaques is believed to be the most important factor leading to neurotoxicity, dementia and AD development (Hensley et al., 1994). Aβ monomers, in fact, can form several assemblies including oligomers, protofibrils and fibrils and among the different Aβ forms, Aβ42 is the most prone to aggregate. Aβ42 species, indeed, is the predominant Aβ form that deposits into amyloid plaques in AD brain and it has been shown to have a central role driving amyloid deposition *in vivo* (Younkin, 1998; McGowan et al., 2005). In addition, the increasing Aβ42/Aβ40 ratio has been correlated with clinical onset of disease in familial AD cases (FAD) (Tang and Kepp, 2018).

The characteristic senile plaques observed in AD brains are mainly generated by deposition of amyloid fibrils, that are large and insoluble aggregates. Aβ oligomers, instead, are soluble and they have been shown to affect synaptic structure and function. Increased level of Aβ oligomers, indeed, is strongly correlated with cognitive decline, due to their synaptotoxic properties (Smith and Strittmatter, 2017). In addition, studies in postmortem brains from either healthy or mild-demented subjects showed that, in a similar plaques density condition, higher oligomers levels are correlating with dementia, indicating a fundamental contribution of soluble Aβ oligomers to synaptotoxicity in AD (Esparza et al., 2013). Interestingly, it has been shown that Aβ oligomers can be sequestered from brain interstitial fluid onto cell membranes where they associate with GM1 ganglioside (Hong et al., 2014). This observation suggests that lipid membrane composition is important for the Aβ oligomers-mediated effect on cellular function.

In an attempt to slow the progression of AD disease and/or improve its symptoms, during the years, different therapeutic approaches have been suggested and many of them focused on reducing levels of toxic forms of Aβ. An approach, aiming to decrease Aβ levels by acting on the enzymes involved in its production, β- and γ-secretase, failed due

to the lack of efficacy or detrimental side effects. More recent approaches focus on the removal or prevention of the Aβ deposits using monoclonal antibodies against Aβ (Cummings et al., 2020).

On 7 June 2021, Aducanumab, a human monoclonal antibody against Aβ was authorized by the United States Food and Drug Administration (U.S. FDA), via an accelerated approval pathway, as the first disease-modifying therapy for AD treatment (Cummings et al., 2020; Bastrup et al., 2021). Nevertheless, this decision was cause of debate due to the many controversies regarding aducanumab's efficacy and performance in the two Phase III trials, namely EMERGE and ENGAGE (Haeberlein et al., 2020; Knopman et al., 2021; Salloway et al., 2021; Haeberlein et al. 2022). Although administration of Aducanumab reduced the Aβ content in the brain, this did not lead to a clinical improvement in the case of ENGAGE. In addition, brain scan analysis revealed amyloid-related imaging abnormalities (ARIA) in some of the patients from both studies, raising questions about the security of the treatment.

For these reasons the European Medical Agency (EMA) decided, on 16 December 2021, to refuse marketing authorization. Recently, on February 2022, the producing company, Biogen, requested a re-examination of EMA´s decision. (https://www.ema.europa.eu/en/medicines/human/withdrawn-applications/aduhelm).

To date, an effective and save cure for AD does not exist.

1.2 Presenilins

1.2.1 Presenilins and γ-secretase

Presenilin 1 (PS1) and presenilin 2 (PS2) are two homologous transmembrane proteins encoded by PSEN1 and PSEN2 genes, respectively. These proteins are synthetized as a full-length (FL) protein of ~50 kDa with nine transmembrane domains (TMDs) (Laudon et al., 2005; Spasic et al., 2006) and share 65% identity at the amino acid level, in human, with most variability within the loop regions (Güner and Lichtenthaler, 2020).

Presenilins (PS) are mainly known to be the catalytic subunit of the γ-secretase complex, a hetero-tetrameric protein complex known to exclusively cleave type I transmembrane proteins. In particular, this complex contains one proteolytically active subunit, presenilin

(PS1 or PS2), and three non-proteolytic subunits: nicastrin (Nct), anterior pharynx defective-1 (Aph1) and presenilin enhancer 2 (PEN-2) (Fig. 1.1).

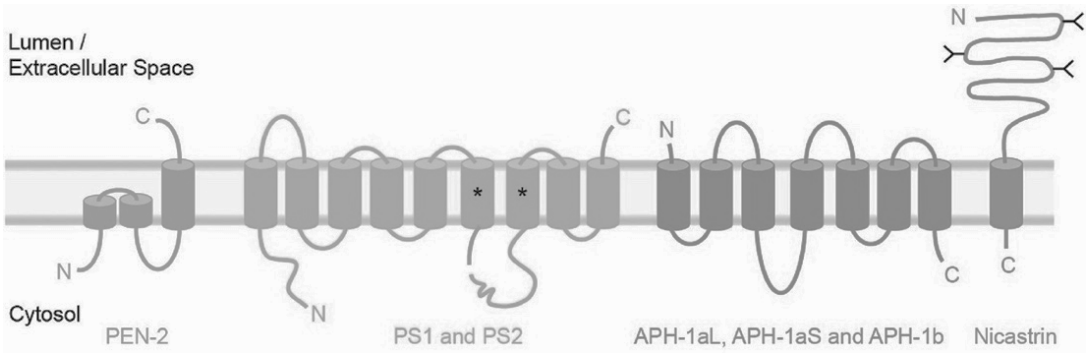

Fig. 1.1: γ-Secretase complex. Schematic representation of the four subunits of γ-secretase. Asterisks indicate the catalytic aspartate residues of PS responsible for the catalytic activity. These residues are located in TMD 6 and 7. Nicastrin subunit is characterized by a large, glycosylated extracellular domain. Picture from (Güner and Lichtenthaler, 2020).

During assembly of the complex, the PS subunit undergoes autoproteolytic cleavage within the large loop between TMD 6 and 7, resulting in stable PS NH2- and COOH-terminal fragment (-NTF, -CTF) heterodimers (Spasic and Annaert, 2008). Two aspartate residues in TMD 6 and 7 of PS (D257/D385 in PS1 and D263/D366 in PS2, respectively) are essential for the catalytic activity (Wolfe et al., 1999; Kimberly et al., 2000).

In human cells and tissues, γ-secretase is present as up to six homologous complexes, due to the different possible subunit combinations, containing either PS1 or PS2 and either one of the three APH-1 homologs (APH-1aL, APH-1aS, and APH-1b) (Hébert et al., 2004; Shirotani et al., 2004).

The γ-secretase complexes differ in their subcellular localization, with PS1-containing complexes found in different secretory pathway compartments as well as the plasma membrane, whereas PS2-containing complexes localize more to endosomes and lysosomes (Meckler and Checler, 2016; Sannerud et al., 2016). As a consequence, some substrates, such as premelanosome protein (PMEL) and tyrosinase-related protein (TRP-1), which localize to lysosome-related compartments, are mostly cleaved by PS2-, but barely by PS1-containing γ-secretase complexes. It is possible, then, that the six different γ-secretase complexes generally have a distinct, but probably overlapping substrate spectrum (Sannerud et al., 2016). In addition, the relative abundance of the γ-secretase complexes may be different among cell types and tissues (Serneels et al., 2009). In fact,

for example, it has been reported that microglia cells predominantly utilize PS2, but not PS1 in the γ-secretase complex (Jayadev et al., 2010).

To date a list of 149 substrates of γ-secretase have been identified (Güner and Lichtenthaler, 2020). Among them the most studied are Notch and APP due to their implication in different pathologies. Impairment in γ-secretase/presenilins activity, indeed, is known to have an impact in developmental disorders, acting on Notch signals, and in AD etiology, affecting APP cleavage (Medoro et al., 2018).

Regarding APP, physiologically, two major proteolytic processing pathways have been identified and both involve cleavage by γ-secretase. In the “non-amyloidogenic pathway”, APP is cleaved first by α-secretases and then by γ-secretase, resulting in release of soluble sAPPα ectodomain, p3 fragment and APP intracellular domain (AICD).

The alternative “amyloidogenic pathway” gives rise to Aβ peptide formation and its extracellular release. APP is first cleaved by beta-site APP-cleaving enzyme 1 (BACE1, or β-secretase) with formation of the soluble sAPPβ ectodomain, and then, by γ-secretase that cleaves the remaining β-CTF (C99) giving rise to AICD and Aβ peptide species (Haass et al., 2012) (Fig. 1.2).

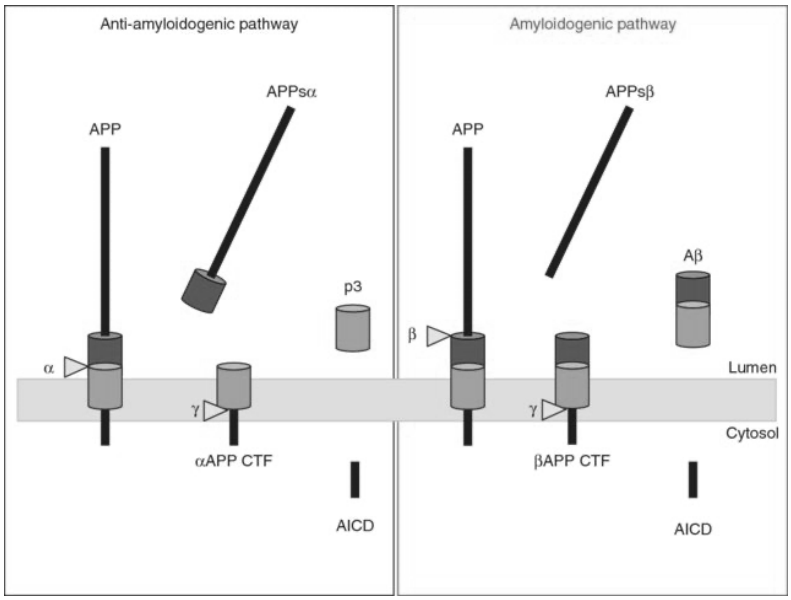

Fig. 1.2: Proteolytic processing of APP. Schematic representation of the non-amyloidogenic (left) and amyloidogenic (right) pathway acting on APP and resulting fragments. Picture from Haass et al., 2012.

The resulting monomeric Aβ species can have slightly different lengths, from 37 to 43 amino acids. Aβ 40 is one of the most soluble species, while Aβ42 and Aβ43, particularly, have the tendency to aggregate and form higher order structures including toxic soluble Aβ dimers, trimers, oligomers and protofibrils.

Beside the role of presenilins in intramembrane proteolysis, associated with γ-secretase cleavage, other functions have been attributed to these proteins. For example, it has been shown that PS1 is a negative regulator of the Wnt/β-catenin signaling pathway (Kang et al., 2002); PS modulate intracellular Ca^{2+} homeostasis (Leissring et al., 1999; Kasri et al., 2006; Cheung et al., 2008; Green et al., 2008; Hayrapetyan et al., 2008) and trafficking of proteins such as the receptor Tyrosine-related kinase B (TrkB) (Naruse et al., 1998), APP (Kaether et al., 2002; Cai et al., 2003) and Nct (Herreman et al., 2003).

A role of PS has been described also in relation with endo-lysosomal trafficking and autophagy. Using different settings *in vitro*, in primary neuronal cultures and fibroblasts, and *in vivo*, in mouse brain samples, it has been shown that PS deficiency causes endo-lysosomal and autophagic abnormalities (Esselens et al., 2004; Wilson et al., 2004; Lee et al., 2010; Neely et al., 2011; Dobrowolski et al., 2012). Ablation of either PS1 or PS2 appears to affect lysosomal function with an increase in the number and size of the vesicles, suggesting an involvement of both proteins in this mechanism (Neely et al., 2011). In addition, the influence on vesicular fusion and autophagy seems to be independent from γ-secretase activity, as demonstrated by lack of alteration of autophagy-related protein upon γ-secretase inhibition and /or depletion of Nicastrin (Lee et al., 2010; Neely et al., 2011). An increase in autophagic vacuoles it has been shown also in neurons from PS1cKO (PS1 conditional KO) mice at 2-3 months of age (Lee et al., 2010). Around the same age, 2 months old, in PS-double knockout (PSDKO) mice it has been describe the start of synaptic impairment and deterioration of memory ability that exacerbates with age resulting in neurodegenerative alterations (Saura et al., 2004). These observations suggested an important role of PS in the endo-lysosomal autophagic system as well as in neuronal function and potential involvement of subcellular vesicular trafficking alterations in the early stage of neurodegeneration.

Additional indications of a γ-secretase-independent role of PS1 in endo–lysosomal / autophagic system emerged from studies regarding ICAM-5 (also known as telencephalin) (Annaert et al., 2001; Esselens et al., 2004), a neuronal intercellular cell adhesion

molecule, forebrain-specific. In PS1 knockout (PS1KO) primary hippocampal neurons, ICAM-5 accumulates in intracellular degradative organelles positive for autophagic markers, but that are not acidified (Esselens et al., 2004; Raemaekers et al., 2012). Accumulation of similar degradative organelles was also noted in another study, where lack of PS1 in neurons led to a pronounced α- and β-synuclein intracellular accumulation (Wilson et al., 2004). Interestingly, PSDKO cells also showed, in addition to extensive clustering of autophagic vacuoles, accumulation of late endosomal multivesicular bodies (Dobrowolski et al., 2012).

Although these studies support the implication of PS in the turnover of endosomal / autophagic cargo, the mechanism remains debated. In particular, it is unclear whether the deletion of PS impairs lysosomal degradation per se or the fusion capacity of the compartments involved. In order to explain these deficits, two major hypotheses have been considered: defective lysosomal acidification and Ca^{2+} homeostasis (Lee et al., 2010; Coen et al., 2012).

A first model suggested that PS1 deficiency/ mutation would compromise the role of endoplasmic reticulum (ER)- localized full-length PS1 as co-factor of the oligosaccharyl transferase (OST) complex in N-glycosylation of the V0a1 subunit of the vacuolar ATPase (v-ATPase; proton pump). As result, V0a1 loses its lysosomal targeting, compromising the proton pump function and, consequently, the lysosomal acidification thereby impairing the activity of lysosomal hydrolases (Lee et al., 2010). However, several other studies failed to reproduce the lysosomal acidification and proteolysis defects as well as impaired N-glycosylation of the V0a1 subunit in PS KO cells (Coen et al., 2012; Zhang et al., 2012).

Alternatively, implication of PS in calcium homeostasis has been proved by several studies. It has been shown, indeed, that PS interacts with a number of calcium channels and pumps including sarco-ER Ca^{2+} ATPase (SERCA) (Green et al., 2008), the inositol 1,4,5-trisphosphate (IP3) receptor (Cheung et al., 2008), and the ryanodine receptor (Payne et all., 2015). Through these interactions PS influence calcium homeostasis in cells by affecting ER calcium stores, as well as capacitive calcium entry (Leissring et al., 1999; Yoo et al., 2000). Moreover, an impairment of lysosomal calcium storage/release, required for lysosomal function and fusion, was observed in PS KO cells and neurons (Neely et al., 2011; Coen et al., 2012).

Interestingly, a similar situation of endo-lysosomal dysfunction caused by significant reduction in lysosomal calcium storage/release is observed in Niemann–Pick disease type-C (NPC) cell model (Lloyd-Evans et al., 2008). NPC is a neurodegenerative lysosomal storage disorder caused by mutations in NPC1 or NPC2 genes and characterized by late endosomal/lysosomal accumulation, among other lipid species, of unesterified cholesterol (Vanier and Millat, 2003).

Although the hallmark of this disease is an aberrant lipid transport and storage, an alteration of the calcium homeostasis it has been proposed as an initial event leading then to the lipid dyshomeostasis (Lloyd-Evans et al., 2008). In particular, an initial accumulation of sphingosine in acidic compartments, due to NPC1 dysfunction, seems to cause a depletion of calcium in lysosomes that impairs endocytic function and leads to lipid storage. This hypothesis is supported by the evidence that a modulation of the cellular calcium levels can induce the fusion of endosomes with lysosomes, rescue the cholesterol accumulation and improve the phenotype of NPC1-/- mice.

Similarly to what was observed in NPC1 disease, a reduced lysosomal calcium level was described in PSDKO MEFs and PS1KO hippocampal neurons. This calcium defect was successfully rescued by re-introduction of WT human PS1 or catalytically inactive human PS1, suggesting a γ-secretase independent function of PS -mediated lysosomal Ca^{2+} regulation (Coen et al., 2012).

All together these observations suggest that PS can exert functions within the γ-secretase complexes, which do not depend on the catalytic activity, but have a fundamental role in cellular homeostasis. Although many insights have been gained regarding the involvement of PS in different cellular mechanisms, much remains to be elucidated.

1.2.2 PS and Alzheimer´s disease.

Because PS are carrying the catalytic activity of γ-secretase complex, many studies have been conducted regarding PS dysfunction, Aβ production and AD pathogenesis.

Regarding APP processing, several studies showed a lower activity of PS2 γ-secretase compared to PS1 γ-secretase (Lai et al., 2003; Lee et al., 2011) meaning a predominant implication of PS1 γ-secretase in the APP cleavage (De Strooper et al., 1998; Yu et al., 2001; Pintchovski A. et al., 2013; Xia et al., 2015). General genetic deletion of PS1 in mice causes a phenotype highly similar to Notch KO characterized by skeletal abnormalities,

midline closure defect and embryonic lethality (E17- P1) (Shen et al., 1997; Hartmann et al., 1999; Handler et al., 2000; Takahashi et al., 2000). The double knockout of both PS genes, as well, is apparently not distinguishable from the Notch KO phenotype (Donoviel et al., 1999; Herreman et al., 2003). These observations indicate the essential role of PS for Notch signaling which is, also, considered as a contributing factor in AD pathogenesis (Costa et al., 2003, 2005; Wang et al., 2004; Woo et al., 2009; Kapoor and Nation, 2021). Interestingly, tissue specific PS1KO in mice forebrain neurons causes mild impairment of spatial memory and subtle changes in neurogenesis (Feng et al., 2001; Yu et al., 2001). In the same mouse brain region deletion of both PS results, already at 2 months of age, in severely impaired memory and synaptic plasticity with synaptic loss and hyperphosphorylation of tau in the total absence of Aβ generation (Saura et al., 2004). These observations suggest an important role of PS in AD development, not necessarily associated with Aβ production.

Beside these studies, that investigate the effect of PS deletions, many others are focusing on specific PS mutations. In fact, mutations in PSEN genes are a major cause in early onset autosomal-dominantly inherited forms of familial AD (FAD).

1.2.3 PS FAD-linked mutations.

The majority of AD cases occurs late in life and without a known cause (sporadic Alzheimer's disease, SAD). Nevertheless, it exists a rare but highly penetrant hereditary form of AD defined as FAD. These FAD forms are inherited as an autosomal dominant trait and, because the disease develops much earlier than sporadic cases, between age of 20 and 65 years, they are also defined has early-onset AD (EOAD).

The first gene found in association with EOAD was APP, localized on chromosome 21, and then the other two were identified: PSEN1 on chromosome 14q24.3 (Sherrington et al., 1995) and PSEN2 on chromosome 1q42.2 (Levy-Lahad et al., 1995; Rogaev et al., 1995). Almost 50% of FAD cases are due to mutations in one of these three genes encoding for APP, PS1 and PS2 and currently, more than 400 FAD associated mutations have been identified in PSEN1 or PSEN2 [ALZFORUM, https://www.alzforum.org/mutations/search?genes%5B%5D=493&genes%5B%5D=494&diseases%5B%5D=145&keywords-entry=&keywords=#results].

The mechanisms by which mutations in these genes result in the EOAD phenotype are still unclear. FAD cases, though with an onset in middle age and dominant genetic inheritance, display essentially the same progression of symptoms and the same plaque and tangle pathology as in SAD.

PS pathogenic mutations can significantly dysregulate γ-secretase activity, affecting APP processing and Aβ generation. The mutant presenilins assemble with other γ-secretase components into full complexes that may or not display a reduction of proteolytic activity. Most of the analyzed PSEN1 mutations, indeed, affect the proteolytic processing of APP increasing the relative amount of Aβ42 versus Aβ40 and promoting neuritic plaque formation (Borchelt et al., 1996; Duff et al., 1996; Scheuner et al., 1996; Sun et al., 2017). This was observed in fibroblasts derived from patients (Citron et al., 1997), in cell lines overexpressing the mutant presenilins (Borchelt et al., 1996; Citron et al., 1997), and in living mice overexpressing the mutant presenilin in brain (Borchelt et al., 1997; Shen and Kelleher, 2007). PSEN1 mutants can also reduce Notch cleavage with consequent inhibition of its signaling (Song et al., 1999).

Independently from the effect on γ-secretase catalytic activity, FAD-related mutations might also alter other PS functions that might contribute to AD pathogenesis. In fact, it has been shown that depletion of PS1 or PS2, as well as some FAD-associated PS1 mutations, in HEK293 and HeLa cells, induce multivesicular endosomes accumulation resulting in increased Wnt signaling. The Wnt signal induction, following PS1 knockdown, was rescued by overexpression of WT human PS1 (hPS1) or protease-inactive hPS1 mutants (D257A and D385A), but not by other FAD-associated PS1 mutations, suggesting a γ-secretase independent effect of PS on Wnt signal (Dobrowolski et al., 2012).

Loss of PS1 has been shown to increase also the level of the epidermal growth factor receptor (EGFR) (Repetto et al., 2007; Zhang et al., 2007). Analysis of EGFR turnover showed a delayed trafficking from endosomes to lysosomes in PS1 deficient cells suggesting a defect in EGFR degradation in these cells. The increased EGFR level in PS KO cells was not rescued by expression of catalytic inactive form of PS1, suggesting a role of the γ-secretase activity in this phenomenon. Nevertheless, pharmacological inhibition of γ-secretase in WT cells failed to mimic the EGFR increase observed in PSKO cells (Repetto et al., 2007). Based on these observations, it can be hypothesized that PS1-

mediated regulation of EGFR is not completely dependent on the catalytic activity of γ-secretase.

In addition to the effect on Wnt and EGFR expression, reduced function in other certain signaling pathways, different from Notch and APP, may be a secondary contributing factor in the EOAD. Evidences indicate that much like lack of PS, also certain FAD-linked mutations can alter the intracellular signaling, leading to pathological tau phosphorylation (Baki et al., 2004) and *in vitro* degeneration of primary neurons (Baki et al., 2008), independently from their catalytic activity. PSEN1 and PSEN2 FAD-associated mutations also correlate with pronounced lysosomal neuropathology in AD neurons (Cataldo et al., 2004) and dysfunctions of multiple cellular processes, such as lipid metabolism (Foley, 2010; Cho et al., 2019a), Ca^{2+} homeostasis (Neely et al., 2011; Coen et al., 2012) and autophagy (Nixon et al., 2005; Lee et al., 2010; Neely et al., 2011; Nixon and Yang, 2011). In numerous studies PS FAD-linked mutations have been showed to cause changes in Ca^{2+} levels (LaFerla, 2002; Zatti et al., 2006; Pendin et al., 2021). In particular, a defective autophagosome-lysosome fusion causing autophagy dysfunction has been described in SH-SY5Y cells carrying a FAD-PSEN2 mutation. This phenomenon was due to a decreased recruitment of the small GTPase RAB7 to the autophagosomes and appeared to be unrelated to γ-secretase activity, but dependent from the PS2 ability to partially deplete ER Ca^{2+} content (Zatti et al., 2004, 2006; Fedeli et al., 2019). Regarding the effects on Ca^{2+}, it was also proposed that PS holoproteins act as passive Ca^{2+} channels in the ER and that PS FAD mutations alter channel conductance (Tu et al., 2006).

Taken all together, these studies suggest that FAD-associated PSEN mutations, in addition to altering the catalytic activity of γ-secretase complex, may also contribute to disease progression via additional impairment of other PS functions. Therefore, a better knowledge of the different implications of PS in cellular homeostasis is fundamental to have a comprehensive understanding of the mechanism underlying AD pathology.

1.3 Cholesterol

1.3.1 Cellular cholesterol metabolism

In cells, cholesterol localizes mainly at the plasma membrane where it regulates fluidity, but also interacts with proteins to control membrane trafficking and signal transduction

(Luo et al., 2019). Because of its importance for the normal function of the cells, cholesterol homeostasis is regulated by several mechanisms, at cellular level: control of uptake and release of cholesterol in complex with lipoproteins, subcellular transport, *de novo* synthesis, storage in and mobilization from cholesterol esters.

To facilitate dietary cholesterol transport to peripheral tissues, cholesterol is bound, mainly in esterified form, to apolipoproteins (Apo) forming LDL particles. These particles are recognized by LDL receptors on the cellular surface and internalized by receptor-mediated endocytosis (Goldstein and Brown, 2009).

After internalization in late endosomes/lysosomes, the soluble luminal protein NPC2 is able to bind the LDL-derived cholesterol and facilitate its transfer to the cholesterol-binding pocket in the N-terminal domain of NPC1 (Liou et al., 2006; Infante et al., 2008; Gong et al., 2016). The interaction between NPC2 and NPC1 is required for the successful egress of cholesterol from the lysosomal compartment to the ER. Levels of cholesterol are sensed in the ER by different proteins such as sterol regulatory element binding protein 2 (SREBP2) (Madison, 2016).

Reduced cholesterol level leads to transfer of the full-length SREBP2 (SREBP2-FL), together with the escort protein SCAP, to the Golgi. Here, SREBP2-FL is cleaved resulting in the release of the N-terminal domain (SREBP-NT) that acts as transcriptional factor after translocation into the nucleus and induces expression of genes involved in cholesterol synthesis and uptake, such as HMG-CoA reductase (HMGCR), HMG-CoA synthase (HMGCS), mevalonate kinase (MVK) and LDLR (Sakai et al., 1997; Madison, 2016; Brown et al., 2018). Conversely, high cholesterol levels inhibit SREBP2 activation and induce cholesterol esterification by acyl-coA: cholesterol acyltransferase (ACAT1) to form cholesterol esters (CE) that are stored in lipid droplets (Chang et al., 1997; Zhang and Liu, 2017). Another effect of high cellular cholesterol levels is the increased export that is mediated through ATP-binding cassette (ABC) transporters, like ABC subfamily A member 1 (ABCA1) and ABC subfamily G member 1 (ABCG1).

Due to the blood brain barrier (BBB), cholesterol metabolism in the brain appears to be different compared to the peripheral tissues. In the central nervous system (CNS), in fact, the BBB limits the exchange between brain and plasma, the majority of cholesterol in the brain is derived from *de novo* biosynthesis, rather than plasma LDL (Dietschy and Turley, 2001; Vance et al., 2005).

In particular, most of the cholesterol is present in an unesterified form, produced by astrocytes and transported to neuron and microglia via ApoE-containing lipoprotein particles. Neurons can take up astrocyte-derived lipoprotein through receptors of the LDL family, of which LRP1 is highest expressed in neurons (Vance and Hayashi, 2010; Zhang and Liu, 2015). Nevertheless, neurons can also activate biosynthesis and synthetize their own cholesterol under certain conditions (Vance et al., 2005; Nieweg et al., 2009).
In microglial cells, astrocytes-derived ApoE particles interact with LDL receptors to be internalized, but also with Triggering Receptor Expressed on Myeloid Cells 2 (TREM2), Toll Like Receptor 4 (TLR-4) to mediate intracellular signaling pathways (Loving and Bruce, 2020).
In neurons, particularly, maintenance on cholesterol homeostasis is essential for the correct functionality. Cholesterol, in fact, is involved in important processes like neuronal integrity, function, differentiation and neurosteroid hormone production. In order to control cholesterol metabolism, neurons contain an additional cholesterol-metabolizing enzyme, cholesterol 24-hydroxylase (CYP46A1), which is CNS and neuron specific (Brown et al., 2004; Ramirez et al., 2008). CYP46A1 converts excess cholesterol to 24S-hydroxycholesterol (24S-OHC) (Lund et al., 2003; Ramirez et al., 2008; Zhang and Liu, 2015; van der Kant et al., 2019), which can be released from cells and cross the BBB through diffusion (Lutjohann et al., 1996; Lund et al., 1999; Xie et al., 2003). Considering that it is specifically produced in neurons, 24S-OHC levels in the blood provide a direct measure of cholesterol turnover in the brain (Sodero, 2021).
Impairment of neuronal cholesterol homeostasis can induce neurodegeneration, as observed in the case of NPC disease, where cholesterol accumulation in late endosomes/lysosomes leads to progressive neurodegeneration (Dulac et al., 2013) characterized by cerebellar dysfunction, mental retardation, and dementia.

1.3.2 Cholesterol metabolism in Alzheimer´s disease.

As mentioned before, Alois Alzheimer originally described a third pathological hallmark in AD brains, “adipose saccules” or “lipoid substances”, suggesting an aberrant lipid metabolism (Foley, 2010). However, a link between lipid metabolism and AD was established with the identification of the ε4 allele of the lipoprotein APOE gene (ApoE4) as the biggest risk factor for SAD (Corder et al., 1993; Saunders et al., 1993; Strittmatter

et al., 1993). Conversely, presence of ε2 allele (ApoE2) is associated with milder AD pathology (Serrano-Pozo et al., 2015), lower cholesterol level in synapses (Oikawa et al., 2014) and reduced amyloid deposition brains (Grothe et al., 2017; Li et al., 2020). Since then, several studies confirmed the implication of cholesterol in different aspects of AD pathogenesis.

In AD patients, in fact, higher cholesterol level has been reported in synapses (Gylys et al., 2007) and cholesterol levels in the brain positively correlated with the severity of dementia (Cutler et al., 2004). Moreover, increased plasma and cerebral spinal fluid (CSF) levels of 24S-OHC, the neuronal specific cholesterol metabolite, have been linked to early AD development (Lütjohann et al., 2000; Papassotiropoulos et al., 2002; Schönknecht et al., 2002; Li et al., 2018). On the contrary, reduction of cholesterol, due to statin use, was associated with lower AD incidence in retrospective studies (Jick et al., 2000; Lin et al., 2015; Zissimopoulos et al., 2017; Zhang et al., 2018).

Studies in APP transgenic mouse models showed that a high cholesterol diet increased Aβ-plaque load, while in WT mice induced Tau hyperphosphorylation (Refolo et al., 2000; Rahman et al., 2005; Glöckner et al., 2011). In addition, a hypercholesterolemic diet in young (4-months old) versus aged (14-months old) rats negatively affected memory performance, at both ages, and increased hippocampal phospho-Tau levels at old age (Ledreux et al., 2016).

A more specific link between cholesterol and Aβ has been observed from different research groups. On one hand, increase of membrane cholesterol facilitates assembly and aggregation of Aβ, since its formation on cell membranes is promoted via interaction with gangliosides, tightly associated with cholesterol (Matsuzaki et al., 2010; Yanagisawa, 2015). In addition, work from Vendruscolo's lab showed a direct effect of cholesterol on Aß aggregation (Habchi et al.,2018). On the other side, cholesterol is also able to affect APP processing directly promoting BACE1 and γ-secretase activity. This was observed in human brain tissue lysates after exogenous cholesterol was added (Xiong et al., 2008), but also in primary mouse neuronal cultures, where treatment with excess cholesterol increased Aβ42 secretion (Marquer et al., 2014). In line, lower cholesterol levels have been shown to decrease Aβ generation via stimulation of the non-amyloidogenic pathway (Simons et al., 1998; Schneider et al., 2006; Grimm et al., 2008).

These phenomena could depend on the fact that increased cholesterol levels promote APP and BACE1 colocalization in lipid rafts, membrane microdomains enriched in cholesterol and sphingolipids, resulting in clathrin-mediated endocytosis and amyloidogenic processing of APP (Cossec et al., 2010; Marquer et al., 2011; Cho et al., 2020). This idea is supported by a recent study in human iPSC-derived neurons, where lowering cholesterol levels reduced the interaction between full-length APP and BACE1 in lipid rafts (Langness et al., 2021). γ-Secretase distribution in microdomain was also reported in mouse cells as well as human brain (Vetrivel et al., 2004; Hur et al., 2008) and appears to be important for its cleavage function on APP (Vetrivel et al., 2005). Enriched cholesterol content in lipid rafts, indeed, has been shown to increase γ-secretase activity in vitro (Osenkowski et al., 2008).

An increased APP localization in lipid rafts has been observed also in CHO cells carrying the FAD-associated PS1ΔE9 mutation, where cellular cholesterol content was significantly increased (Cho et al., 2019a). In this model, treatment with γ-secretase inhibitor did not increase the APP localization to lipid raft, suggesting that this phenomenon may be independent from the PS1 catalytic activity. Interestingly, in PS1ΔE9 cells, inhibition of Lanosterol 14a-demethylase (CYP51), enzyme involved in cholesterol *de novo* production, reduced cellular cholesterol levels and APP localization in lipid rafts.

Additional evidence for the implication of cholesterol metabolism in regulation of phospho-Tau levels was obtained in iPSC-derived neurons from FAD patients, where administration of drugs that decreased cholesterol ester levels, also reduced phospho-Tau due to its increased proteasomal degradation (van der Kant et al., 2019). In mice, genetic inhibition of ApoE-mediated cholesterol transport from astrocytes to neurons also reduced neuronal phospho-Tau levels (Wang et al., 2021a) suggesting that an exogenous source of cholesterol can contribute to formation of neuronal tangles.

All these studies proved the important role of cholesterol homeostasis in AD and how an increased level of cholesterol can contribute to the pathogenesis of the disease.

Beside this, a relationship between the clinical presenilin mutations and cellular cholesterol metabolism is also suggested by several studies. For example, in mouse embryonic fibroblasts (MEFs) it was reported that pharmacological or genetic inhibition of γ-secretase or expression of PS1 FAD mutation increases cholesterol levels (Grimm et al., 2005; Tamboli et al., 2008; Area-Gomez et al., 2012).

Furthermore, in MEFs lacking PS expression as well as fibroblasts from patients harboring clinical PS mutations, an upregulation of cholesterol biosynthesis and increased level of cholesteryl ester and lipid droplet were found (Grimm et al., 2005; Tamboli et al., 2008; Gutierrez et al., 2020).

Although these studies proved a correlation between presenilin dysfunction, due to mutations or genetic depletion, and alteration of cholesterol levels, the possible mechanisms through which the PSs can influence cellular cholesterol level are still unclear.

Increased cellular cholesterol levels are also able to facilitate the cleavage of the C-terminal domain of APP (C99) by γ-secretase. The C99 fragment, indeed, contains a cholesterol binding motif (Beel et al., 2008; Barrett et al., 2012; Song et al., 2013) and the C99-cholesterol complex seems to be sensitive to pH levels with an increased stability at a low pH condition (Panahi et al., 2016). It has been hypothesized that dimerization of C99 protect the fragment from γ-secretase cleavage and high cholesterol levels, destabilizing the interaction between the C99 monomers, facilitates instead the cleavage process (Stange et al., 2021). As mentioned before, γ-secretase localizes in cholesterol rich microdomains and its activity is influenced by cholesterol concentration, therefore, binding to cholesterol may recruit C99 to lipid rafts domains and facilitate its cleavage.

1.4 Protein N-glycosylation.

The term “glycosylation” refers to the process through which carbohydrate chains, called glycans, are covalently linked to lipid or protein molecules. The biological functions of glycosylation differ based on the glycan type and glycan-binding protein or lipid involved. However, it is possible to classify the biological roles of glycans in categories such as structural/modulatory roles, including protein folding and functional switching; extrinsic recognition of glycans, involved in immune response; intrinsic recognition of glycan, as for example intracellular glycoprotein and lipid degradation and trafficking or intracellular signaling (Varki, 2017).

Due to these broad functions, it is not surprising that glycosylation has a critical role in several cellular mechanisms and its disruption leads to different pathologies. In the past twenty years there has been a rapid progression in the discovery of human glycosylation

disorders. The majority of them are related to genetic defects in pathways of protein glycosylation (congenital disorders of glycosylation, CDG).

Deficiency in enzymes or proteins involved in glycolipid degradation is also known to cause several pathologies with many of them (e.g. Tay-Sachs, Sandhoff, Metachromatic leukodystrophy, GM1/2 gangliosidosis) showing, amongst other clinical symptoms, impairment of the nervous system (Varki, 2017).

Protein glycosylation is divided into *N*-linked glycosylation, where the carbohydrate is attached to the nitrogen atom of an asparagine residue of the protein, and *O*-linked glycosylation, where the sugar is attached to the oxygen atom of a serine or threonine residue of the protein. N-glycosylation, in particular, is known to be one of the most common co- and post-translational modifications of secretory proteins in eukaryotes.

N-glycan synthesis starts in the endoplasmic reticulum (ER) where assembly of initial sugar residues on the lipid, the dolichol pyrophosphate (Dol-PP), takes place on the cytosolic side (Bieberich, 2014). The oligosaccharide synthesis is carried by glycosyltransferases encoded by asparagine-linked glycosylation (ALG) pathway genes (Breitling and Aebi, 2013). Assembly of the lipid-linked olisaccharide (LLO) starts with addition of GlcNAc-P to the Dol-P lipid carrier by Alg7. This initial step of the glycosylation process is targeted by tunicamycin, an antibiotic able to inhibit Alg7 and, consequently, block N-glycosylation (Elbein and Heath, 1984). Following Alg7, other five glycosyltransferases, on the cytosolic side of the ER, act on the glycan precursor to obtain $Man_5GlcNAc_2$. To be further elongated, the LLO is then translocated across the ER membrane to the luminal side by a flippase (Rush, 2015). Into the ER lumen, other four mannose residues are added by specific mannosyltransferases (Aebi et al., 1996; Frank and Aebi, 2005). Mutations in glycosyltransferases and flippase lead to a spectrum of diseases called congenital disorders of glycosylation type I (CDG type I) which often display symptoms in the nervous system (Aebi, 2001; Leroy, 2006).

The resulting $Man_9GlcNAc_2$ oligosaccharide is then completed by the action of three highly specific glucosyltransferases Alg6, Alg8 and Alg10 (Stagljar et al., 1994; Reiss et al., 1996). Once complete, the oligosaccharide is transferred from the DoL-PP to the selected asparagine residues on the protein by the oligosaccharyltransferase complex (OST). Addition of the terminal glucose residues to the oligosaccharide bound to Dol-PP is a key factor for substrate recognition by oligosaccharyltransferase (Aebi, 2013). A defect in this

step results in accumulation of biosynthetic intermediates and a hypoglycosylation of proteins. The protein hypoglycosylation, due to the reduced number of glycostructures attached to the protein and reduced number of glycosylated proteins, and not the transfer of incomplete oligosaccharides, is the primary cause for the severe symptoms observed in patients with CDG (Freeze and Aebi, 2005). OST complex consists of eight subunits that in mammals are encoded by DAD1, TUSC3, ribophorin I and II (RPN1, RPN2), OST48, STT3A and STT3B (Mohorko et al., 2011). Although the OST complex has a high substrate specificity for the lipid linked oligosaccharide, it is able to modify numerous proteins by recognizing the consensus sequence NxS/T (where x can be any amino acid except proline) (Bause, 1983). The composition of the OST complex, including STT3A or STT3B isoform, has been suggested to influence OST activity. In particular, in mammalian cells, STT3A OST isoform appears to glycosylate substrate proteins co-translationally, while STT3B isoforms can glycosylate post-translationally sites that were skipped by STT3A complexes (Ruiz-Canada et al., 2009).

Once attached to the nascent protein, the N-linked $Glc_3Man_9GlcNac_2$ oligosaccharides are further trimmed by ER α-glucosidase I and II, encoded by MOGS and GANAB genes, respectively. This cleavage of the terminal glucose residues is crucial for the chaperone function of calnexin and calreticulin. These chaperones, in fact, are able to recognize and bind monoglucosylated, $GlcMan_9GlcNac_2$, N-glycoproteins and mediate their folding (Hammond and Helenius, 1994; Deprez et al., 2005; D'Alessio et al., 2010). If the protein cannot reach the proper conformation in a given period of time, it is degraded by the ER-associated protein degradation (ERAD) machinery, which first shuttles the protein into the cytosol, where it is ubiquitinated and then degraded by the proteasome (Banerjee et al., 2007). Deoxinojimimycin (DNJ) is one of the inhibitors of α-glucosidase I and II thereby it interferes with the correct N-linked glycan synthesis and cause aberrant protein glycosylation (Hughes and Rudge, 1994; Wang et al., 2021b).

If the N-glycosylated protein is correctly folded, the α-glucosidase II removes the last glucose forming the $Man_9GlcNac_2$ N-glycan which is then released from the calnexin/calreticulin cycle. Sequentially, a series of mannosidases in the ER, encoded by MAN1A and MAN1B genes, start the removal of mannose residues. This process is also tightly associated with ERAD that is able to recognize misfolded $Man_8GlcNac_2$ bearing N-glycoproteins. One of the most known glycosylation inhibitors acting on MAN1A and

MAN1B is kifunensine (Elbein and Heath, 1984; Zhou et al., 2021). Once the process of the N-glycan and the folding is complete, the N-glycoproteins can be transported to the Golgi compartment. Here, Golgi mannosidases I, encoded by MAN2 gene, removes other residues to form Man5GlcNac2 (Dunphy et al., 1981; Helenius and Aebi, 2004; Stanley, 2011) that can be further modified by addition of N-acetylglucosamine and other structures, such as sialic acid, galactose and fucose residues, with formation of complex N-glycoproteins (Moremen and Robbins, 1991; Moremen, 2002).

As already mentioned, N-linked protein glycosylation is an essential process in eukaryotic cells, in fact, its complete absence is lethal (Marek et al., 1999). Over 130 types of CDG have been reported (Freeze et al., 2014; Jaeken and Péanne, 2017) and although these diseases are indeed different in their pathogenesis, most of them are due to glycosylation defects in the ER or Golgi compartment. Among the N-linked protein glycosylation defects PMM2-CDG is the most frequent cause of CDG worldwide (Matthijs et al., 1997). It is caused by mutations in phosphomannomutase 2 (PMM2) gene leading to a shortage of GDP-Man, indispensable for the synthesis of the oligosaccharide core. Consequences of this pathology include seizures, hypotonia, ataxia, dysmetria, dysarthria, peripheral neuropathy, cerebral and cerebellar atrophy and myasthenia (Chang et al., 2018). Mutation of another N-glycosylation related gene, ALG6, also leads to several neurological clinical effects such as hypotonia, psychomotor retardation, epilepsy, hypokinesia and cortical atrophy (Dercksen et al., 2012).

These observations prove that primary alteration of the protein N-glycosylation have a huge impact on the general brain functionality and it has been also observed that glycosylation alterations are involved in neurological diseases such as AD.

In fact, many proteins affected in AD are glycosylated themselves, APP, BACE1, Nicastrin, APOE and TREM2. Different studies, indeed, showed an altered protein glycosylation pattern in AD patients. In particular, increased level of N-glycans with more than two branches (bisecting GlcNAc), generated in the Golgi, as well as the responsible enzyme N-acetylglucosaminyltransferase-III (GnT-III), encoded by *Mgat3*, have been found increased in AD patients (Akasaka-Manya et al., 2010; Wang et al., 2019). In mice, lack of GnT-III (*Mgat3*) results in drastic reduction of Aβ deposition and improvement of short-term memory due to the low APP cleavage by BACE1 (Kizuka et al., 2015). In fact, in GnT-III KO cells BACE1 is relocated from the early endosomes, where it efficiently

cleaves APP (Tan and Evin, 2012; Toh and Gleeson, 2016), to the late endosomes/lysosomes where BACE1 can be eventually degraded.

Also sialylation, the terminal attachment of sialic acid to glycans, appears to be decreased in AD patients serum, CSF and brains (Maguire and Breen, 1995; Fodero et al., 2008).

Several studies focused on understanding how aberrant glycosylation of the most common AD-related proteins could contribute to AD pathogenesis (for comprehensive reviews refer to Kizuka et al., 2015; Haukedal and Freude, 2021).

Regarding γ-secretase, nicastrin is the only subunits known to be N-glycosylated with an immature form containing oligomannose N-glycans and a mature form carrying complex N-glycans (Yang et al., 2002; Herreman et al., 2003). In order to achieve the complete maturation, nicastrin has to reach the Golgi compartment where complex N-glycan synthesis occurs. Absence of both PSs in cells leads to the complete loss of mature form of nicastrin mainly due to impaired trafficking of the protein to the Golgi.

This observation implicates that PSs are required for correct nicastrin maturation (Herreman et al., 2003). Treatment with the mannosidase inhibitor kifunensine also blocks nicastrin maturation, but does not affect its cell surface expression or interaction with PS1 and γ-secretase assembly suggesting that the complete glycan maturation of nicastrin is not required for its function (Shirotani et al., 2003).

Although PSs are not glycosylated themselves, their regulatory role in glycosylation of other proteins directly or by affecting their cellular localization was proved by several studies (Schedin-Weiss et al., 2014). PS1 and PS2, in fact, affect the glycosylation and sialylation of the neural cell adhesion molecule (NCAM) (Farquhar et al., 2003), as well as glycosylation, maturation and subcellular localization of the receptor TrkB (Naruse et al., 1998). The effect of PS1 deletions or mutations on N-glycosylation of V0a1 was also observed in study examining lysosomal proteolysis and autophagy (Lee et al., 2010) although this could not be confirmed in other studies (Coen et al., 2012; Zhang et al., 2012).

Considering that glycan alterations was observed in patients with mild cognitive impairment that progressed to AD, it is plausible that glycan alterations precede the clinical onset of AD. This consideration highlights how glycan alteration in humans can be a potential biomarker for early AD diagnosis (Palmigiano et al., 2016). Furthermore, the

restoration of the glycosylation homeostasis could be a possible interesting therapeutic strategy (Wang et al., 2019).

2. Aims

For many years AD research field has been focused on studying the role of Aβ and Tau in relation to the pathology. Although presence of senile plaques and tangles are the hallmarks that define AD pathology, insight of the relevance of cholesterol were already described by Alzheimer himself at the time of his discovery. In the last thirty years many studies supported the important role of cholesterol in AD pathogenesis. Observations regarding increased cellular cholesterol level upon PS dysfunction suggest a link between these events. Alteration of PS functions leading to increased cellular cholesterol, therefore, might have an important contribution in accelerating and/ or aggravating the course of the disease.

In this contest, the purpose of this project is to try to acquire new knowledge about the connecting mechanism between PS function and cellular cholesterol homeostasis.

Observation of altered cholesterol metabolism in models with depletion of both PS (double knockout, PSDKO) have been previously reported. In this study we aim to dissect the contribution of the single PS using specific knockout for PS1 and PS2. The comparison between these models can give interesting hints regarding common pathways as well as highlight potential differences between the two homologous proteins.

An initial purpose is to characterize the cholesterol phenotype *in vivo* using mouse brains from either single or both PS KO mice. These experiments can provide information regarding the cholesterol levels in different brain regions and cell types.

For further analysis of molecular mechanisms, mouse fibroblasts from single knockout mice are here used as *in vitro* model. In these cells, the aim is to characterize the cholesterol phenotype by analysis of the cholesterol levels, its subcellular distribution and expression of proteins involved in cholesterol metabolism. These experiments can provide information regarding potential altered step in the cholesterol metabolism.

PS functions are involved in several cellular processes; therefore, their deletion can affect cholesterol homeostasis through different mechanisms. Perturbation of potentially involved pathways and/or rescue of their alteration might help to discern among the different possibilities.

3. Materials and methods

3.1 Cell lines.

Mouse Embryonic Fibroblasts (MEFs).
MEF WT, MEF PS1KO, MEF PS2KO and MEF PSDKO were cultivated in Dulbecco's Modified Eagle's Medium (DMEM) / Glutamax Medium (Thermo Fisher: 3196621) supplemented with 10 % inactivated FCS, 1 % Penicillin / Streptomycin (50 U/ml Penicillin, 50 g/ml Streptomycin). Cells were maintained at 37 °C and 5 % CO_2. MEFs transfected with NPC1His-EGFP construct were cultivated with the same medium supplemented with 200 µg/ml G418.

Chinese hamster ovary cell (CHO).
CHO WT and CHO NPC1null cells were cultivated in Ham´s F-12 (Sigma: N6658) supplemented with 10% FCS, 1% Penicillin/Streptomycin and 2 mM L-Glutamine at 37 °C and 5 % CO_2.

3.2 Mouse brain samples.

A total number of eighteen hemibrains from 2 months old (62, 64, 66 or 69 days of age) female and male mice were obtained from Dr. Kang Jongkyun and Dr. Jie Shen, Harvard Medical School:

- 6 WT (fPS1 / fPS1; PS2+/+); 4 males and 2 females
- 6 PS1cKO (fPS1 / fPS1; PS2+/+; CamK2α-Cre); 4 males and 2 females
- 3 PS2KO (fPS1 / fPS1; PS2-/-); 3 males
- 3 PSDKO (fPS1 / fPS1; PS2-/-; CamK2α-Cre); 2 females and 1 male.

Additional six hemibrains (3 WT and 3 PS2KO) from 6 months old female mice were provided by Dr. Lutgarde Serneels from Dr. Bart De Strooper Lab in Leuven.
After extraction, the brain hemispheres were separated and one hemibrain was immersion-fixed in 4 % PFA. After shipping, the brains were cryoprotected in 30 % sucrose for 48 hours and snap frozen in isopentane (2-methylbutane) precooled at - 80 °C. 16-20 µm sections were obtained by cryostat, collected in PBS and maintained at 4 °C until the moment of use.

3.3 Immunofluorescence staining.

Cells.

Cells were seeded on coverslips and fixed with 4 % PFA, 20 min at RT. Then coverslips were washed three times with 1x PBS and maintained at 4 °C until the moment of use. For staining, the coverslips were incubated with the Blocking solution (10 % BSA in PBS) with addition of Filipin 100 µg/ml, freshly dissolved in DMSO, for 1 hour at RT. This step was followed by three washings with PBS and incubation with primary antibodies (Tab. 1) dissolved in 5 % BSA in PBS overnight at 4 °C. Secondary fluorophore-conjugated antibodies (Tab. 2), dissolved in 5 % BSA in PBS, were added to the coverslips after three washing steps with PBS and incubated for 1 hour at RT in the dark. Coverslips were then washed three times with PBS, two times with dH_2O and mounted with Immunomount solution (Immu-Mount, Shandon, Thermo Scientific). All the incubation steps were performed in a humid chamber.

Mouse brains.

Brain sections were transferred to the coverslip and surrounded with a hydrophobic pen (ImmEdge Pen, Vector laboratories). For ß-Tubulin staining, the sections have been subjected to heat-induced antigen retrieval, using a microwave, in Sodium citrate buffer (10 mM sodium citrate, 0.05 % Tween-20, pH 6.0) 90 °C for 30 min. Stainings were performed following the same protocol described above. Filipin concentration was increased to 200 µg/ml.

3.4 Imaging and analysis

Images were acquired using AxioVert 200 fluorescence microscope and ZEN microscopy software (Zeiss) or VisiScope CSU-W1 spinning disk confocal microscope and VisiView Software (Visitron Systems GmbH). Lasers and exposure time settings were maintained constant through all the acquisitions and images were obtained using a 63x immersion objective with z-step size on 0.25 µm. For each experiment, at least six images per coverslip were randomly taken and used for quantification. Image processing was performed using the free software ImageJ Fiji and analysis of Pearson´s coefficient was performed using Squassh, a tool of the MosaicSuite macro (Rizk et al., 2014).

3.5 Mass spectrometry analysis

Sterol mass spectrometry analysis

WT, PS1KO and PS2KO MEFs were cultivated in 10 cm dishes to be confluent. After remotion of the medium, the cells were washed once using cold PBS and collected with 1.5 ml cold HBSS by scraping. This step was followed by centrifugation at 4 °C for 3 minutes at 1,000 g. Supernatant was then removed and the pellet snap frozen at – 80 °C. Mass spectrometry analysis for sterols was performed by our collaborator prof. Dr. Dieter Lütjohann, Institute of clinical Chemistry and clinical Pharmacology, University of Bonn.

Glycostructures mass spectrometry analysis

Mass spectrometry analysis for glycostructures was performed by our collaborator Dr. Hirokazu Yagi, Gratuate School of Pharmaceutical Science, University of Nagoya.

3.6 Protein expression analysis

3.6.1 Cell lysis, subcellular fractionation and protein estimation

Cells from 6 or 10 cm dishes were washed with 1x PBS and collected in 600 µl or 1 ml cold Hypotonic Buffer (TrisHCl pH 7.4 10 mM, 1x Complete® protease inhibitor [ROCHE] in dH2O, 1x PhosphoStop [ROCHE]) by scraping and maintained on ice. To separate the nuclear fraction, the cell lysate was resuspended through a 0.6 mm cannula and centrifuged at 1,000 g for 5 min at 4 °C. The supernatant was then collected in a separate tube and further centrifugated at 16,000 g for 60 min at 4 °C to separate the membrane and cytoplasmic fractions. The membrane fractions obtained, after addition of an appropriate volume of Hypotonic Buffer (100 - 150 µl), were homogenized by sonication (3 sec, minimum power).

The protein estimation was performed following the Pierce BCA Protein Assay Kit (Item No. 23225, Thermo Fisher Scientific) protocol. The standard curve was calculated based on sequential dilution of 2.0, 1.0, 0.5, 0.25 and 0.125 µg/µl BSA while, for the blank, only hypotonic buffer was used at the following concentrations: 2.0, 1.0, 0.5, 0.25, 0.125, and 0.0 µg/µl BSA. 10 µl of each standard or sample were added into 200 µl pre-mixed solution A and B (ratio 1:50) from the kit. Standard and samples were incubated at 65 °C for 3 minutes, then pelleted and transferred onto 96 wells plate. The absorbance was measured at 562 nm

on the Tecan plate reader. Protein concentration was calculated by the standard curve formula. The working dilution was prepared mixing the amount of sample required to obtain the desired concentration of protein (µg/µl) with 4x Laemmli buffer (62.5 mM Tris pH 6.8, 2 % SDS, 10 % glycerol, 5 % 2-mercaptoethanol, 0.001 % bromophenol blue, 40 mM DTT). The samples were stored at -20 °C if not used immediately.

3.6.2 Sodium dodecyl sulfate polyacrylamide gel electrophoresis (SDS Page)

In order to separate the proteins accordingly to their size, the samples dissolved in Laemmli Buffer were subject to SDS page. This technique allows to separate proteins depending on the individual mobility in a polyacrylamide gel. The presence of SDS and DTT in the sample buffer remove the effect of different shapes and charges of proteins on the migration. The same amount of samples was loaded into 4 % - 12 % gradient Bis-Tris NuPage gels using MOPS or MES SDS running buffer, under 140 mA for ~ 1.5 hours.

3.6.3 Western immunoblotting

After electrophoresis, the gel was rinsed in Transfer Buffer (Tris Base, Glycin, pH 11, 10 % methanol) with Whatman paper and 0.2 µm nitrocellulose membrane. The transfer was obtained using a wet system, in a tank containing Transfer Buffer, under 400 mA for 3 - 4 hours. The membrane was then washed once in dH_2O and incubated with Ponceau S (for protocol see below). Incubation in blocking solution (5 % milk powder in TBS containing 0.05 % Tween 20) for 1 hour at RT, was followed by three washing steps with TBST (TBS containing 0.05 % Tween) and incubation with diluted primary antibody solution (Tab. 1) overnight at 4 °C in permanently agitation. On the following day, the membrane was washed three times with TBST and incubated with secondary antibody solution (Tab. 2) for 1 hour at RT shaking. Protein detection was performed using ECL solutions.

Tab. 1: Primary Antibody list

Antibodies	Target	Dilution	Species	Company
ABL-93-c	Lamp2	1:1000	Rat	Iowa hybridoma bank
B-3	Rab7	1:200	Mouse	Santa Cruz
PM062	EEA1	1:300	Rabbit	MBL
234003	Iba1/AIF1	1:300	Rabbit	Synaptic Systems
Mab377	NeuN	1:500	Mouse	Sigma-Aldrich
Ab15568	Beta tubulin	1:1000	Rabbit	Abcam
GFAP (D1F4Q)	GFAP	1:300	Rabbit	Cell Signaling
NB400-148SS	NPC1	1:1000	Rabbit	Novus Biologicals
HPA000835	NPC2	1:250	Rabbit	Merk
ERP3724 (ab92544)	LRP1	1:1000	Rabbit	Abcam
NB400-105	ABCA1	1:1000	Rabbit	Novusbio
EP1553Y	LDLR	1:1000	Rabbit	Abcam
Ab30682	SREBP2	1:1000	Rabbit	Abcam
BD557037	SREBP2	1:1000	Mouse	BDbiosciences
13431-1-AP	Cyp51A1	1:1000	Rabbit	Proteintech
BD610920	N-Cadherin	1:1000	Mouse	BDbiosciences
924301	Giantin	1:1000	Rabbit	Biolegend
PA5-30048	Golgin 97	1:200	Rabbit	Invitrogen

Tab. 2: Secondary Antibody list.

Fluorophore-conjugated Antibodies	Dilution	Catalog number	Company
Donkey anti-Rabbit Alexa Fluor 546	1:1000	A10040	Invitrogen
Goat anti-Rabbit Alexa Fluor 546	1:1000	A11010	Invitrogen
Donkey anti-Mouse Alexa Fluor 488	1:1000	A21202	Invitrogen
Goat anti-Mouse Alexa Fluor 488	1:1000	A11001	Invitrogen
Goat anti-Rat Alexa Fluor 546	1:1000	A11081	Invitrogen
Goat anti-Mouse Alexa Fluor 546	1:1000	A11003	Invitrogen
Goat anti-Rabbit Alexa 647	1:500	A21244	Invitrogen
Peroxidase-conjugated Antibodies	**Dilution**	**Catalog number**	**Company**
Anti-Rabbit IgG	1:10000	A9169	Sigma-Aldrich
Anti-Mouse IgG	1:10000	A9044	Sigma-Aldrich
Anti-Rat IgG	1:10000	612-103-120	Rockland

3.6.4 Normalization of Western Immunoblotting.

Although protein amount was quantified using BSA Protein Assay Kit and each sample was diluted in order to apply the same protein amount for western blot, we also normalized the protein signal, obtained from detection with ECL, on Ponceau S staining. Before

selecting this method, we compared its reliability against normalization based on commonly used standards, such as Calnexin and Actin.

Because some of our proteins of interest can be detected at low amounts (for example NPC1, LRP1 and CYP51), we prepared a standard curve using membrane fraction samples from WT MEFs at the following amounts: 1, 2 and 4 µg.

The experiment was performed twice with three technical replicates for each amount of protein. Quantification of NPC1 protein signals correlated well with the loaded protein in a linear relationship (Fig. 3.1C). Amongst the three normalization methods analyzed, Ponceau S staining showed the best linear correlation, while the Actin signal appeared not to be reliable for amounts of protein below 2 µg. The correlation of Calnexin was similar to Ponceau staining. However, Calnexin co-migrates with LRP1 and varies with the PS genotype. For these reasons we proceeded using Ponceau S staining to normalize the protein bands for quantification.

3.6.5 Ponceau S staining.

Nitrocellulose membranes were placed in a plastic box and submerged with Ponceau S solution (0.5 g Ponceau S, 25 ml acetic acid, dH_2O up to 500 ml), 1 min at RT in agitation. The membranes were then washed three times with dH_2O and imaged. The staining was removed washing the membranes with TBST thrice for 10 min at RT with shaking.

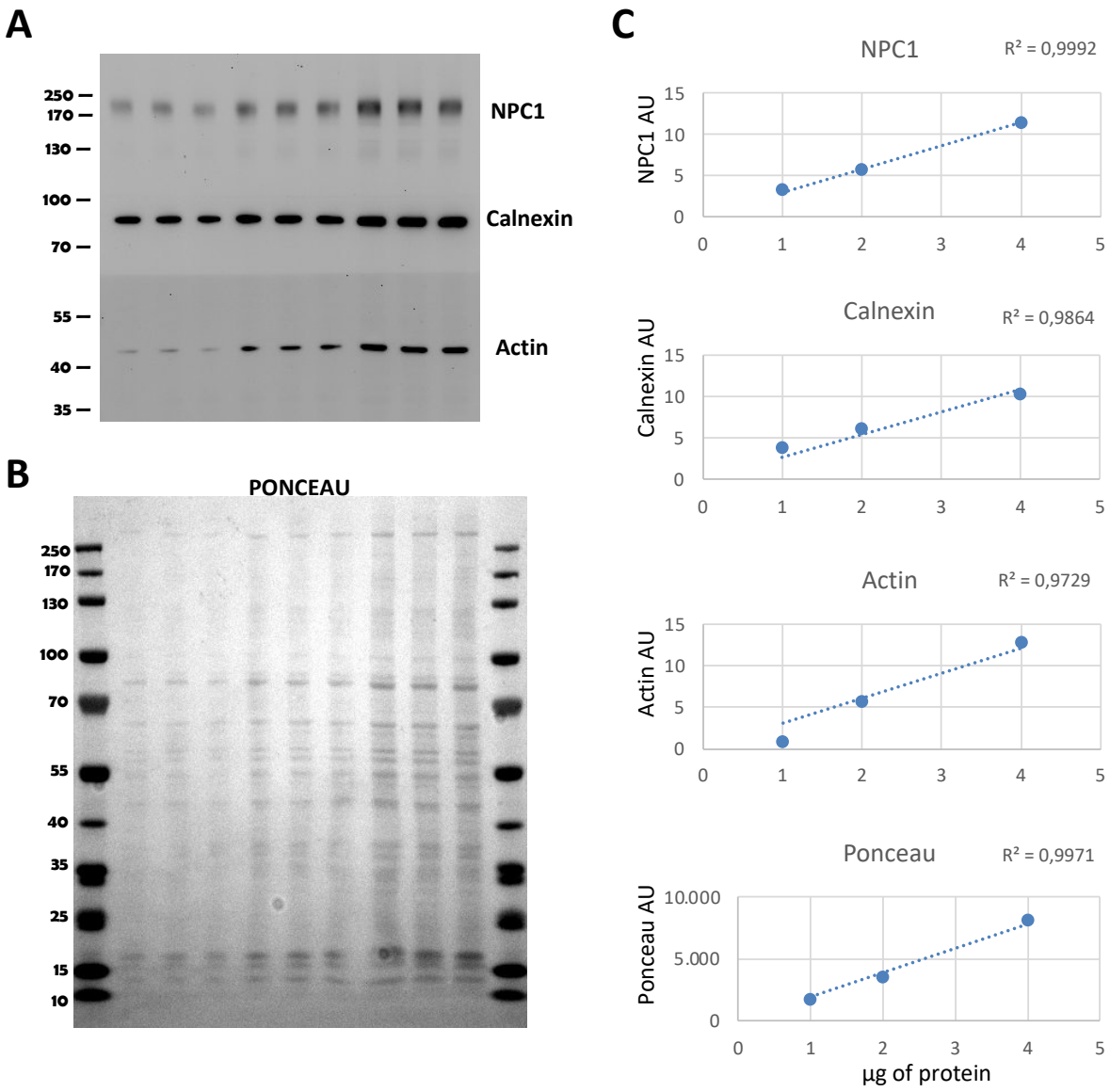

Fig. 3.1: Comparison of different methods of Western Immunoblotting normalization A) Representative western immunoblotting of NPC1, Calnexin and Actin proteins detected on the same membrane and relative B) Ponceau image. C) Graphs showing the variation from the linear regression for each quantified protein or ponceau staining.

3.7 Deglycosylation assay.

Deglycosylation of membrane proteins was obtained using PNGase F (New England Biolabs, #P0704), according to the suggestion of the manufacturer.
In particular, 1 - 20 µg of membrane fraction samples were combined with 1 µl of 10x Glycoprotein Denaturing Buffer and H_2O (if necessary) to make a 10 µl total reaction volume. Denaturation of glycoprotein was obtained by heating the samples at 45 °C for 10 min. Then, a reaction volume of 20 µl was obtained by adding 2 µl 10X GlycoBuffer 2, 2 µl 10 % NP-40, 6 µl H_2O. After addition of 1 µl of PNGase F enzyme or H_2O (for the controls), the reactions were incubated at 37°C for 1 hour. Samples were, then, pelleted and mixed with 7 µl of sample buffer (4x Laemmli buffer) and either stored at -20 °C or immediately used for western blotting analysis to assess mobility shifts.

3.8 Pharmacological treatments

3.8.1 Treatments with glycosylation inhibitors

To perform the treatments with the different inhibitors, starting from a confluent 10cm dish, cells were first detached, pelleted and resuspended in cultivation medium. 10µl of cell suspension was applied to a Neubauer counting chamber to estimate the number of cells per ml (cells/ml). An appropriate number of cells (1 x 10^4 cells/cm^2) were then seeded on 10 cm dishes, 6 cm dishes or on coverslip in 24 wells plate using normal cultivation medium. The day after, the medium was removed and replaced with fresh medium supplemented with an appropriate concentration of each component:

- Tunicamycin, 6 ng/ml (T7765-5MG, Sigma-Aldrich, stock solution 5 mg/ml in DMSO);
- 1-Deoxynojirimycin, 1 mM (Item No. 21500, Cayman, stock solution 61 µM in DMSO);
- Kifunensin, 0.1 µM (Item No. 109944-15-2, Cayman, stock solution 61 µM in dH_2O);
- Swainsonine, 0.01 µM (Item No.16860, Cayman, stock solution 58.8 µM in DMSO).

Cells were cultivated for 6 days and the supplemented medium was changed every other day. In control cells, normal medium was used and changed every other day. At the end of the experiments, cells were washed once with PBS and collected in Hypotonic Buffer or fixed using 4 % PFA (as previously described).
To perform the short time Tunicamycin treatments, the day after seeding, medium was supplemented or not (for control cells) with 2 µM of Tunicamycin and the cells were

collected at different time point (30min, 1h, 3h, 6h, 9h, 16h, 18, 24h). Treatment for 24 hours resulted in apparent toxicity.

3.8.2 Treatments with DAPT

WT MEFs were counted and seeded on 10 cm dishes or coverslips on 24 wells plate using normal cultivation medium. The day after, the medium was removed and replaced with fresh medium supplemented with 5 or 10 μM of DAPT (tert-Butyl (S)-{(2S)-2-[2-(3,5-difluorophenyl) acetamido] propanamido} phenylacetate), D5942, Sigma-Aldrich, stock solution 10 mM in DMSO). Cells were cultivated for 6 days and the medium was changed every other day with or without (for control cells) addition of DAPT. At day 7 cells were washed once with PBS and collected in Hypotonic Buffer or fixed using 4 % PFA (as previously described).

3.8.3 Treatments with calcium modulators

To perform the treatments the cells were counted and seeded on 10 cm dishes or on coverslip in 24 wells plate using normal cultivation medium. The day after, the medium was removed and replaced with fresh medium supplemented with an appropriate concentration on each component:

- Thapsigargin, 0.01 and 0.03 μM (T9033, Sigma-Aldrich, stock solution 10 mg/ml);
- DHBP (1,1′-diheptyl-4,4′-bipyridinium dibromide), 1 μM (Item No. HY-101237, MedChemExpress, stock solution 10 mM in DMSO);
- Dantrolene, 30 and 100 μM (Item No. 14326, Cayman, stock solution 2 mg/ml in DMSO);
- Xestospongin C, 0.3 and 1 μM (Item No. 64950, Cayman, stock solution 30 mM in EtOH);
- Concanamycin A, 0.01 and 0.001 μM (Item No. C9705, Sigma-Aldrich, stock solution 10 mM in DMSO)
- ML-SA1, 10 and 30 μM (Item No. HY-108462, MedChemExpress, stock solution 6 mM in DMSO)

- TransNed19, 0.3, 1, 3 and 10 μM (Item No. 17527, Cayman, stock solution 4 mM in DMSO)

Cells were cultivated for 6 days and the supplemented medium was changed every other day. In control cells, normal medium was used and changed every other day. At the end of the experiments, cells were washed once with PBS and collected in Hypotonic Buffer or fixed using 4 % PFA (as previously described).

3.8.4 Treatments with U18666A

WT MEFs was seeded on 10 cm dishes or on coverslips in 24 wells plate using normal cultivation medium. The day after, the medium was removed and replaced with fresh medium supplemented or not (for control cells) with U18666A at 1 or 2 μM concentration. Cells were cultivated for 6 days and the supplemented medium was changed every other day. At day 7, cells were washed once with PBS and collected in Hypotonic Buffer or fixed using 4 % PFA (as previously described).

3.8.5 Treatments with Arimoclomol maleate

WT, PS1KO and PS2KO MEFs were counted and seeded on 10 cm dishes or coverslips on 24 wells plate using normal cultivation medium. The day after, the medium was removed and replaced with fresh medium supplemented or not (for control cells) with 300 or 400 μM of Arimoclomol maleate (Item No. HY-106443A, MedChemExpress, stock solution 50 mM in DMSO). Cells were cultivated for 6 days and the medium was changed every other day with or without addition of Arimoclomol maleate. At day 7 cells were washed once with PBS and collected in Hypotonic Buffer or fixed using 4 % PFA (as previously described).

3.9 Cell transfection.

3.9.1 Vector characterization

NPC1 His6 EGFP was a gift from Matthew Scott (Addgene plasmid #53521) (Fig. 3.2). The plasmid was sent in bacteria as agar stab and, after arrival, bacteria were plated in agar plates containing Kanamycin (50 μg/μl). The day after several colonies were picked

and each of them was inoculated in 5 ml LB broth supplemented with Kanamycin for 24 hours. The plasmid was then extracted using the Miniprep kit, (QIAprep Spin Miniprep Kit, Qiagen) following the suggested protocol and the DNA concentration was determined using the Nanodrop device (NanoDrop, Thermo Scientific). The accuracy of the plasmid was confirmed by sequencing and, in addition, by obtaining the expected fragments size after cleavage of the plasmid with restriction enzymes (NheI, KpnI).

Fig.3.2. Map of the NPC1 His6 EGFP plasmid: Full sequence map of NPC1 His6 EGFP (plasmid #53521). Picture downloaded from addgene website.

3.9.2 Transfection with lipofectamine

One day before transfection with NPC1His-EGFP plasmid, WT and PS KO MEFs were counted and $2*10^5$ cells were seeded in 6 wells plate cell culture dishes in normal medium without antibiotics. The next day, the transfection was performed using Lipofectamine

2000 Transfection Reagent (Item No. 11668019, ThermoFisher Scientific), according to the suggestion of the manufacturer.

In particular, for each transfection sample:

a) 3.75 µl of Lipofectamine was diluted in 100 µl Opti-MEM, mixed by tapping and incubated 5 min at RT = Solution A;
b) 3.5 µg of DNA plasmid was mixed in 100 µl Opti-MEM Reduced Serum medium (Item No. 31985070, ThermoFisher Scientific) = Solution B;
c) solutions A and B were combined, gently mixed by pipetting and incubated for 20 min at RT.

Meanwhile, cells were washed twice with pre-heated PBS and 2 ml of Opti-MEM medium was added in each well. 200 µl of Lipofectamine-plasmid complexes were, then, added dropwise to each well. Cells were incubated at cell culture conditions for 24 hours. After this time, the cells where splitted and seeded on 10 cm dishes or on coverslips, in 24 wells plate, using normal medium supplemented with 200 µg/ml G418 for selection of cells expressing the gene of interest. After 48 hours the cells were washed once with PBS and collected in Hypotonic Buffer or fixed using 4 % PFA (as previously described).

3.10 3´mRNA sequencing

3.10.1 RNA extraction

RNA from WT and PS KO MEFs samples from two different preparations was extracted using Trizol (Invitrogen) following the manufacturer's instructions.

3.10.2 3´ mRNA sequencing

3' mRNA sequencing was performed by Dr. André Heimbach in the Next Generation Sequencing (NGS) Core Facility of the Medical Faculty, University of Bonn. Libraries were prepared using the QuantSeq 3'-mRNA-Seq Fw. Library Prep Kit (Lexogen, New Hampshire, United States). The data was preprocessed using the options recommended by the manufacturer: quality control was performed using fastqc v0.11.8 (Babraham Bioinformatics Institute, Cambridge, UK)) followed by trimming using bbduk. Alignment was done with STAR aligner 2.6.0a (using the options recommended by the manufacturer) against the GRCm38 mouse (Ensembl release 102) genome (Dobin et al. 2013). The R-

package DESeq2 was used for statistical analysis with settings as recommended by the provider (normalization of raw counts, dispersion estimation and negative binomial Wald test with Benjamini-Hochberg multiple test correction) (Love at al. 2014). Adjusted p-values < 0.05 were defined as significant. Raw reads processing and differential expression analysis was performed by Dr. Simon Bohleber.

3.11 Statistical analysis

Ordinary one-way ANOVA followed by Dunnett´s correction was used for statistical analysis using GraphPad Prism. The data are represented as mean ± standard error of the mean (SEM).

4. Results

4.1 Cholesterol accumulation in PS KO mouse brain

4.1.1 Increased Filipin intensity in neurons from PS KO mouse brains

Brain samples of mice with conditional deletion of PS1 in excitatory forebrain α-calcium-calmodulin-dependent kinase II (CaMK2α) positive neurons (PS1cKO), constitutive deletion of PS2 (PS2KO), conditional ablation of PS1 using the Cre/loxP system in PS2KO mice (PSDKO) and controls (WT) were provided by Dr. Kang Jongkyun and Dr. Jie Shen (Dhaliwal et al., 2018).

Mouse brains were used to study if the lack of presenilins can affect the cholesterol level in neurons *in vivo*. Therefore, the intensity of the Filipin staining, a compound able to bind the free cholesterol, was examined in TUJ1/NeuN double positive cells. Cells from several brain regions were analyzed: cortex, striatum, dentate gyrus (DG), CA1, CA2, CA3.

Neurons from PS1cKO mice showed a significant increase in cholesterol in cortex, DG and CA1 as compared to WT mice (Fig. 4.1). In the striatum area, instead, filipin intensity was similar between PS1cKO and WT. Considering that CamK2α neurons, in the striatum, are less than 1% (Erondu and Kennedy, 1985), an overall similarity of the Filipin signal in this region, between PS1cKO and WT, was expected.

In mice lacking PS2 expression, the significant increase in free cholesterol level is observed in all the examined brain regions except the DG.

Deletion of both presenilins, in PSDKO mice, led to an increased cholesterol level in cortex, striatum, CA1 and CA3 but not in DG and CA2. These results suggest that, in a PS2KO background, deletion of PS1 in CamK2α positive neurons does not significantly affect the cholesterol levels in the DG. Apart from this interesting brain region dependent phenotype in hippocampal areas, these data show that lack of presenilins in brain affects cholesterol levels in neurons. Single or combined deletion of PS1 and PS2, indeed, led to a significant cholesterol accumulation in cortex and CA1 regions.

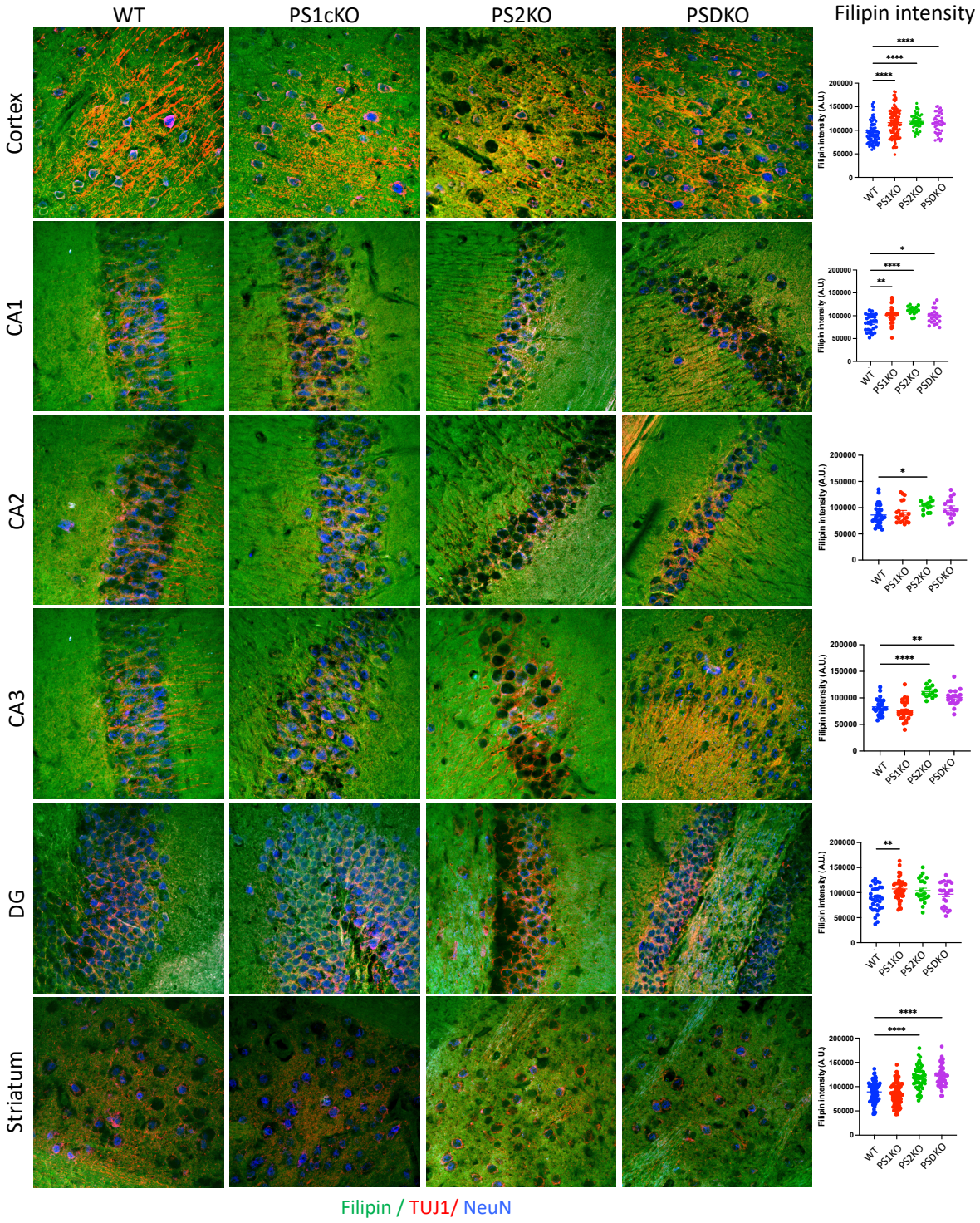

Fig. 4.1: Neuronal cholesterol accumulation in PS KO mouse brains. Representative co-immunostaining of Filipin (green) with ßTubulin (TUJ1, red) and NeuN (blue) in different brain regions from WT, PS1cKO, PS2KO and PSDKO mice. Three (PS2KO and PSDKO) or six (WT and PS1cKO) brains per genotype were analyzed. At least four images per brain region were taken from each sample. The graphs show the Filipin intensity quantified in double positive TUJ1/NeuN cells; each point correspond to a single cell. A.U., arbitrary

units, one-way ANOVA with Dunnett´s correction; *, P<0.05; **, P<0.005; ***, P<0.0005; ****, P<0.0001.

4.1.2 Decreased Filipin intensity in Iba1-positive cells from PS2KO mouse brains

Considering the previous results obtained in mouse brain neurons, the next step was to analyze the possibility that presenilin deletion affects cholesterol levels also in other cell types, different from neurons.

For this purpose, brains from mice with constitutive deletion of PS2 (PS2KO) gene and relative controls (WT) provided by Bart De Strooper's lab were analyzed.

The different cell types were identified performing a co-staining with Filipin and specific cellular markers: Ionized calcium-binding adapter molecule 1 (IBA1) for microglia, βTubulin/NeuN for neurons and Glial fibrillary acidic protein (GFAP) for astrocytes. Different brain regions were analyzed and the results, displayed in the graphs, show the intensity of the Filipin signal colocalizing with each specific cellular marker.

The filipin intensity in IBA1 positive cells was significantly decreased in PS2KO mice brains compared with the WT mice in all the analyzed brain regions (Fig. 4.2 A).

An opposite result was observed regarding the βTubulin/NeuN positive cells, were the Filipin signal is significantly increased in all the brain region, except for the dentate gyrus (Fig. 4.2 B). These results are in line with the previous observation in PS2KO mouse brains from Dr. Shen´s lab.

Regarding astrocytes, no significant changes in the free cholesterol content was observed between WT and PS2KO mice in the different brain regions investigated (Fig. 4.2 C).

These data suggest that lack of PS2 can affect cellular cholesterol metabolism, in mouse brain, in a cell type-dependent manner with increased levels of cholesterol in neurons and reduced levels in microglia cells. However, the underlying mechanisms are unclear and there may be other possibility to explain this phenomenon.

Overall, our results confirmed that in PS2KO mice cholesterol accumulates in neurons from several brain regions *in vivo*, consistently with what observed in the previous experiment.

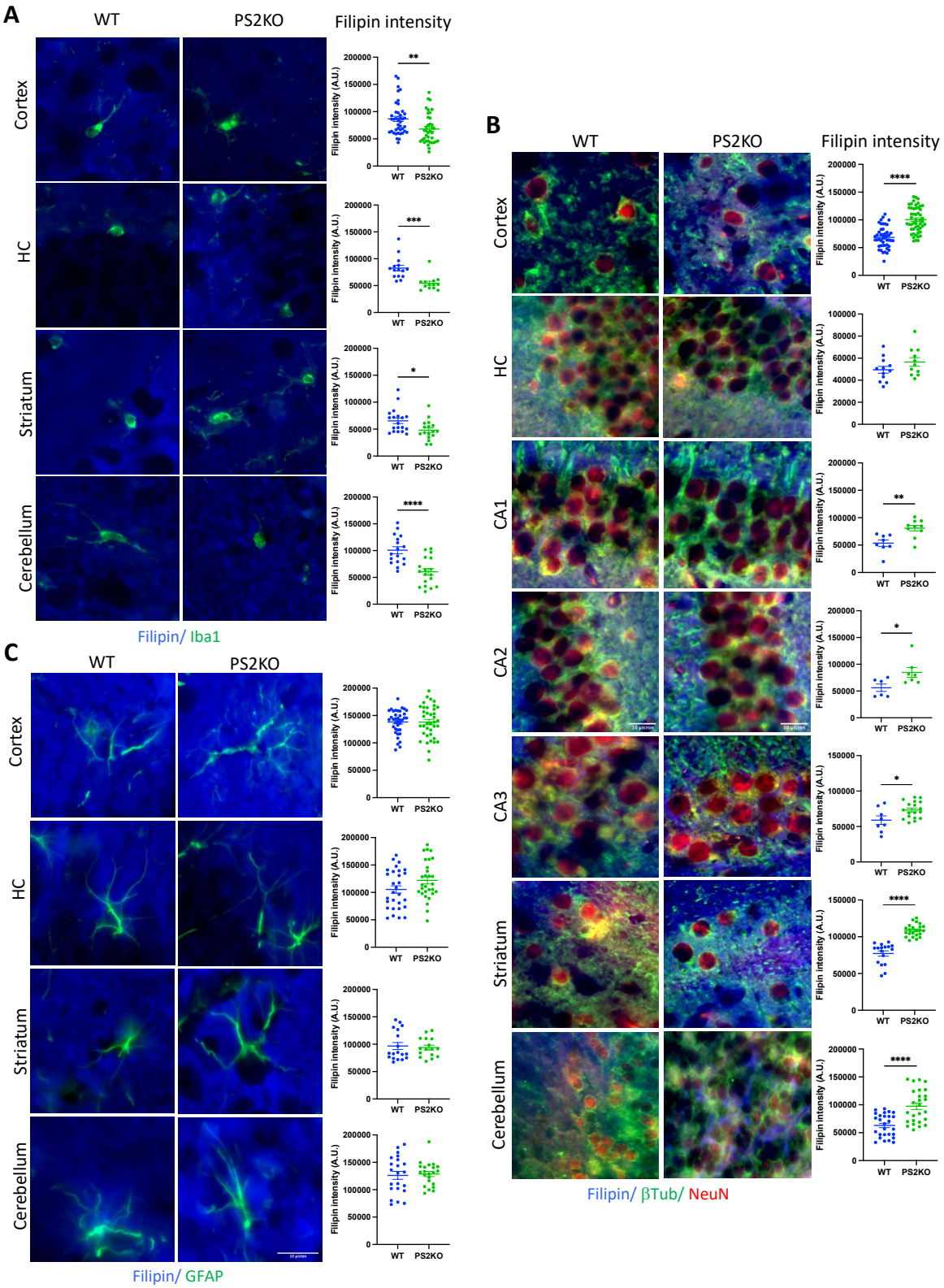

Fig. 4.2: Cholesterol accumulation in PS2KO mouse brains. Representative co-immunostaining of Filipin (blue) with IBA1 (green; A), βTub/NeuN (green/red; B) and GFAP (green; C) in different brain regions from WT and PS2KO mice. Three brains per genotype were analyzed. At least four images per brain region were taken from each

sample. Scale bar 10 µm. Graphs show the Filipin intensity; each point correspond to a single cell. A.U., arbitrary units; one-way ANOVA with Dunnett´s correction; *, P<0.05; **, P<0.005; ***, P<0.0005; ****, P<0.0001.

4.2 Cholesterol accumulation in PS KO MEFs

4.2.1 Endo-lysosomal accumulation of cholesterol in PS KO MEFs

To further investigate the molecular mechanism behind the increase of cholesterol level following presenilins deletion, mouse embryonic fibroblast (MEFs) derived from PS KO and WT mice were selected as the *in vitro* model.

First of all, level of cholesterol and its precursors were analyzed performing mass spectrometry (MS). The results show significantly increased levels of desmosterol, lathosterol and cholesterol itself in PS1- and PS2- KO MEFs as compared with WT (Fig. 4.3 A) indicating an increased cholesterol production in PS1 and PS2 deficient cells.

In these cells, immunofluorescence staining was performed to further characterize the cholesterol content and its subcellular distribution. Free cholesterol was visualized by Filipin while cellular compartments were stained with specific antibodies. The Filipin signal is evidently increased in both PS1- and PS2KO MEFs compared with WT, in line with results from the MS analysis. Moreover, while in the WT MEFs the Filipin signal appears mainly in the plasma membrane, in both PS KO cells the Filipin signal is predominant in cytoplasmic vesicular compartments.

Co-staining with antibodies against different cellular compartments, Early Endosome Antigen 1 (EEA1) for early endosomes, Ras-related protein Rab-7a (Rab7) for late endosomes and Lysosome-associated membrane protein 2 (LAMP2) for lysosomes, revealed the subcellular distribution of free cholesterol in PS1- and PS2KO MEFs.

In particular, the colocalization analysis shows an increased overlap of Filipin with LAMP2- and Rab7-positive compartments in PS KO compared to WT MEFs, while no significant differences were observed regarding the cholesterol distribution in early endosomal compartments (Fig. 4.3 B).

The obtained data proved that also in our *in vitro* model deletion of presenilins induces an increased cellular cholesterol level recapitulating what was observed in neurons from PS KO mouse brains. Therefore, PS KO MEFs can be used as a model to investigate the molecular mechanism connecting presenilins to cholesterol metabolism. In addition, the

cholesterol distribution in PS KO MEFs provides evidences of a specific accumulation in endo-lysosomal compartments.

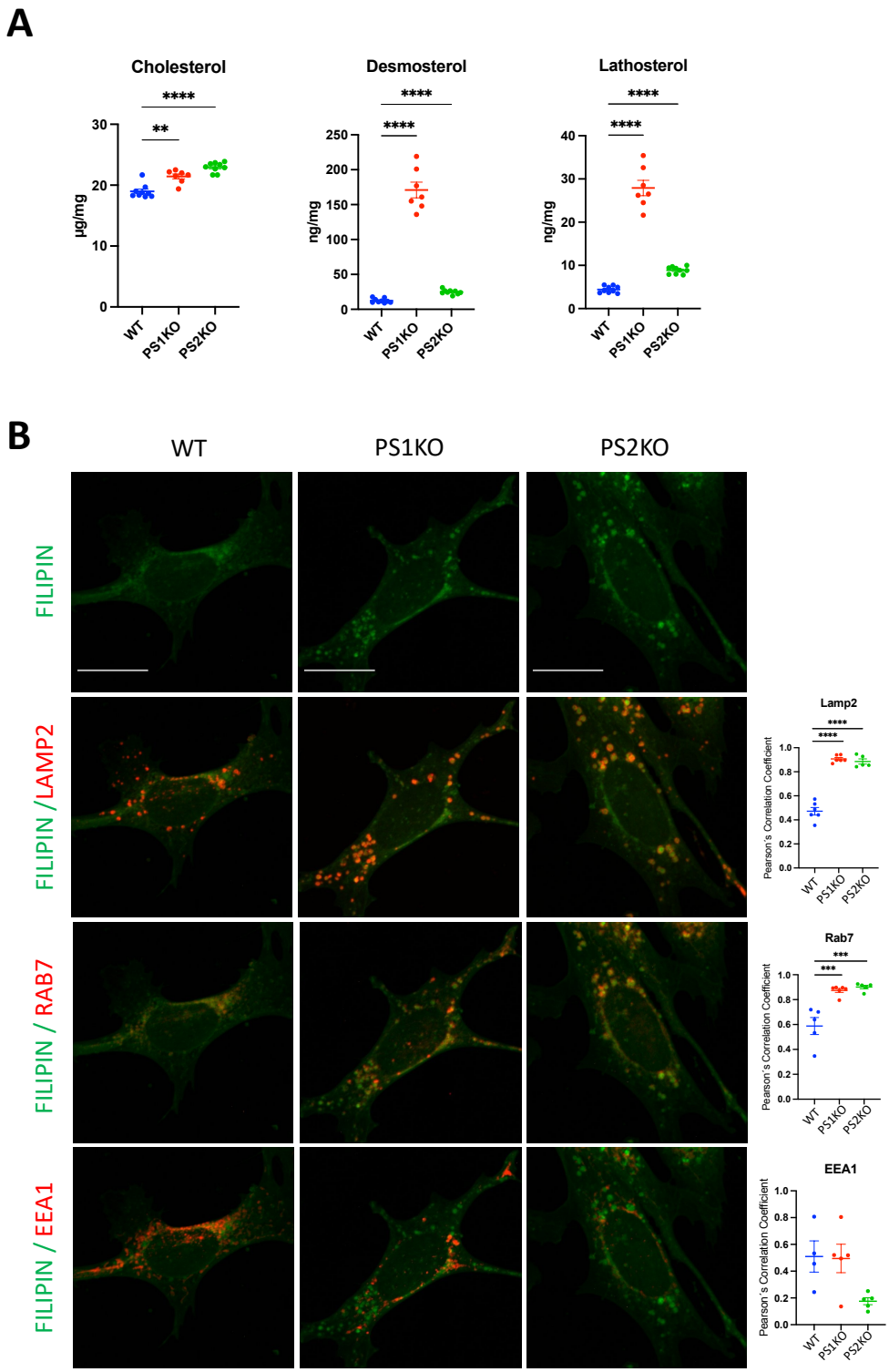

Fig. 4.3: Cholesterol accumulation in PS1- and PS2KO MEFs. A) Cholesterol and its precursors, desmosterol and lathosterol, measured by mass-spectrometry in MEFs WT, PS1- and PS2KO. Brown-Forsythe and Welch ANOVA multiple comparison test, Dunnett

correction; ***, P<0.0005; ****, P<0,0001. B) Representative co-immunostaining of Filipin (green) with Lamp2, Rab7 or EEA1 (red). Scale bar 20 µm. Six pictures per each sample were taken. Graphs show the Pearson´s Correlation Coefficient obtained from 3 independent preparations (n=3). A.U., arbitrary units; ordinary one-way ANOVA with Dunnett´s correction; ***, P<0.0005; ****, P<0,0001.

4.2.2 Altered expression level of cholesterol related proteins in PS KO MEFs

To further dissect the processes that lead to the observed cholesterol accumulation in PS KO MEFs, the expression level of cholesterol metabolism related proteins was analyzed in these cells by western immunoblot analysis (WB; Fig. 4.4 A). Although the general aim was to study the effect of deletion of individual PSs on cholesterol homeostasis, in this experiment, PSDKO MEFs were included. Here, the PSDKO are used as an additional control considering that previous studies from our lab already reported the level of some cholesterol metabolism related proteins in these cells (Tamboli et al., 2008).

The results show an opposite effect regarding the level of Low-Density Lipoprotein receptor (LDLR) between PS1- and PS2KO compared with WT MEFs (Fig. 4.4 B). In particular, lack of PS1, as well as both PSs, increases the level of LDLR, while its expression is decreased in PS2KO cells. Upon deletion of PS1 or both PS, an increase in the expression level of the ATP-binding cassette transporter ABCA1 is also observed. The expression level of the Low-density lipoprotein receptor-related protein 1 (LRP1) is significantly decreased in PS2KO and PSDKO MEFs.

Interestingly, the expression level of Niemann-Pick C1 (NPC1), an intracellular cholesterol transporter that when mutated leads to a lysosomal cholesterol accumulation in neurons, is significantly decreased in PS KO MEFs. Conversely, Niemann-Pick C2 (NPC2) protein, a transporter which acts in concert with NPC1, is increased in PS KO cells compared with WT.

Regarding the Sterol regulatory element-binding protein (SREBP), the precursor protein (Full Length, FL) is anchored in the endoplasmic reticulum and, when the sterol levels in the cell are low, it is cleaved. The resulting amino terminal fragment (NT, N-terminal) migrates into the nucleus where it acts as a transcriptional factor (Sakai et al., 1997; Madison, 2016). The results show that the level of both SREBP-2 forms, FL and NT are increased in the PS KO compared with the WT MEFs. Lanosterol 14a-demethylase (CYP51), that catalyses the demethylation of lanosterol, an essential step of the

cholesterol synthesis (scheme in Fig. 4.18 A), is also significantly increased in PS KO cells. Lanosterol 14a-demethylase (CYP51), that catalyses the demethylation of lanosterol, an essential step of the cholesterol synthesis (scheme in Fig. 4.18 A), is also significantly increased in PS KO cells.

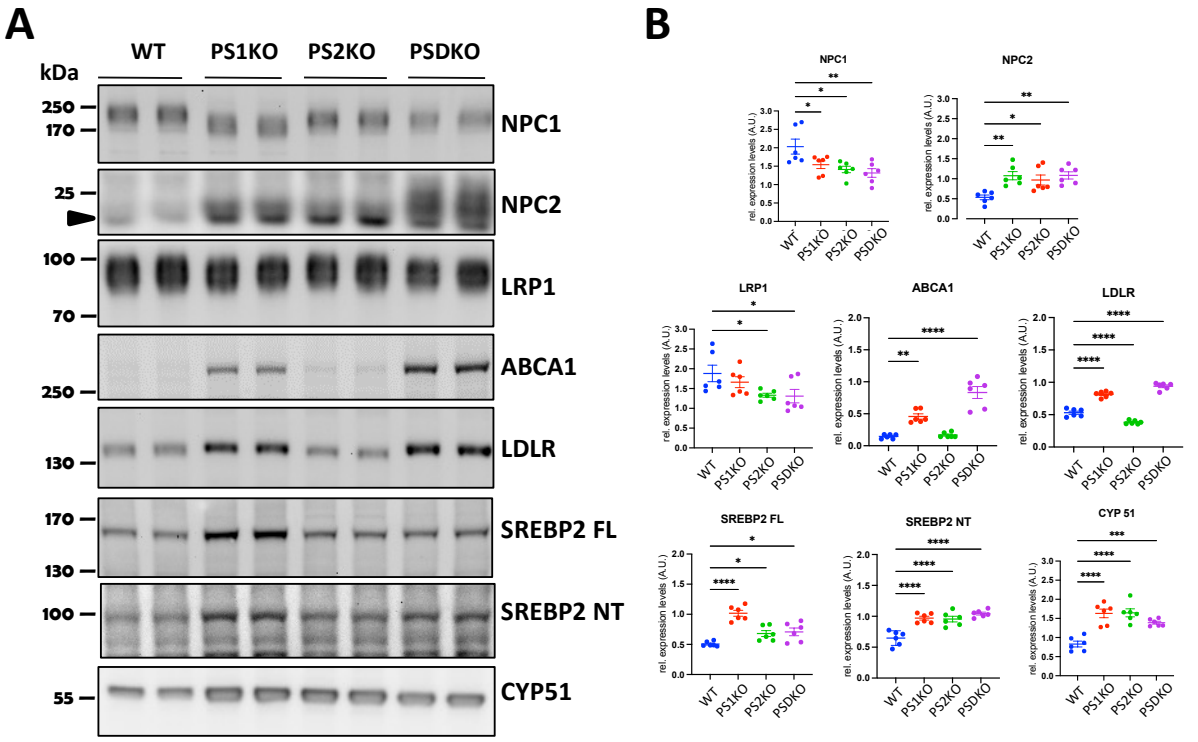

Fig. 4.4: Abnormal expression of proteins related to cholesterol metabolism in PS1- and PS2KO MEFs. A) Representative western immunoblotting of proteins involved in cellular cholesterol metabolism and B) relative quantification. Arrowhead indicates the band relative to NPC2. Signal intensities were normalized to Ponceau. Values were obtained from three independent experiments with two biological replicates (n=3). A.U., arbitrary units; Ordinary one-way ANOVA with Dunnett´s correction; *, P<0.05; **, P<0.005; ***, P<0.0005; ****, P<0,0001.

All together these results suggest that the lipid uptake via LDLR, as well as the cholesterol and phospholipids efflux via ABCA1, is affected by lack of PSs. Moreover, the increased levels of SREBP-2 and CYP 51 indicate an enhanced cholesterol synthesis in all the PS KO cells. In addition, the decreased NPC1 expression level in PS KO MEFs suggests an impairment of cholesterol transport, in particular in the lysosomes, in these cells.

4.3 Protein glycosylation is affected in PS KO MEFs

4.3.1 Altered N-glycosylation underlies differential migration of select membrane proteins from PS KO cells

An interesting aspect that emerged from the previous experiments is that NPC1 band showed a faster migration in SDS gels in PS KO MEFs compared with the WT bands (Fig. 4.4 A). This different migration is more evident in PS1KO MEFs and is observed also in regard to the LRP1 band. NPC1 and LRP1 are N-glycosylated proteins containing in their sequence numerous glycosylation sites (16 for NPC1, 51 for LRP1).

In order to understand if the observed shift of the bands is specific for these proteins or it is a general effect on membrane glycoproteins, the expression of other two glycosylated membrane proteins, N-cadherin and Lamp 2, was analyzed. As shown in figure 5A, an evident difference in the mobility of these proteins was detected in samples from PS KO compared with samples from WT MEFs (Fig. 4.5 A).

The altered migration might be caused by different structures of the glycol moieties and/or differential usage of glycosylation sites. To test this hypothesis, the samples were treated with PNGase F, an enzyme cleaving all the N-linked oligosaccharides from glycoproteins. After treatment, it is possible to observe by WB analysis a faster migration of all the protein bands, as expected, similar among the different genotypes (Fig. 4.5 B).

These results indicate that the altered migration of the protein bands observed in the PS KO MEFs could involve abnormal protein glycosylation and, the fact that different membrane proteins are affected, suggest a general impairment of the N-glycosylation machinery in these cells.

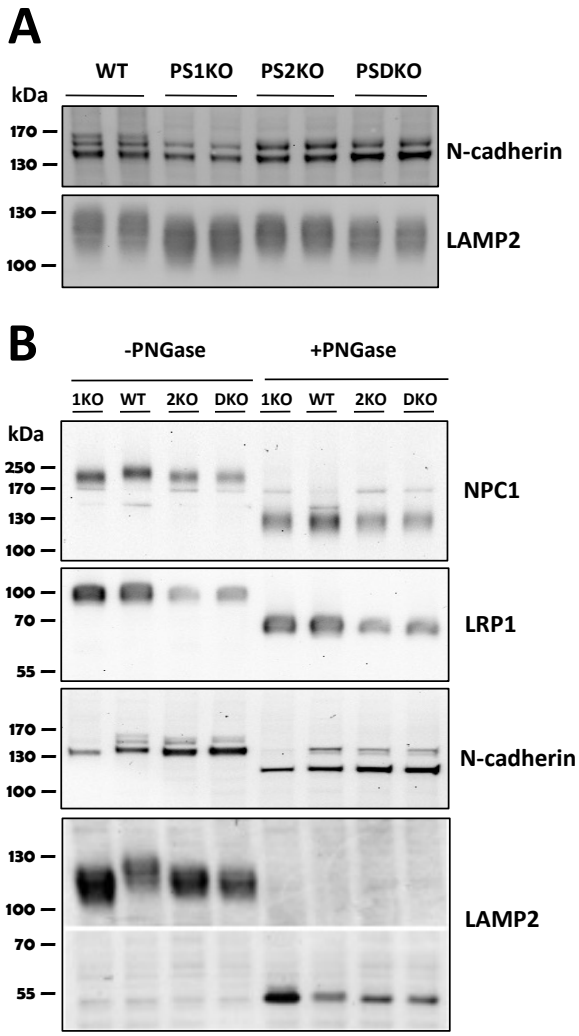

Fig. 4.5: Membrane protein glycosylation is impaired in PS1- and PS2KO MEFs.
A) Western immunoblotting of glycosylated membrane proteins N-cadherin and Lamp2 that shows the shift down of the relative bands in PS KO MEFs compared to WT. B) Membrane fraction samples from MEFs WT and PS KO were exposed to PNGase or water (controls, - PNGase) and applied for western blot to evaluate the migration of the bands after complete cleavage of the glycans.

4.3.2 Mass spectrometry analysis reveals that low mannose glycostructures are decreased in PS KO MEFs compared with WT

Considering the previous observation regarding the general impairment of protein glycosylation in PS KO MEFs, we sought to analyze if the formation of a specific glycostructure is impaired in these KO models. Samples of cellular membranes from WT

and PS KO MEFs were sent to Dr Hirokazu Yagi, Nagoya city University, for mass spectrometry.

The results of Dr. Yagi showed a statistically significant decrease in low mannose glycostructures in PS KO MEFs when compared to WT (Fig 4.6). In particular, the species affected in both PS KO cells, $Man_5GlcNAc_2$ (M5), is the glycostructures with the lower mannose content.

High mannose N-glycans, $Man_9GlcNAc_2$ (M9), are synthetized in the ER and modified by addition of glucose molecules to obtain specific oligosaccharide, ($Glc_3Man_9GlcNAc_2$) that is recognized and transferred by the OST complex to the nascent protein. Once attached to the protein, the ER Mannosidase, MAN1B1, trims the central branch of the mannose residue to produce $Man_8GlcNAc_2$ (M8), and allow the protein to be transported to the Golgi apparatus for further processing of the N-glycan. In the Golgi the MAN1A1, MAN1A2, and MAN1C1 mannosidases trim the mannose residues of M8 to $Man_5GlcNAc_2$ (M5). This last specie is then processed by specific enzymes in the medial and trans-Golgi compartments to obtain oligosaccharide complexes.

The decreased level of M5 N-glycan suggests a defect in the trimming process in PS KO MEFs, but it could have different reason.

Although the mechanism behind this change of glycostructure in PS deficient cells is not clear, these findings support the previous observations of an altered protein glycosylation in PS KO MEFs.

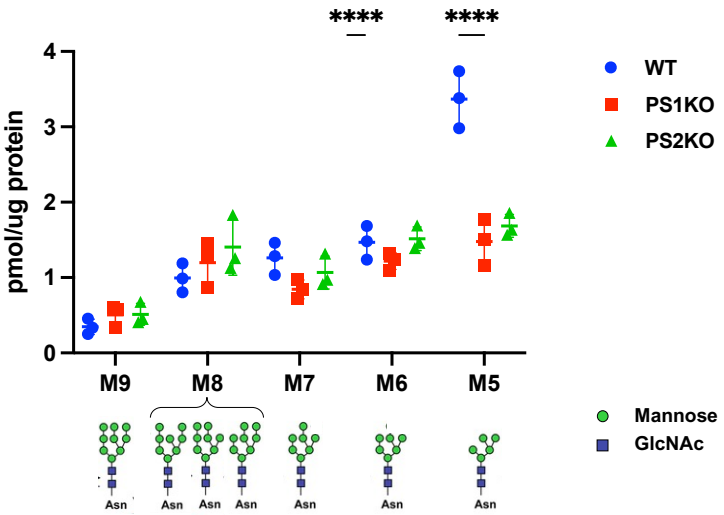

Fig. 4.6: Decreased amount of M5 glycostructure in PS1- and PS2KO MEFs. Graph showing the amount of specific N-glycan structure measured by mass spectrometry. The

results are from 3 independent sample preparations. Ordinary two-way ANOVA with Dunnett´s correction. ****, P< 0.0001

4.3.3 Glycosylation inhibitors treatments in WT MEFs partially mimic the glycoprotein migrational shift observed in PS KO MEFs

Considering that in the previous experiments the mobility shift of the bands is observed in NPC1, LRP1, Lamp2 and N-cadherin, proteins that undergo to *N*-glycosylation, we focused on this process. At the beginning, a precursor oligosaccharide is transferred to the nascent protein in the ER lumen; then the *N*-glycan is processed by several enzymes located in ER and Golgi apparatus.

Using different inhibitors, known to be specific for certain enzymatic step of the process, it was aimed to mimic in the WT the mobility shift observed in the PS KO MEFs.

Four compounds were selected:

- Tunicamycin (TUN); an antibiotic that inhibits the first step in the biosynthesis of N-linked glycans managed by a glycosyltransferase, ALG7, with a possible impairment of the protein folding and transport of the protein through the ER.
- 1-Deoxynojirimycin (DNJ); inhibitor of α-glycosidase I and α-glycosidase II in ER.
- Kifunensine (KIF); inhibitor of endoplasmic reticulum α-1,2-mannosidase I and members of the Golgi subfamily of the class I mannosidases (Golgi α-mannosidase IA, IB, and IC), that prevents the trimming of mannose residues from high mannose N-glycans interfering with the synthesis of complex N-glycans.
- Swainsonine (SW); inhibitor of lysosomal α-mannosidase and Golgi α-mannosidase II.

Tunicamycin treatment is usually limited to 24 hours using high concentration. In order to verify the effect of this treatment in our cell model, the WT cells were treated and collected at different time points using the highest non-toxic drug concentration (2μg/ml). The results show that NPC1 and Lamp2 expression starts to decrease already after 6h treatment with tunicamycin, but no evident changes in the migration of the bands are observed. Regarding N-cadherin, after 6h of treatments it is possible to detect only the signal of the immature, un-glycosylated protein (Fig. 4.7 A).

Because the aim of using glycosylation inhibitors was to mimic in WT MEFs the potential chronic glycosylation impairment observed in PS KO cells and analyze its effect on cholesterol metabolism, a time frame of 6 days treatment was established. To prolong the

Tunicamycin treatment for 6 days, lower concentration of this compound was used. Under these conditions, Tunicamycin treatment leads to a decreased expression and faster migration of the bands representing NPC1, LRP1 and LAMP2. In the case of Nicastrin, the treatment seams to increase the lower band, corresponding to the immature form of the protein. Inhibition of α-glycosidase I and II in ER, by DNJ treatment, induces also a shift of all the protein bands, but effect on the expression level is observed only for LRP1 (Fig 4.7B). Interference with later ER and early Golgi glycosylation by Kifunensine treatment, as well as inhibition of lysosomal and Golgi α-mannosidase by Swainsonine, induced also a downward shift of the bands relative to the examined glycosylated proteins, similarly to what observed in PS KO MEFs, with no decrease in the protein levels except for LRP1 (Fig. 4.7 C).

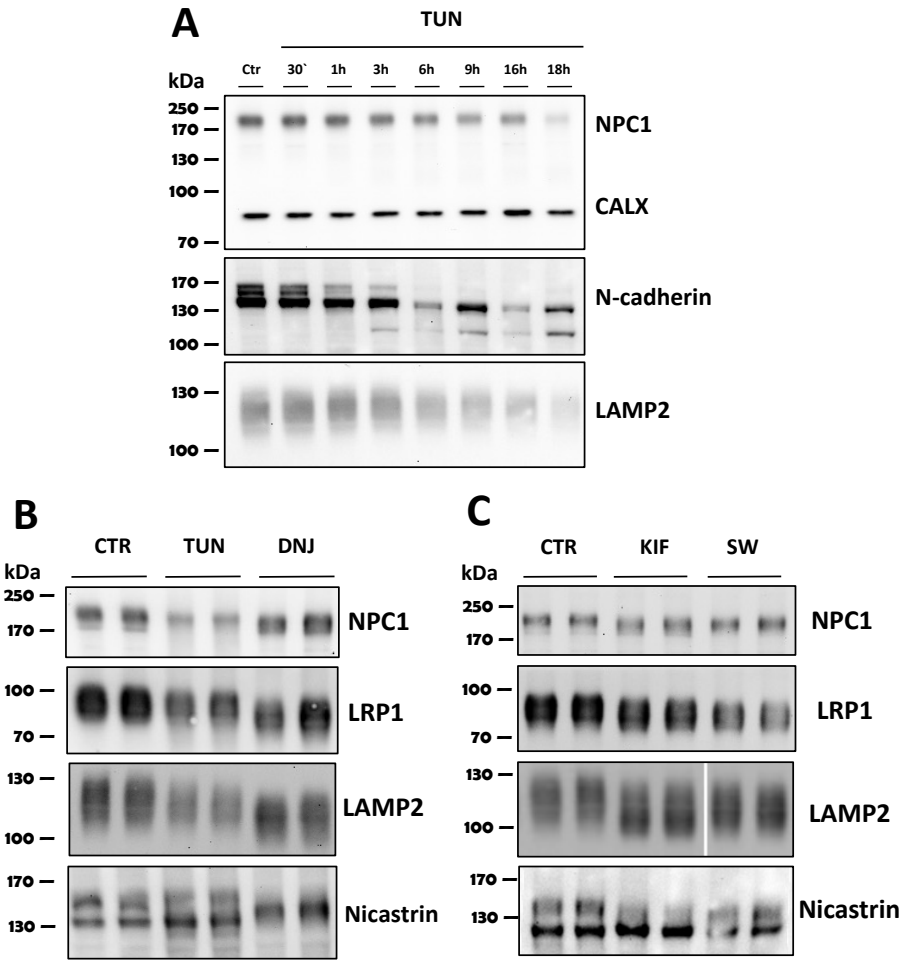

Fig. 4.7: Treatment with glycosylation inhibitors induces a mobility shift of the protein bands in WT MEFs. A) Western immunoblotting of the time dependent effect of TUN (Tunicamycin) treatment at high concentration (2 µg/ml) on glycosylated membrane proteins. B) Representative western immunoblotting of WT MEFs treated for 6 days with

TUN and DNJ (Deoxynojirimycin) at 6 ng/ml and 1 mM respectively or C) with KIF (Kifunensin) and SW (Swainsonine) at 0.1 µM and 0.01 µM. The blots show the mobility shift of the bands as consequential effect of the glycosylation inhibition.

Altogether, treatment of WT MEFs with glycosylation inhibitors partially mimicked altered migration of glycoproteins from PS KO cells, suggesting that PS deficiency impairs glycosylation of membrane proteins and offering a model to investigate the potential consequences of this impairment on cellular cholesterol levels.

4.3.4 Disruption of the initial phase of protein glycosylation in WT MEFs induces the accumulation of cholesterol

In order to understand if impaired protein glycosylation state can alter cholesterol metabolism in MEFs, the effect of glycosylation inhibitors on cholesterol metabolism related proteins was analyzed by WB.

For the treatments, the same experimental design applied previously was followed. Significant changes in the protein levels similarly to that observed in PS KO MEFs were detectable only upon Tunicamycin treatment. In particular, the decrease in NPC1 and the increase of ABCA1, as well as CYP 51 protein levels indicates the importance of protein glycosylation in the expression of key proteins involved in cholesterol trafficking and metabolism (Fig. 4.8 A, B).

Alteration of some of the cholesterol metabolism related proteins expression and/or migration was detectable also upon DNJ treatment, while affection of glycosylation at the Golgi stage, by KIF and SW, had almost no effect on the expression of the tested proteins (Fig. 4.8 C, D). These results indicate that, despite all the compounds used were able to decrease the glycosylation state of the proteins, only interference with the early glycosylation stages occurring in the ER can partially mimic the altered expression of cholesterol metabolism related proteins and their migration in SDS gels as observed in PS KO MEFs.

The next step was to analyze if affection of protein glycosylation can induce accumulation of cholesterol in MEFs. For this purpose, immunostaining analysis using Filipin and markers for subcellular compartments was performed on WT MEFs treated with glycosylation inhibitors.

Analysis of the colocalization between Filipin signal and intracellular vesicles showed that the free cholesterol is accumulating in Lamp2 positive and Rab7 positive compartments only after treatment with Tunicamycin. The other three compounds don't significantly affect cholesterol distribution in these compartments (Fig 4.9 A, B). These results show that, in WT MEFs, blocking protein glycosylation at the early ER stages can induce cholesterol accumulation in endo-lysosomal compartments, thereby phenocopying alterations observed similarly to what was observed in PS KO MEFs.

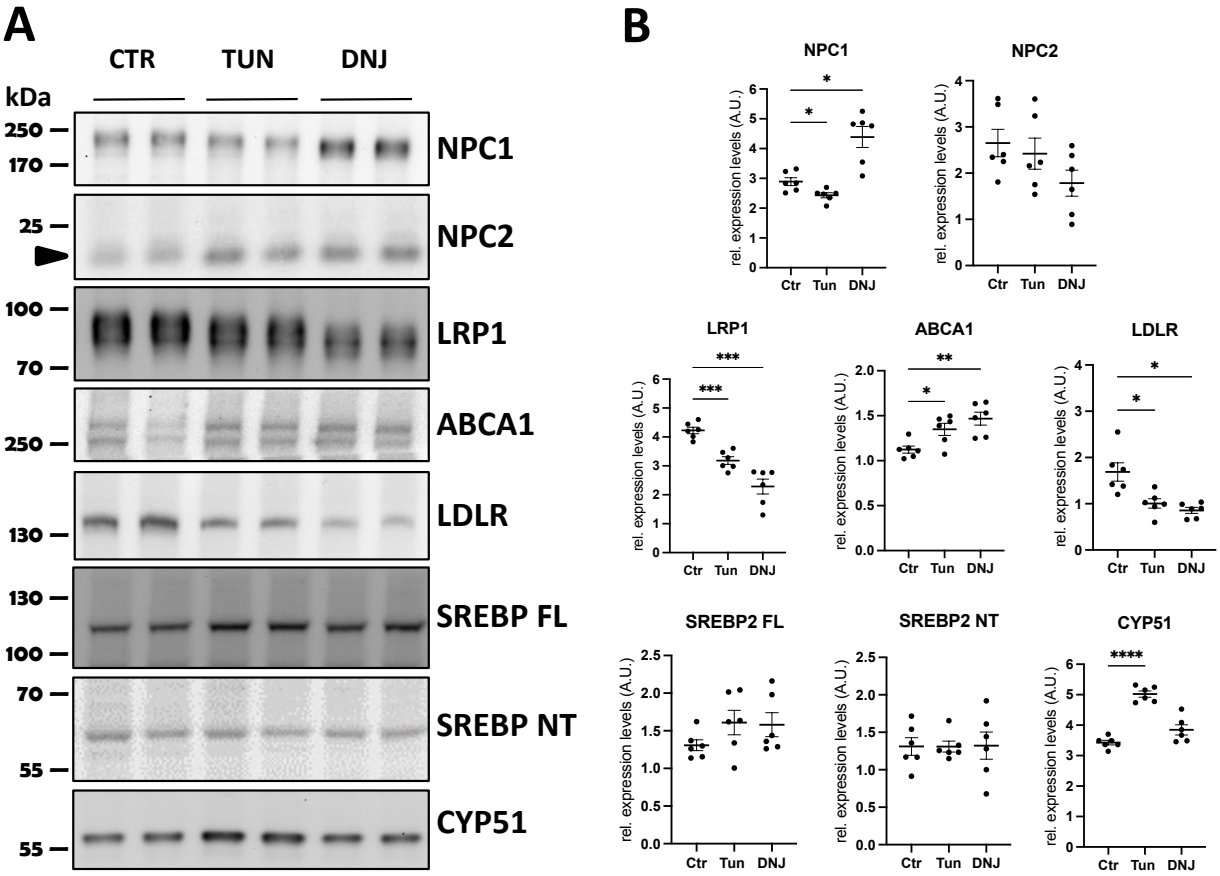

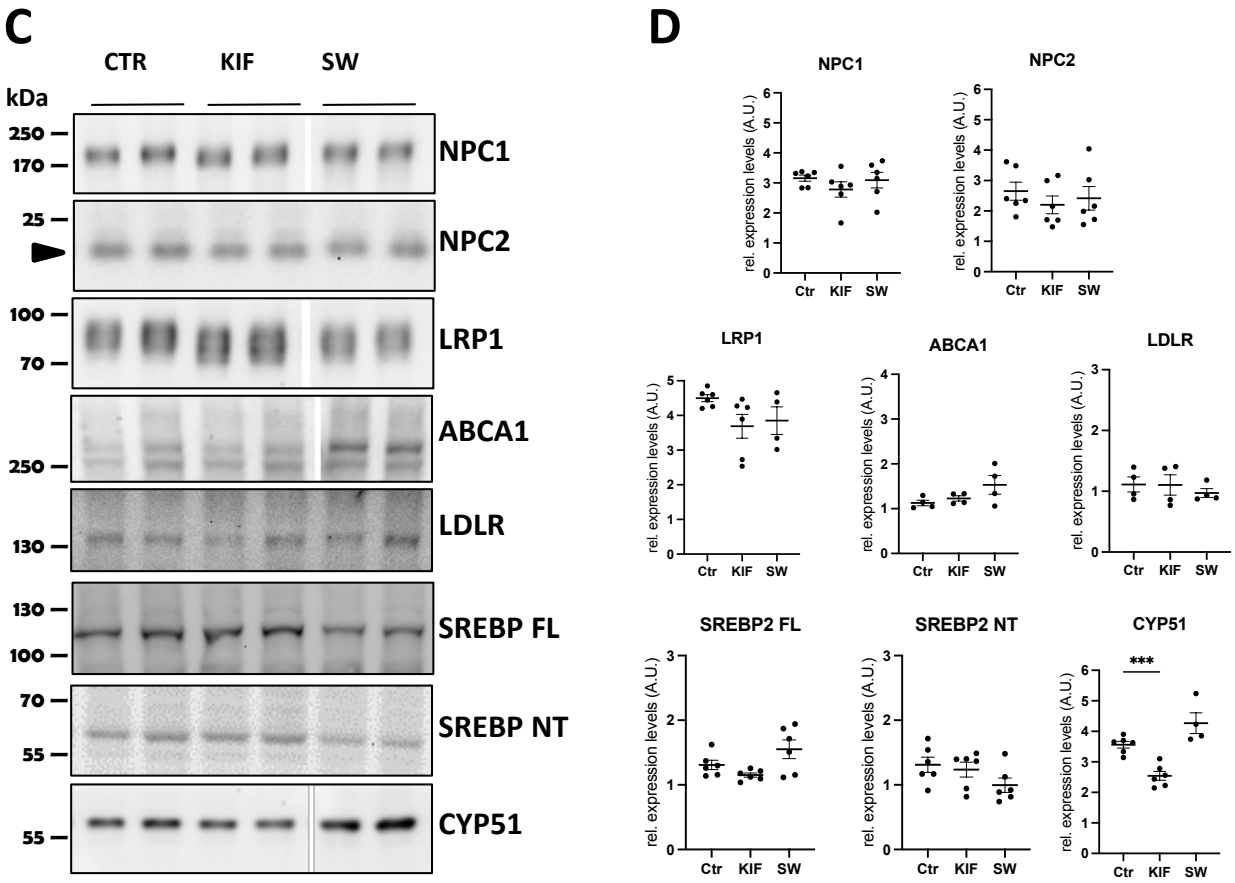

Fig. 4.8: Impairment of protein glycosylation using inhibitors affects cholesterol metabolism in WT MEFs. A) Representative western immunoblotting of the effect of TUN (Tunicamycin) and DNJ (Deoxynojirimycin) treatments on protein related to cholesterol metabolism and B) relative quantification. C) Representative western blotting showing the effect of KIF (Kifunensin) and SW (Swainsonine) treatments on protein related to cholesterol metabolism and D) relative quantification. Arrowhead indicates the band relative to NPC2. Signal intensities were normalized to Ponceau. Values were obtained from three independent experiments with two biological replicates (n=3). AU, arbitrary units; Ordinary one-way ANOVA with Dunnett´s correction; *, P<0.05; **, P<0.005; ***, P<0.0005; ****, P<0,0001.

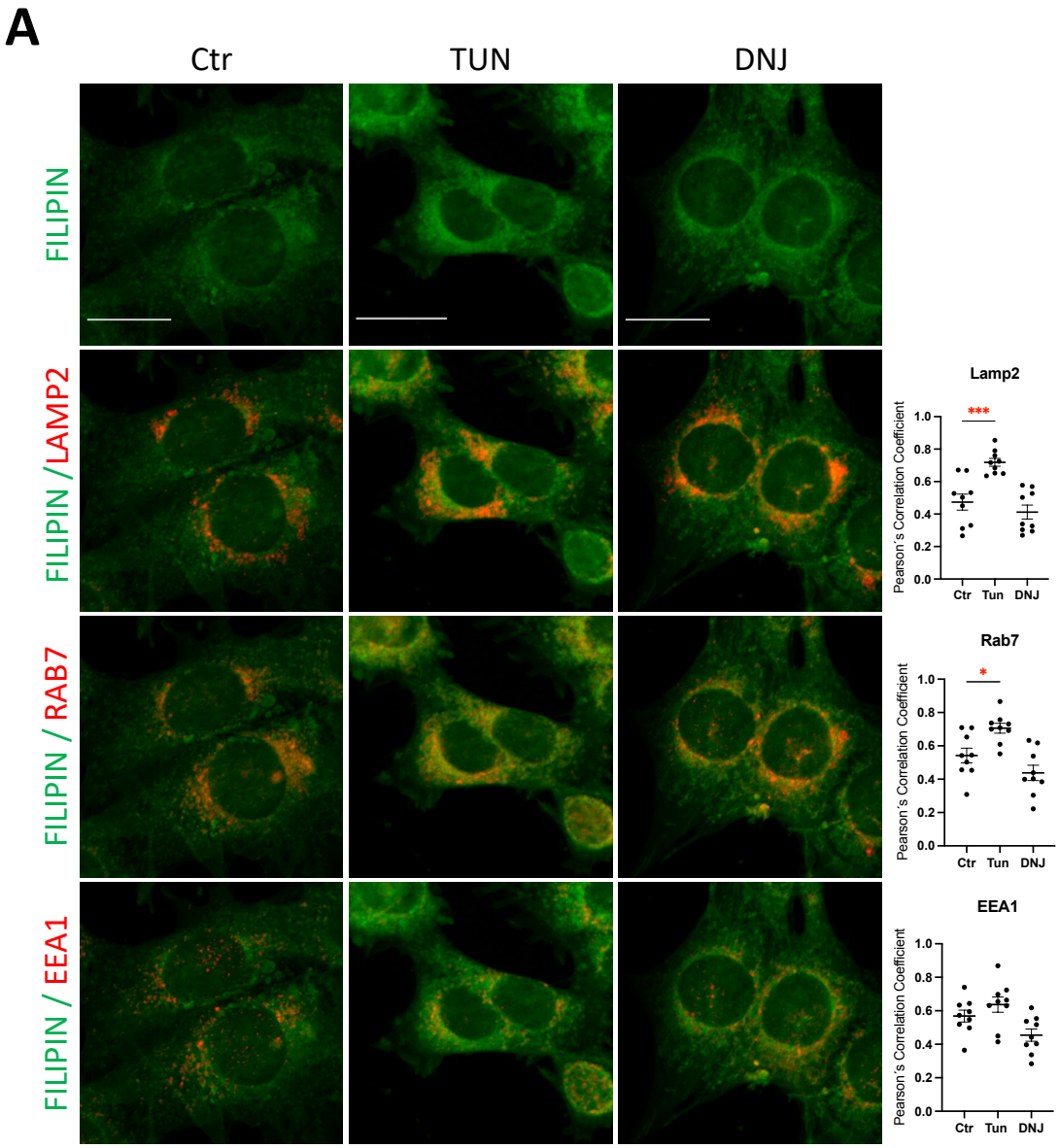
A
Ctr
TUN
DNJ
FILIPIN
FILIPIN /LAMP2
FILIPIN / RAB7
FILIPIN / EEA1
Lamp2
Rab7
EEA1
Pearson's Correlation Coefficient
1.0
0.8
0.6
0.4
0.2
0.0
Ctr
Tun
DNJ
***
*

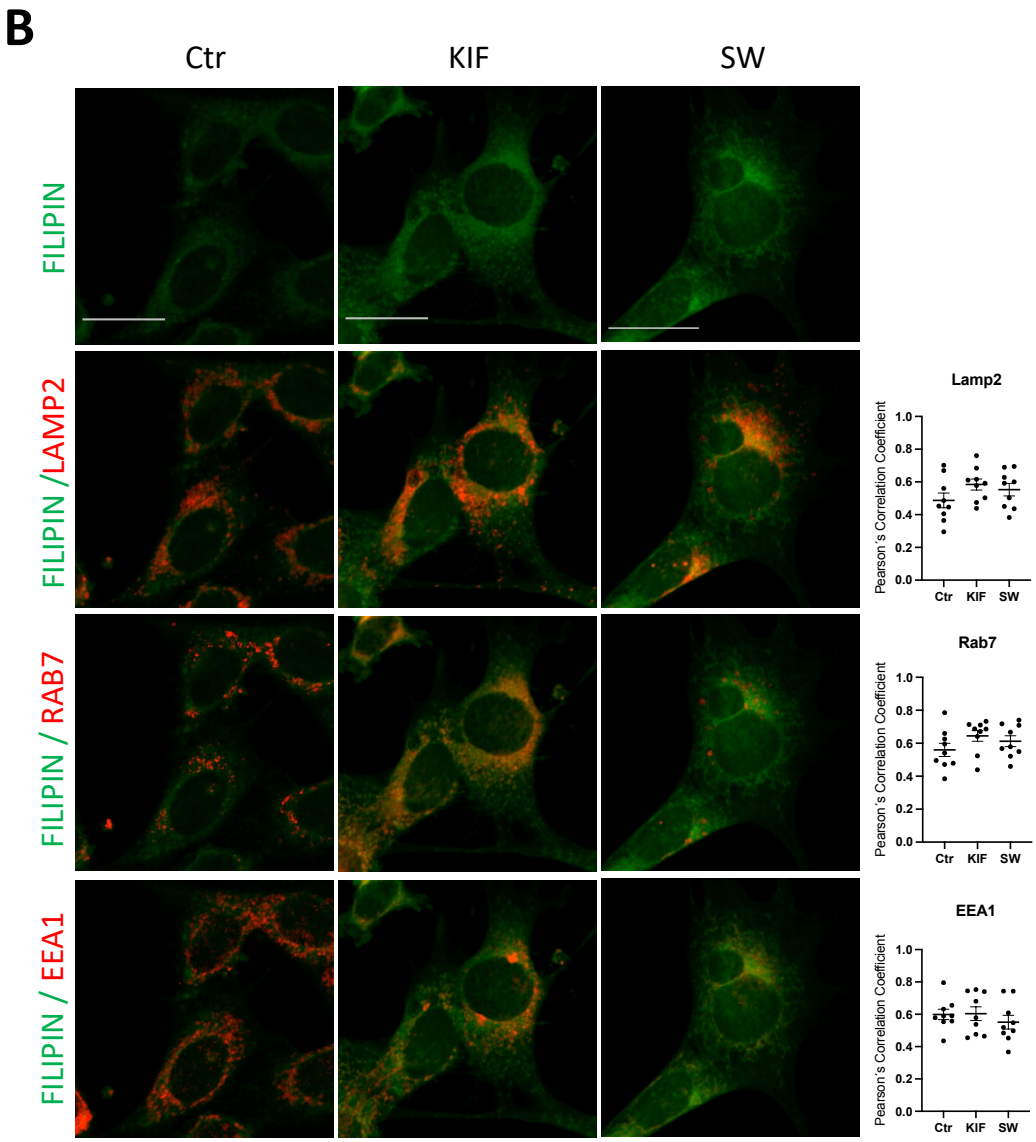

Fig. 4.9: Cholesterol subcellular distribution upon treatments with glycosylation inhibitors in WT MEFs. Representative co-immunostaining of Filipin (green) with Lamp2, Rab7 or EEA1 (red) in WT MEFs untreated (Ctr) or treated with TUN and DNJ (A) or KIF and SW (B) and relative co-localization analysis. Scale bar 20 µm. Six pictures per each sample were taken. Graphs show the Pearson´s Correlation Coefficient obtained from 3 independent preparations (n=3); Ordinary one-way ANOVA with Dunnett´s correction; *, P<0.05.***, P<0.0005.

4.3.5 Inhibition of γ-secretase activity by DAPT does not affect protein glycosylation in MEFs

Presenilins are mostly known for being the catalytic subunit of the γ–secretase complex (De Strooper and Annaert, 2010). Therefore, the absence of one of these proteins, as in

our PS KO models, highly decreases the enzymatic activity of the complex causing an accumulation of the protein substrates.

In order to examine if the reduction of γ-secretase activity can affect protein glycosylation in MEFs, we inhibited the enzymatic complex using DAPT. Although the accumulation of APP C-terminal fragments confirmed the effective inhibition of γ-secretase activity upon treatment, no effects are observed regarding the glycosylation state and the expression level of the examined glycoproteins, NPC1, LRP1 and Lamp2, or expression levels of CYP51 (Fig. 4.10).

These observations suggest that the impairment of protein glycosylation in absence of PS1 or PS2 may be independent from the catalytic activity of the γ -secretase complex and rather related to additional functions of these proteins.

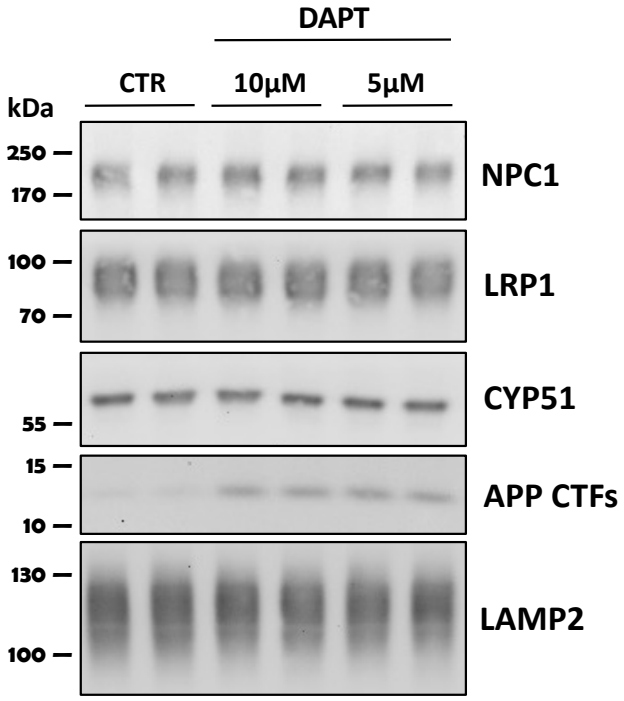

Fig. 4.10 Effect of γ-secretase inhibition on protein glycosylation: Representative western immunoblotting of WT MEFs treated with 10 or 5 μM DAPT for 6 days. Two independent experiments with two biological replicates (n=2) were performed.

4.3.6 Calcium modulators treatments do not affect protein glycosylation in MEFs

Beside the catalytic function in the γ-secretase complex, presenilins are known to be involved in several cellular processes such as calcium homeostasis. It has been demonstrated by several groups, indeed, that mutations or lack of presenilins can alter cellular calcium level, independently from the catalytic activity of the γ-secretase complex, although the specific mechanism is still debated (Yoo et al., 2000; Cheung et al., 2008; Green et al., 2008; Payne et all., 2015).

The results shown above demonstrate that lack of presenilin affects protein glycosylation in MEFs. A perturbation of the cellular calcium levels due to lack of presenilin could be the cause of the observed glycosylation impairment in PS KO MEFs.

To examine this hypothesis, treatments with different compounds, able to perturb the calcium concentration in ER and cytosol or lysosomes, were performed on WT MEFs and the mobility shift of NPC1 was evaluated.

Compounds acting at ER level:

- Thapsigargin (TAPSG); an inhibitor of sarco/endoplasmatic reticulum Ca^{2+} ATPase (SERCA) that impairs the influx of Ca^{2+} into ER;
- 1,1'-diheptyl-4,4'-bipyridinium dibromide (DHBP); an antagonist of ryanodine receptors (RyRs) that inhibits the release of Ca^{2+} from sarcoplasmic reticulum;
- Dantrolene (DANTR); another inhibitor of ryanodine receptors (RyRs)
- Xestospongin C (XEST); an antagonist of IP_3 receptor inhibiting the calcium release from ER.

Compounds acting at lysosomal level:

- Concanamycin A (ConcA); an inhibitor of vacuolar type H+ ATPase activity (v-ATPase) that impairs lysosomal acidification;
- ML-SA1; a lysosomal TRPMLs agonist that inhibits Ca^{2+} release from lysosomes;
- TransNED19 (TNED); an antagonist of NAADP activation of endo-lysosomal TPC2 that inhibits Ca^{2+} release from lysosomes.

Only Concanamycin treatments seams to decrease NPC1 expression level without affecting the migration of the band, but more experiments would be required to support this notion. Alteration of calcium levels in ER or lysosomes, induced by administration of

all the other substances, do not affect NPC1 expression or its glycosylation state (Fig. 4.11).

These observations suggests that the impaired protein N-glycosylation detectable in the absence of presenilins in MEFs may not be related to a perturbation of intracellular calcium homeostasis in these cells.

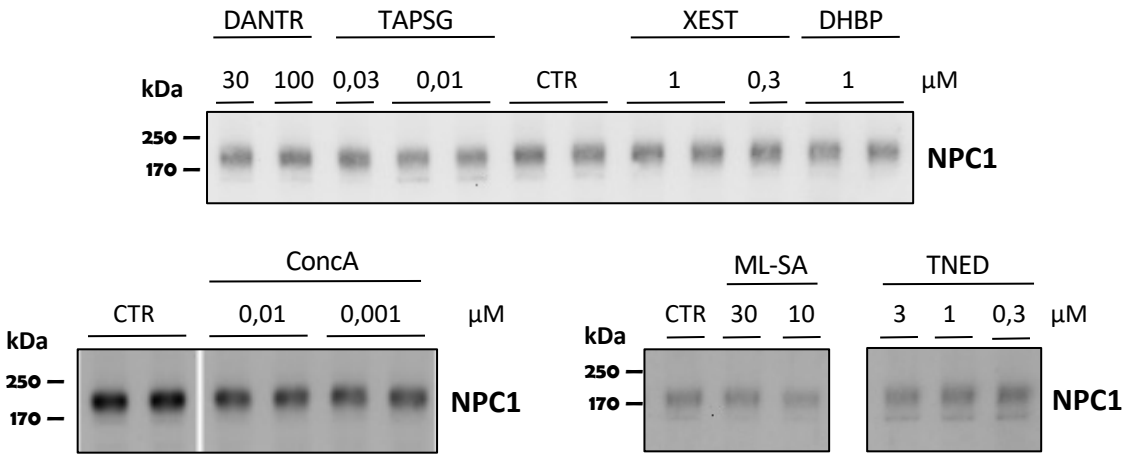

Fig. 4.11: Calcium modulators do not affect NPC1 glycosylation in WT MEFs. Western immunoblotting of WT MEFs treated for 6 days with lysosomal calcium modulator ConcA (Concamycin A), ML-SA, TNED (TransNED) or ER calcium modulator DANTR (Dantrolene), TAPSG (Tapsigargin), XEST (Xestospongin C) and DHBP at different concentrations.

4.3.7 Induced lysosomal cholesterol accumulation by UA18666A does not affect protein glycosylation in MEFs

The present data indicate that lack of presenilins in MEFs is associated with cholesterol accumulation in endo-lysosomal compartments and reduces protein glycosylation. The next step, then, was to investigate the functional relationship between these two events. The results obtained using glycosylation inhibitors, suggest that the altered protein glycosylation observed in PS deficient cells could underlie cholesterol accumulation in these cells. Nevertheless, the possibility of a reverse sequence of events, where a cholesterol dysregulation could affect protein glycosylation, was not excluded. For this reason, lysosomal cholesterol accumulation was induced in WT MEFs to analyze the effect on membrane protein glycosylation. Cells were administered with UA18666A, a compound commonly used to block NPC1 activity and induce lysosomal cholesterol

storage (Elgner et al., 2016). As expected, the treatment on WT cells with UA18666A causes a dramatic cholesterol accumulation in lysosomes (Fig. 4.12 A). In spite of this, no effects are observed regarding the protein level or migration state (Fig. 4.12 B).

These results indicate that cholesterol accumulation in lysosomes, induced by pharmacological inhibition of cholesterol transport, does not lead to altered protein glycosylation in MEFs.

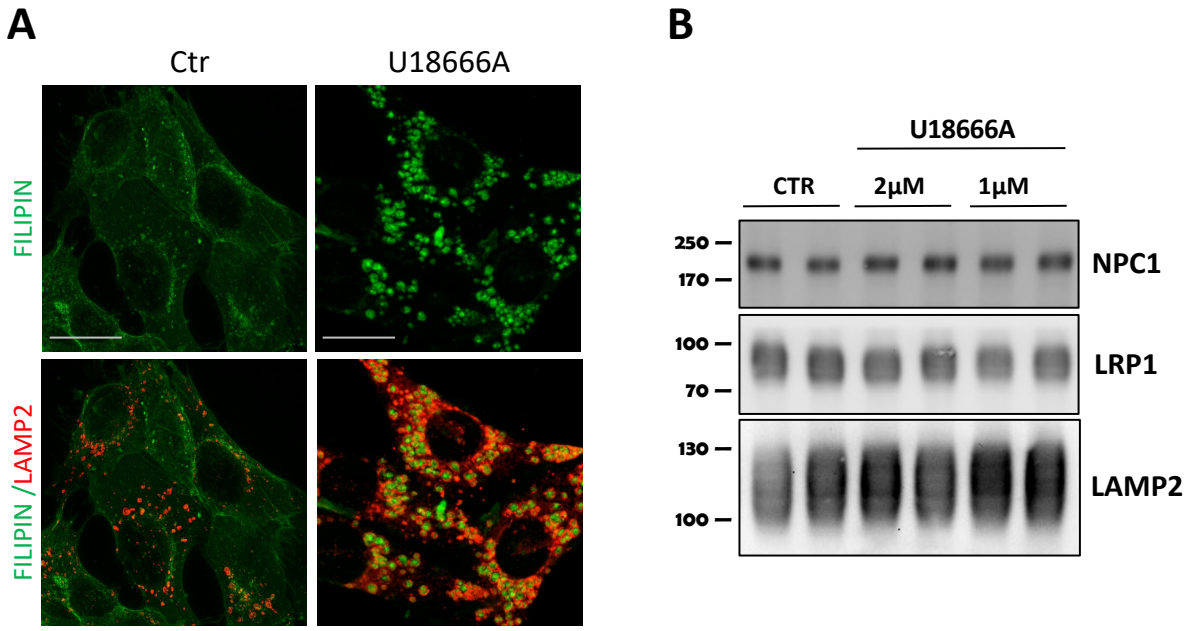

Fig. 4.12: Lysosomal cholesterol accumulation does not affect protein glycosylation in WT MEFs. A) Co-immunostaining of Filipin (green) with Lamp2 (red) in WT MEFs untreated (Ctr) or treated with 2 µM U18666A. Scale bar 20 µm. B) Representative western immunoblotting of the effect of the treatments on glycosylated membrane proteins. Two independent experiments with two biological replicates (n=2) were performed.

4.4 Chaperone inducer Arimoclomol maleate increases NPC1 level and rescues lysosomal cholesterol accumulation in PS-KO MEFs

In PS KO cells, NPC1 level is significantly decreased and its glycosylation state reduced. As mentioned before, NPC1 is a cholesterol transporter and mutations in this protein are known to cause the lysosomal cholesterol storage disorder Niemann-Pick´s type C, associated with neurodegeneration. The significantly decreased level of NPC1 could be, then, the cause of the endo-lysosomal accumulation of cholesterol observed in PS KO

MEFs. To test this hypothesis, the chaperone inducer Arimoclomol maleate was used to increase the NPC1 protein level in PS KO MEFs and then analyze the subcellular cholesterol distribution. As shown in figure 4.13, the treatment increases NPC1 expression and reduces the CYP51 level in both PS KO MEF (Fig. 4.13 A). Moreover, staining of free cholesterol and lysosomes with Filipin and anti-Lamp2 antibodies, respectively, revealed that cell treatment with Arimoclomol maleate, reduced the lysosomal cholesterol accumulation in PS KO cells, and the size of lysosomes (Fig. 4.13 B).

These results show that lysosomal cholesterol accumulation resulting from lack of PSs can be partially normalized by increasing NPC1 protein level and stabilization even if the protein glycosylation state is not rescued. To exclude the possibility that reduction of cholesterol in lysosomes upon Arimoclomol maleate treatment is due to effects on proteins different from NPC1, we used CHO-NPC1 null cells. In this model the chaperone induction treatment failed to reduce the cholesterol storage in lysosomes (Fig. 4.14 A). Interestingly, we found that in absence on NPC1 the level of CYP51 is significantly increased in CHO cells, similar to observations in PS KO MEFs (Fig. 4.14 B).

These data support the assumption that NPC1 impaired glycosylation and folding is involved in the cholesterol phenotype observed in MEFs lacking PS. Considering that NPC1 is responsible for the egress of cholesterol from the lysosomes to the ER, an impairment of this function can affect the ER sensing of cholesterol level and be implicated in the induction of the *de novo* cholesterol production.

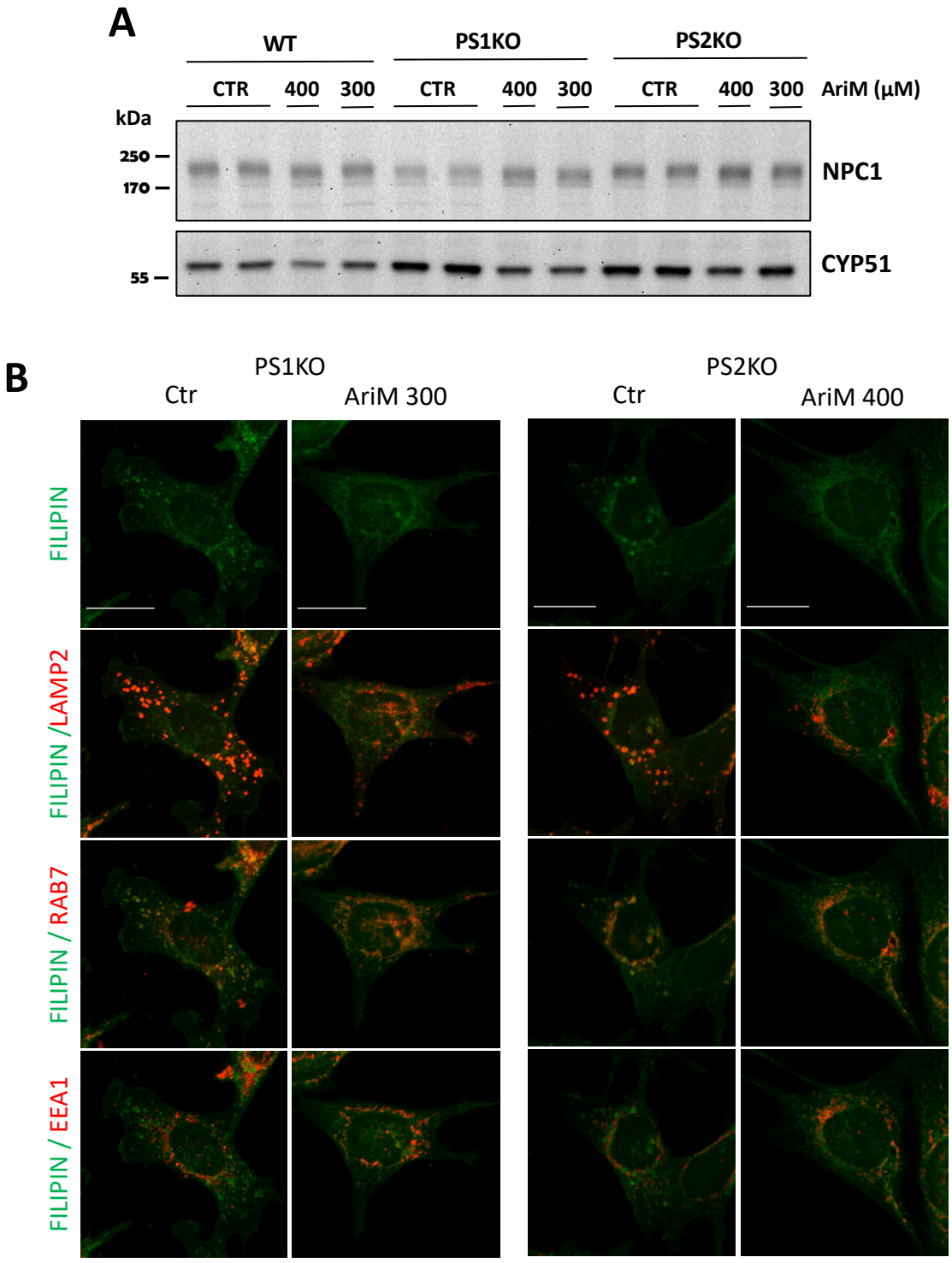

Fig. 4.13: Chaperon inducer treatment increases NPC1 expression and reduces lysosomal cholesterol sequestration in PS KO MEFs. A) Representative western blotting showing the effect of Arimoclomol maleate (AriM) treatments on protein expression in WT, PS1 and PS2 KO MEFs. Two independent experiments (n=2) were performed. B) Co-immunostaining of Filipin (green) with LAMP2, RAB7 or EEA1 (red) in

PS KO MEFs untreated (Ctr) or treated with AriM. Two independent experiments (n=2) were performed. Scale bar 20 µm.

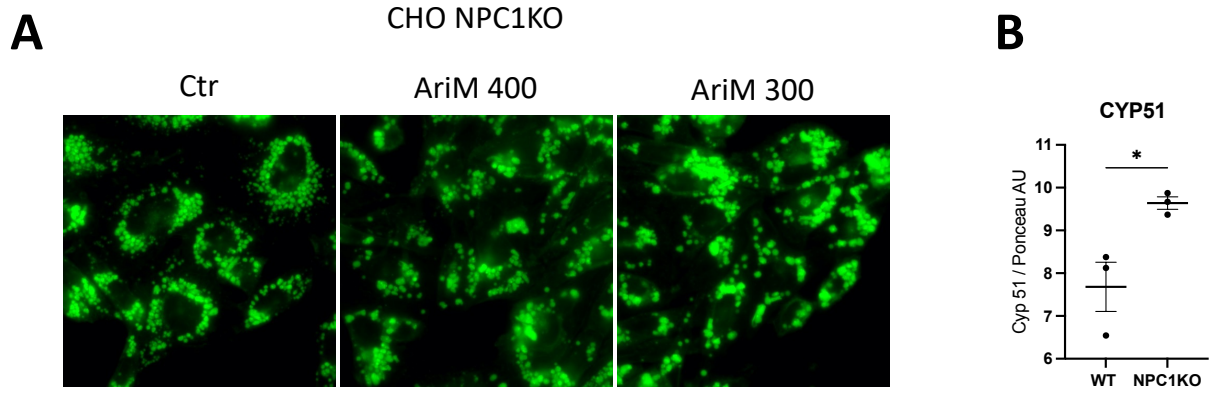

Fig. 4.14: Chaperon inducer treatment failed to reduce cholesterol accumulation in NPC1KO CHO cells. A) Immunostaining of Filipin (green) in CHO NPC1KO untreated (Ctr) or treated with Arimoclomol maleate. B) Quantification of WB relative to CYP51 expression level in CHO WT and NPC1KO. Three independent experiments (n=3) were performed. Signal intensities were normalized to Ponceau. Unpaired t test; *, P <0.05.

4.4.1 Overexpression of NPC1 in PS KO MEFs rescues the lysosomal cholesterol accumulation in PS-KO MEFs

The previous results show an involvement of NPC1 transporter in endo-lysosomal cholesterol accumulation upon PS deletion. In order to further test whether reduced level of NPC1 is the cause of the abnormal cholesterol distribution in PS KO MEFs, the protein was overexpressed in PS1 and PS2 KO cells. A construct encoding NPC1-eGFP was transiently expressed in PS1 and PS2 KO MEFs and visualized by immunofluorescence microscopy. NPC1-eGFP appears mainly in the lysosomes indicating that the protein is correctly processed and reached the expected functional localization. Co-staining with Filipin revealed decreased lysosomal cholesterol accumulation selectively in NPC1-EGFP expressing as compared with the non-transfected neighboring cells (Fig. 4.15).
These observations are consistent between PS1 and PS2 KO MEFs, strongly supporting the involvement of NPC1 in endo-lysosomal cholesterol accumulation in both PS1 KO and PS2KO cells.

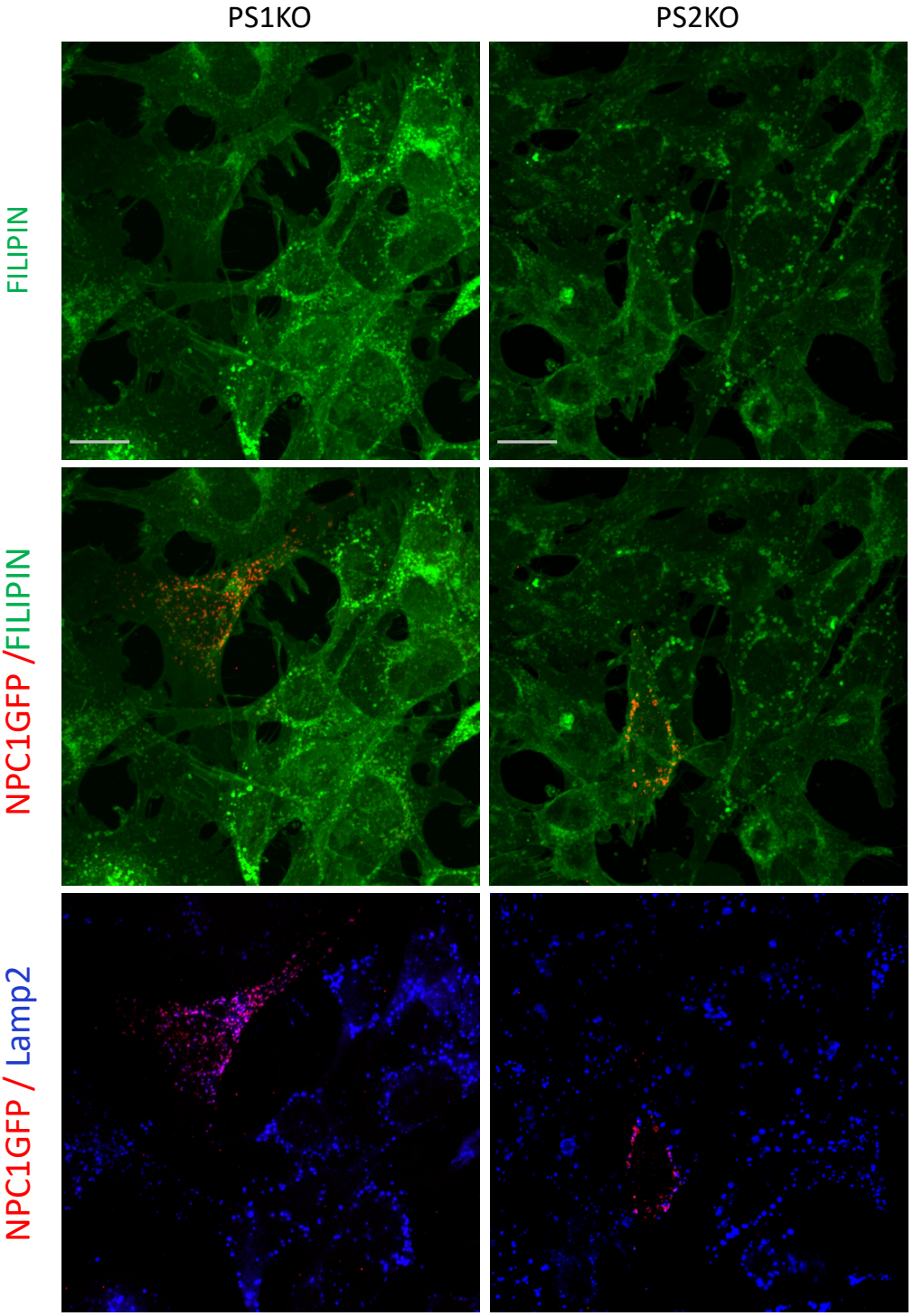

Fig. 4.15: NPC1 overexpression rescues the lysosomal cholesterol accumulation in PS1- and PS2KO MEFs. Representative immunostaining of Filipin (green) with NPC1His-EGFP construct (red) and LAMP2 (blue) in PS1 and PS2KO MEFs. Two independent experiments and six pictures per condition were taken. Scale bar 20µM.

4.5 Expression profiling in PS-KO MEFs

The data, so far, indicate that in MEFs lacking PS1 or PS2, reduced protein N-glycosylation and impaired NPC1 function leads to cholesterol accumulation in endo-lysosomal compartments and increased cholesterol biosynthesis.

To further examine effects of PS1 and/or PS2 deficiency on gene expression, 3´mRNA sequencing was performed. Samples from two independent library preparations were analyzed and the initial quality control process shows negligible batch effect, and clustering by genotype (Fig 4.16). Samples from PSDKO are most closely related to PS1KO implying that the gene expression pattern of the PSDKO is mostly determined by the lack of PS1. Of all the detected mRNAs (17812, 16646 and 18390 in PS1, PS2 and PSDKO MEFs, respectively), the levels of 8101 mRNAs in PS1KO, 7423 in PS2KO and 7423 in PSDKO were significantly changed compared to WT MEFs. This initial observation demonstrates that lack of presenilins dramatically affects gene expression in MEFs.

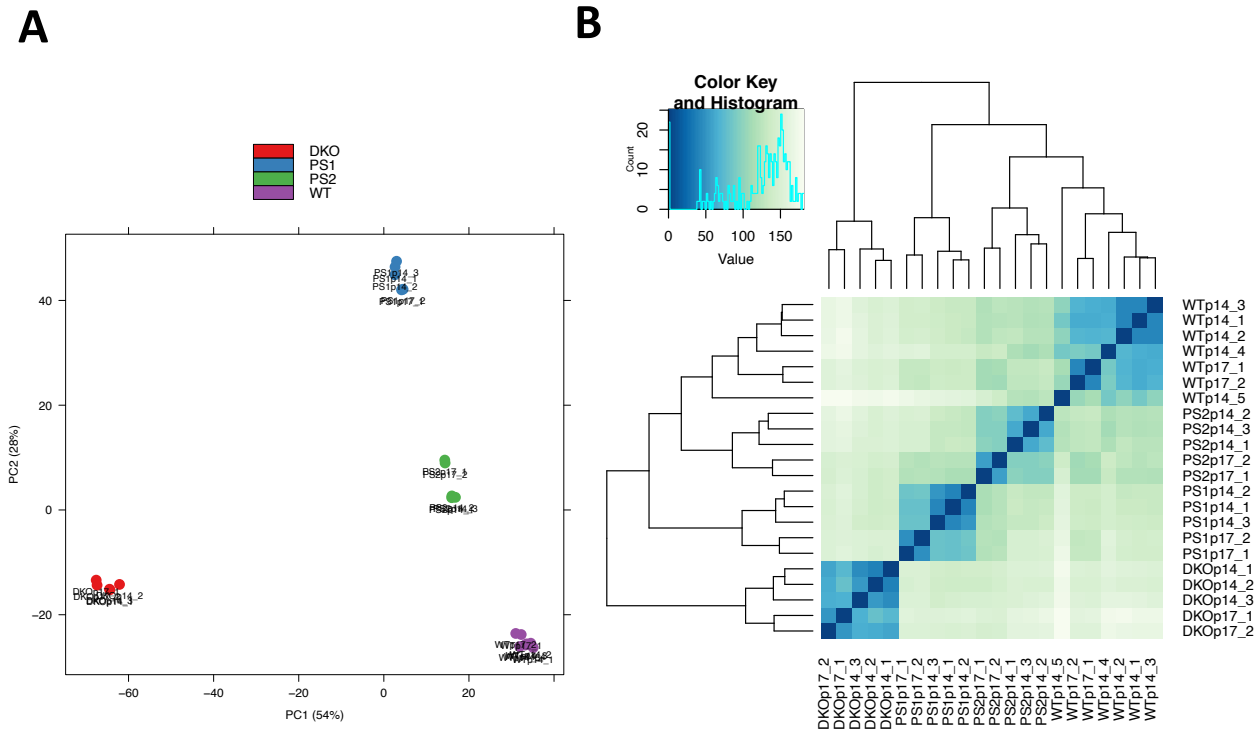

Fig. 4.16: Quality control of the samples applied for 3´mRNA sequencing shows a group-wise clustering. A) Principal components analysis-plot (PCA-Plot) and B) hierarchical clustering of samples showing the distribution of the different genotypes. P14 and P17 denote cells harvested at passages 14 and 17, respectively.

Although the amount of data resulting from this experiment offers numerous possibilities to investigate the changes in different cellular pathways, the analysis was focused on the cellular processes relevant for the current investigation: cholesterol metabolism and protein N-glycosylation.

A first analysis regarded the expression of the proteins involved in cholesterol metabolism. In particular, the mRNA levels relating to the proteins previously examined via western blot analysis were checked. As shown in the heatmaps, some of the analyzed genes, such as *Abca1, Npc1* and *Cyp51*, exhibit the same trend observed at the protein level indicating a regulation already at the mRNA level (Fig. 4.17).

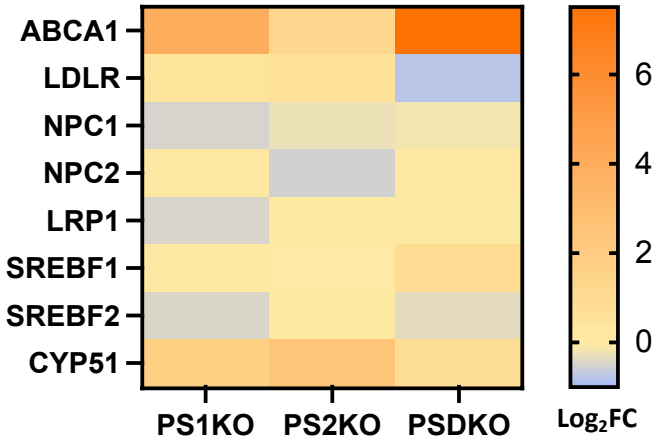

Fig. 4.17: Differential expression of proteins involved in cellular cholesterol metabolism in PS KO MEFs. Heatmap of differentially expressed genes in PS KO MEFs (average of 5) compared to WT (average of 7). Up-regulated and down-regulated genes are indicated in orange and blue, respectively.

Next, the expression of enzymes involved in cholesterol biosynthesis was analyzed using a KEGG pathway (map00100) as a reference (Fig. 4.18 A). Expression of all considered genes is represented in the heatmap, while the significant changes ($P < 0.05$) of PS KO MEFs compared to WT are shown in the graph as Log2fold changes (Fig. 4.18 B, C). What appears clear from these results is that the expression of genes involved in cholesterol synthesis is differentially affected by the PS genotype. Most changes were detected in PS1KO and PSDKO cells. PS2KO cells showed much less changes in the mRNA expression of cholesterol metabolism related genes. Notably, a significant upregulation of *Cyp51* was detected in all three PS KO genotypes indicating an enhanced

cholesterol production in line with the previous results from mass spectrometry regarding the levels of cholesterol and its precursors. Also, *Soat1* and *Soat2* levels are reduced in PS KO cells compared to the WT meaning that the cholesterol storage mechanism is downregulated.

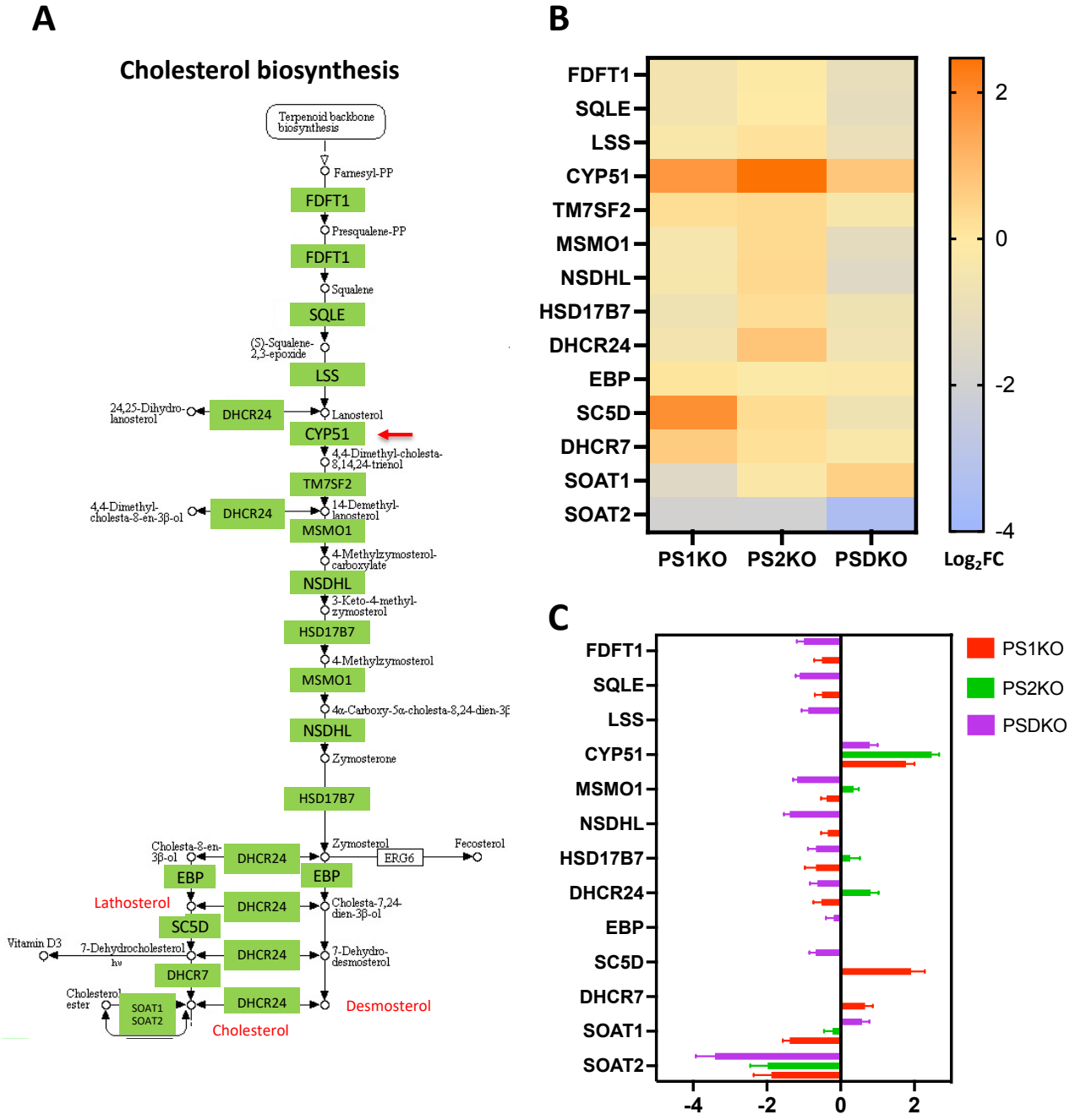

Fig. 4.18: Differential expression of mRNAs of enzymes involved in cellular cholesterol synthesis in PS KO MEFs. A) Scheme modified from KEGG pathways (map00100) showing the enzymatic steps of cholesterol biosynthesis. B) Heatmap of

differentially expressed genes in PS KO MEFs (average of 5) compared to WT (average of 7). Up-regulated and down-regulated genes are indicated in orange and blue, respectively. C) Significantly changed genes (P <0.05). Graph reporting the Log2fold change ± SEM in KO MEFs compared to WT.

For expression analysis of protein glycosylation related genes, the N-glycan biosynthesis KEGG pathway (map00510) was used as a reference. This pathway can be divided into four sub-pathways: N-glycan precursor biosynthesis; N-glycosylation by oligosaccharyl-transferase; N-glycan precursor trimming and complex type N-glycan biosynthesis. Each of these sub-pathways involves different enzymes. An overview of this complex process is shown in Fig. 4.19 A.

Expression of all considered genes is displayed in the heatmaps, while the genes among them with significantly changed expression (P <0.05) are shown in graphs (Fig. 4.19 B, C).

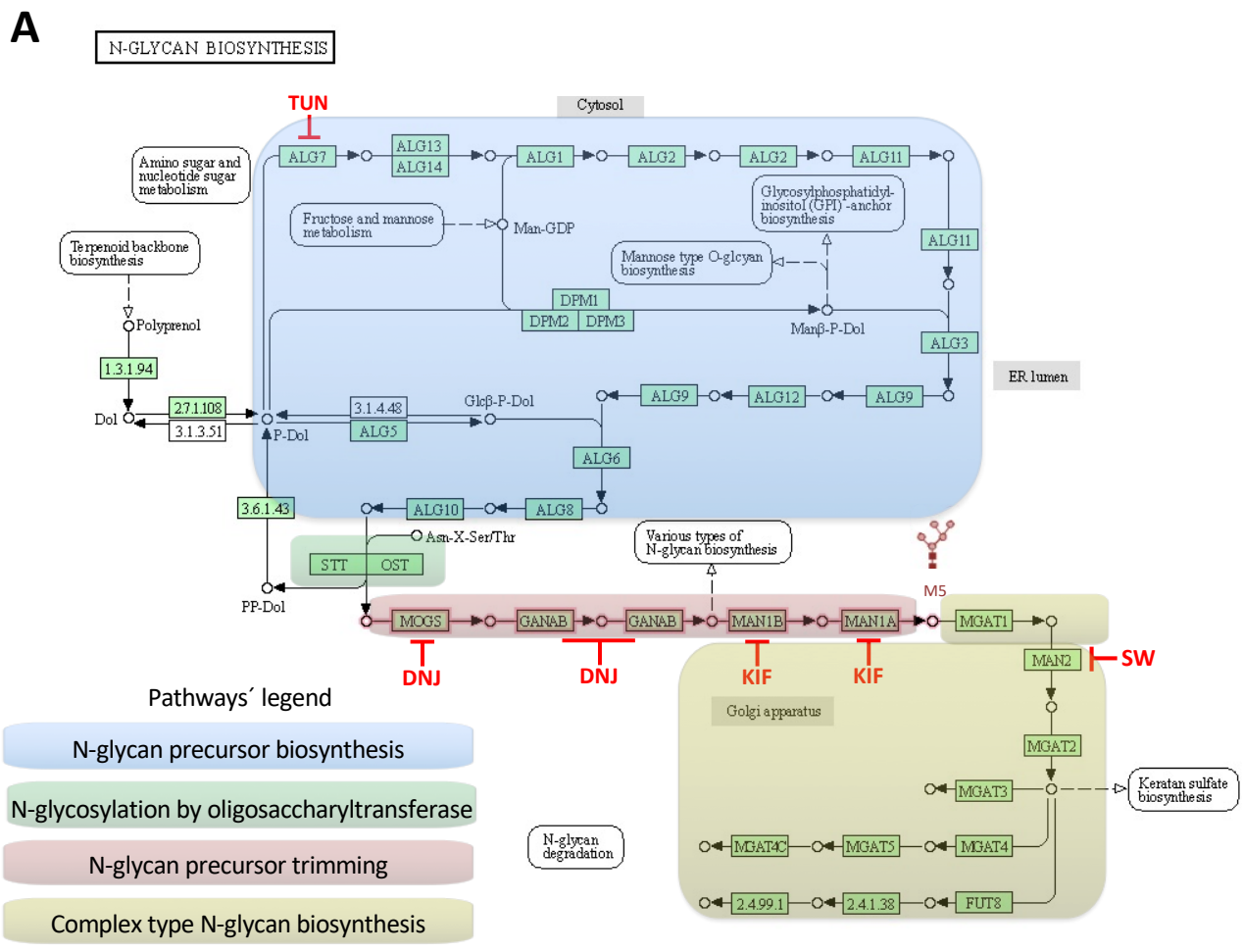

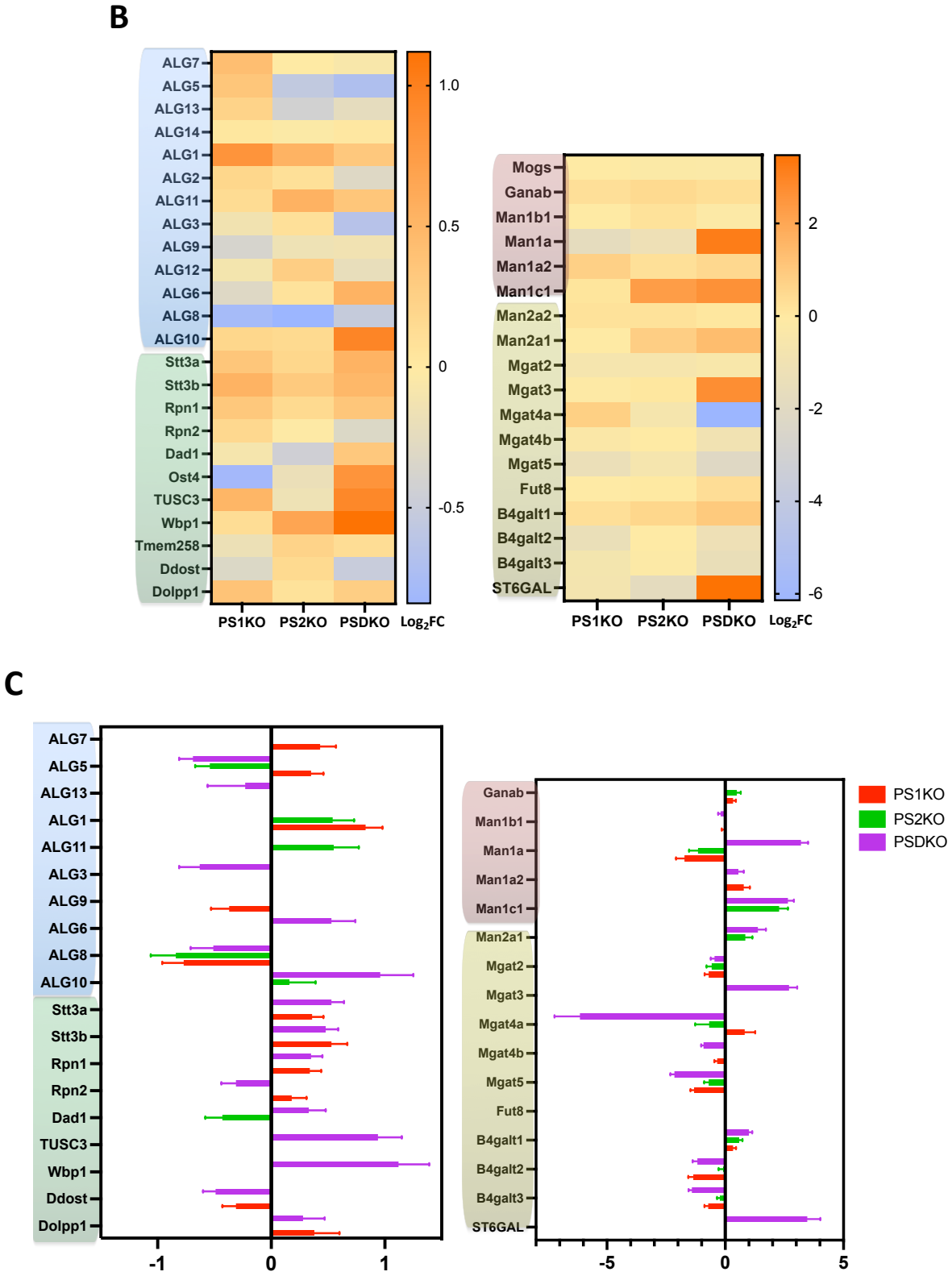

Fig. 4.19: Differential expression of mRNAs of enzymes involved in N-glycan precursor biosynthesis in PS KO MEFs. A) Scheme modified from KEGG pathways (map00510) showing the enzymatic steps of N-glycan biosynthesis. The different sub-

pathways are listed in the legend and highlighted using a color code. M5 N-glycan species is reported in correspondence with the enzymes responsible for its synthesis. Glycosylation inhibitors and relative target enzymes are indicated in red. B) Heatmap of differentially expressed genes in PS KO MEFs (average of 5) compared to WT (average of 7). Up-regulated and down-regulated genes are indicated in orange and blue, respectively. The different sub-pathways are highlighted using a color code. C) Significantly changed genes ($P < 0.05$). Graph reporting the Log2fold change ± SEM in KO MEFs compared to WT. The different sub-pathways are highlighted using a color code.

Although expression of genes related to cholesterol metabolism appeared to be similar between PS1KO and PSDKO MEFs, a divergent effect, with most of the genes having an opposite regulation between these two genotypes, is observed regarding N-glycan biosynthesis. Nevertheless, the results show a consistent decrease, across genotypes, in the mRNA level of the ALG8 enzyme, involved in the formation of specific oligosaccharide, ($Glc_3Man_9GlcNAc_2$) that is recognized and transferred to the nascent protein.

The transfer of the newly synthetized N-glycan to the nascent proteins involves two complexes, STT and OST. Each of them consists of several subunits whose level has been analyzed individually. PS1KO and PSDKO showed predominantly an up-regulation of the mRNA levels of STT and OST complex components, while PS2KO cells have very similar expression of these genes compared to WT.

After the attachment to the protein, the N-glycans undergo the trimming process during which two glucose residues are removed. This step happens in the ER and Golgi compartments and it is fundamental for recognition by the protein quality control machinery. Most of the enzymes involved in the trimming pathway were the targets for the glycosylation inhibitors in prior experiments (Fig. 4.7, 4.8, 4.9). The results show that genes encoding the enzymes targeted by DNJ treatment are not significantly changed (*Mogs*), or even upregulated (*Ganab*) in PS1 and PS2KO MEFs compared to WT. The fact that DNJ treatment failed to mimic the cholesterol accumulation observed in PS KO may be due to the fact that activity of these enzymes is not involved in causing the PS phenotype. A similar explanation can be found regarding Kifunensin treatment. In fact, although the expression of one of the gene inhibited by Kifunensine, *Man1a*, is significantly decreased in PS1 and PS2KO MEFs, the expression of its second target, *Man1b*, is not affected by lack of PS. Assuming that a decrease in mRNA expression

corresponds to a reduction in the enzyme levels and therefore their activity, it is possible that Kifunensin treatment only partially can mimic the conditions observed in PS KO MEFs.

Despite these considerations regarding the inhibitor treatments, it is interesting to notice the significant decrease in the *Man1a* level in PS1 and PS2KO MEFs compared to the WT cells. An opposite effect is observed in PSDKO where expression of this enzyme is upregulated. The function of this MAN1A is to trim the M9 species, in the Golgi compartment, in order to obtain M5 so a decrease in this process, at least in PS1- and PS2KO MEFs, could reflect a decrease in the substrate.

The last sub-pathway of the N-glycan biosynthesis analyzed is the formation of complex type N-glycans. This process takes place entirely in the Golgi compartment and the initial step, for which the MAN2 enzyme is responsible, is the one inhibited by Swainsonine treatment. The expression of *Man2a2* is not significantly changed in PS KO MEFs compared to the WT, while the *Man2a1* mRNA level is rather increased in PS2 and PSDKO. Once more this could be the reason why the inhibition of these enzymes by Swainsonine failed to reproduce the PS KO phenotype in WT MEFs. Regarding the overall expression of genes included in this pathway, it can be noticed that the biggest effect concerns PSDKO with most of the genes showing a reduced mRNA expression and some an increased expression level.

Data obtained from the expression profiling of PS KO MEFs show an additional proof that lack of PS affects expression of genes related to cholesterol metabolism and N-glycosylation processes. Although the changes in mRNA levels do not necessarily correlate to changes in the corresponding protein levels, it was possible to observe the same variation regarding NPC1 and CYP51 proteins in PS KO compared to WT MEFs, confirming their regulation already at the mRNA level.

Also, regarding the protein N-glycosylation, the results show that PS deficiency changes expression of genes involved in this process with a different regulation between PS1 and PS2KO, most of the time. Complete deletion of both PS shows different results meaning that the lack of both PS does not necessarily result in additive effects of the single PS deletion. Although data obtained from the 3´mRNA sequencing, did not fully elucidate the mechanism connecting PS to protein glycosylation, they offer an important and interesting

addition to the previous experiments. In particular, they provide the opportunity to have a more complete overview of this complex cellular process.

5. Discussion

The present work revealed that genetic deletion of presenilin genes affects cholesterol homeostasis *in vivo* and *in vitro*. This work shows that mice with genetic deletion of presenilins displayed a significant increase in neuronal cholesterol levels in cortex and hippocampal area CA1. Similarly, cultured fibroblasts with genetic inactivation of presenilins showed increased cholesterol levels, specifically free cholesterol accumulating within endo-lysosomal compartments. In line with these observations, expression of proteins associated with cholesterol metabolism was altered. For example, CYP51 a key enzyme involved in cholesterol *de novo* synthesis, was upregulated in PS KO cells along with its mRNA as measured by 3´RNA sequencing. On the contrary, the level of the cholesterol transporter NPC1 was significantly decreased. N-glycosylation of NPC1 (and also other N-glycosylated proteins) was impaired, most likely decreasing its function. Interfering with NPC1 N-glycosylation in WT MEFs through the application of Tunicamycin reduced NPC1 expression, increased CYP51 protein levels, and led to accumulation of lysosomal cholesterol to a similar extent as in PS KO MEFs. Conversely, a chemical chaperone that is known to enhance NPC1 expression, increased its protein abundance in PS KO MEFs. It also reduced CYP51 expression and normalized lysosomal cholesterol levels. Along the same lines, NPC1 overexpression reduced lysosomal cholesterol accumulation in PS KO MEFs.

5.1 Presenilin deficiency increases neuronal cholesterol level

Analysis of the free cholesterol in neurons by Filipin staining shows a significant increase in cortex and CA1 region in brains from 2 months old PS single and double KO mice compared with WT (Fig. 4.1). Accumulation of cholesterol is detected also in the striatum from PS2 and PSDKO mice, but not in the striatum of PS1-deficient mice. However, in the PS1KO mice, the genetic inactivation of PS1 is conditional on the forebrain-specific expression of a CamK2α-Cre recombinase. Since CamK2α, hence Cre, is not expressed in striatal neurons, it cannot be excluded that neuronal PS1 deletion in the striatum would also increase cholesterol levels. The effects of PS gene inactivation may be region-dependent, e.g., in the dentate gyrus, lack of PS1, but not PS2, increases the cellular cholesterol level.

Nevertheless, lack of PS increases neuronal cholesterol in cortex and CA1 *in vivo*.

This conclusion is in line with previous studies where deletion of presenilins has been shown to affect cholesterol level in mouse brain. In particular, in cortex from 2-month-old PSDKO mice, quantification of lipid content showed an increase in cholesterol and sphingomyelin levels (Grimm et al., 2005). Also, in 21 month-old mice carrying FAD-related mutations in APP and PS1 encoding genes (APPSLxPS1) altered cholesterol metabolism was reported with an increase in the level of desmosterol in hippocampus, cortex and cerebellum (Vanmierlo et al., 2010).

The previous findings from PSDKO mice are refined in the current study which shows that accumulation of cholesterol is observed upon deletion of either PS1 or PS2. Therefore, both PS are involved in neuronal lipid homeostasis *in vivo* suggesting a common mechanism through which lack of the PS proteins increases cellular free cholesterol.

Elevated cholesterol level in neurons has been previously associated with alteration of neuronal functions and neurodegeneration (Dulac et al., 2013). In the human disease, Niemann Pick type C, for example, the lysosomal cholesterol accumulation alone leads to neurodegeneration (Brady et al., 1989; Vanier and Millat, 2003). The concomitant presence of an increased neuronal cholesterol with other AD-related alterations due to PS dysfunction, such as γ-secretase activity, could be an aggravating factor that enhance or accelerate the AD pathology.

Considering that in PS2KO mice deletion of PS2 is constitutive, this model offers the possibility to investigate the effect of PS2 deletion on cholesterol metabolism also in other brain cells such as astrocytes and microglia. In a second experiment, 6 months old PS2KO mouse brains were compared to age-matched controls. Analysis of free cholesterol in neurons confirmed the neuronal increase described in the previous data (Fig. 4.2 B). In addition, this experiment revealed a novel finding: Filipin staining was significantly decreased in Iba1 positive microglia in PS2KO (Fig 4.2 A). No differences in cholesterol staining where observed, instead, in astrocytes between PS2KO and WT (Fig. 4.2 C).

These observations suggest that deletion of PS2 causes cell-type specific effects on cholesterol metabolism. Although the present data do not offer an explanation for these differences, the description of this phenomenon is intriguing and may motivate dedicated studies on PS2 in microglia.

5.2 Presenilin deficiency increases cholesterol level and alters cholesterol-related protein expression in MEFs.

To investigate the underlying molecular mechanism through which ablation of PS can increase cellular cholesterol level, MEFs from PS1 or PS2KO mice were selected as *in vitro* model.

Quantification of the cellular content of cholesterol and its precursors shows a significant increase in PS1- and PS2KO MEFs compared to the WT (Fig 4.3 A). This result independently supports the previous observation of an important role of both PS in the cellular cholesterol homeostasis. Likewise, the signal obtained by Filipin staining appears brighter in both KO MEFs compared to the control. In addition, analysis of cholesterol distribution by co-staining with subcellular compartment markers reveals an accumulation in late endosomes and lysosomes in PS KO MEFs (Fig. 4.3 B). An impairment of vesicular trafficking upon PS1- or PS1/PS2 deletion (PSDKO) was already known from previous studies where altered fusion events were found to contribute to impaired autophagy and lysosomal activity (Neely et al., 2011; Zhang et al., 2012). Despite these observations, a specific accumulation of cholesterol in late endosomal/lysosomal compartments following PS1 or PS2 deletion was never reported so far.

Taken together and in line with observations in mouse brain, the similar phenotype of PS1- and PS2KO MEFs is consistent with the existence of a common mechanism through which ablation of each PS can induce accumulation of cholesterol in endosomal/ lysosomal compartment. This conclusion is further corroborated by altered expression of proteins involved in cellular cholesterol metabolism (Fig. 4.4). Increased expression of CYP51, SREBPs and LDLR, was already reported in a previous study on PSDKO MEFs (Tamboli et al., 2008). Our study here, follows up on the previous work and extends it by investigating the individual effects of PS1 and PS2 deletion in MEFS.

Protein levels of the membrane cholesterol transporter ABCA1 and the LDL receptor differ between the single PS KO genotypes (increased expression levels observed in PS1KO and decreased in PS2KO). Nevertheless, increased protein expression of SREBP- FL/ NT and CYP51 indicated a common enhancement of cholesterol synthesis in all PS KO MEFs. Additional confirmation of the affected expression levels of cholesterol-related protein was obtained by gene expression analysis of PS KO MEFs compared to WT (Fig. 4.17). Increased mRNA levels of *Abca1* in PS1 and PSDKO MEFs and *Cyp51* in all the

PS KO genotypes suggested transcriptional induction of these genes. Decreased expression of *Soat2* in PS1 and PS2 KO MEFs (Fig. 4.18), suggested that the cholesterol storage mechanism is reduced upon PS deletion.

An involvement of CYP51 in lipid alterations was not only observed in PSDKO MEFs (Tamboli et al., 2008), but also in CHO cells, where a pathogenic mutant in PS1 derived from a FAD patient led to increased cellular cholesterol level that could be rescued by decrease of CYP51 expression (Cho et al., 2019b). Hence, both a loss-of-function mutation of PS1 as well as a pathogenic missense mutation have the same effect on CYP51 in different cell models derived from different species. The results presented here, accordingly, show that deletion of either PS significantly increases the expression of *Cyp51* through activation of SREBP-2. In line with such a mechanism, increased SREBP-2 NT protein was found in PS1, PS2, and PSDKO MEFS (Fig. 4.4).

The enhanced synthesis of cholesterol, while it is accumulated in the lysosomes, suggests a dysfunction of its subcellular trafficking. In fact, an impaired transport of cholesterol to the ER can induce its *de novo* synthesis thought SREBP activation and induction of *Cyp51* (Halder et al., 2002). The hypothesis of impaired cholesterol trafficking is supported by significantly diminished expression of the cholesterol transporter NPC1 in PS KO MEFs. Decreased levels of this protein could limit transport of cholesterol from lysosomal compartments to the ER.

NPC1, in fact, is a crucial cholesterol transporter localized in the late endosome/lysosome compartments. Its importance in neuronal function is made clear by the fact that inactivating mutations in the encoding gene cause the neurodegenerative disorder Niemann-Pick disease type C (NPC) (Brady et al., 1989). Previous studies showed the presence of an Alzheimer-like phenotype in NPC. In particular, progressive neurodegeneration with abnormal cholesterol metabolism, diffuse Aβ cortical deposits, and hyperphosphorylation of tau protein are observed in NPC (Malnar et al., 2014). Studies in different models, and NPC patients, showed that disruption of cholesterol trafficking in NPC affects APP cleavage and increases Aβ production (Burns et al., 2003; Jin et al., 2004; Malnar et al., 2010; Mattsson et al., 2011). Moreover, in models where NPC1 function is pharmacologically or genetically impaired, an increase of Aβ42 production associated with the localization of APP in lipid rafts and endosomal abnormalities were observed (Jin et al., 2004; Malnar et al., 2010).

Additionally, an accumulation of PS1 in late endosomal/lysosomal compartments, associated with an increased γ-secretase activity and production of Aβ40 and Aβ42 peptides has been described in neurons where NPC1 activity was inhibited (Runz et al., 2002; Burns et al., 2003).
Importantly, depletion of cholesterol rescues the increase in Aβ levels in NPC1 KO cells suggesting that APP mis-trafficking and increased cleavage depends on the cholesterol accumulation more than on the loss of NPC1 itself (Malnar et al., 2012). Additional studies regarding phosphorylated tau accumulation further emphasized the similarity between NPC pathology and AD (Sawamura et al., 2001; Ohm et al., 2003).
Beside these observations that connect the NPC1-dependent cholesterol accumulation and impaired endo/ lysosomal trafficking with altered APP processing and Aβ production, a direct link between PS dysfunction and NPC1 level, as proposed in this work, was not previously put forward.

5.3 Presenilin deficiency affects N-glycosylation of membrane proteins.

Analysis of protein expression by WB not only shows that in PS KO MEF the level of NPC1 is reduced but also that the migration of the band in SDS gel is faster compared to that from the WT cells. A similar effect, albeit to a lesser degree, can be observed for LRP1 (Fig 4.4 A). In addition, the bands corresponding to N-cadherin and LAMP2 in PS KO cells also show increased mobility (Fig. 4.5 A). Treatment with PNGase suggested that this effect is due to reduced N-glycosylation of the membrane proteins (Fig. 4.5 B).
Increased mobility in SDS-PAGE can either be the result of a decreased number of N-glycans attached to a protein or a reduction in their complexity, or a combination of both. The finding that in PS KO MEFs several membrane proteins show aberrant N-glycosylation could indicate a general impairment of the N-glycosylation machinery upon PS deletion. Independent confirmation of an altered N-glycosylation state of membrane proteins in PS KO MEFs was obtained by mass spectrometry, where the levels of the different N-glycans attached to membrane proteins was measured. The results show that a particular species, M5, is significantly decreased in PS KO MEFs compared to WT (Fig. 4.6). In line with this result, the expression level of the gene encoding for the enzyme responsible for M5 production, *Man1a* (Mannosidase Alpha Class 1A Member 1), was decreased by more than 50 % in PS1 and PS2 KO compared to WT MEFs (Fig. 4.19 C).

Inhibition of enzymes in the late glycosylation steps at ER level or in the Golgi, through treatment with DNJ, Kifunensin and Swainsonine, does not affect cholesterol-related protein expression in WT MEFs (Fig. 4.8). In contrast, Tunicamycin treatment alone was able to reduce NPC1 expression level and increase CYP51, inducing cholesterol accumulation in Rab7 and Lamp2 positive compartments, as shown by immunocytochemistry (Fig. 4.8 A). Thus, it is possible to speculate that interference particularly in the initial ER stages of N-glycosylation impairs cholesterol transport and synthesis.

Complete abrogation of protein glycosylation by a high concentration of Tunicamycin is lethal to the MEFs after 24h of treatment. For this reason, in order to allow prolonged treatment of the cells, a lower, non-toxic, concentration of Tunicamycin was chosen in the final experimental design. Nevertheless, the selected concentration is still able to reduce protein glycosylation, as indicated by increased mobility of the glycosylated proteins (Fig 4.7 B). It is likely to assume, then, that this lower concentration of tunicamycin only partially blocks the glycan synthesis.

The fact that in WT MEFs Tunicamycin treatment alone is able to decrease NPC1 expression level and, at the same time, phenocopy the cholesterol accumulation observed in PS KO MEFs, supports the hypothesis of a key role of NPC1 in mediating the effect of PS KO on cholesterol levels.

Several studies show that dysfunctional NPC1 is subject to ERAD (ER-associated protein degradation), a quality control process that takes place in the ER and is triggered by protein misfolding (Gelsthorpe et al., 2008; Nakasone et al., 2014; Schultz et al., 2018). Interestingly, the most relevant pathological mutation in the *NPC1* gene, $NPC1^{I1061T}$, affects the NPC1 glycosylation state and, consequently, its migration on electrophoresis (Gelsthorpe et al., 2008; Nakasone et al., 2014).

These observations are in line with our results, where impairment of NPC1 glycosylation in cells lacking PS or treated with Tunicamycin reduced NPC1 levels.

Gene expression analysis of enzymes involved in the N-glycan synthesis revealed individual steps of this complex process that are affected by deletion of PS1, PS2 or both proteins in MEFs (Fig. 4.19). Although we do not have information regarding the levels of N-glycan species before the transfer onto the protein, expression of enzymes involved in their synthesis appears dysregulated in all the PS KO MEFs. In particular, a decrease in

the mRNA level of *Alg8* is observed in all PS KO MEFs compared to the WT (Fig. 4.19 B). Expression of *Alg7*, the enzyme inhibited by Tunicamycin treatment, does not appear to be affected by PS ablation. The expression of genes related to proteins of the OST complex, which is responsible for the transfer of the mature N-glycan to the nascent proteins, appears increased mainly in PS1 and PSDKO MEFs (Fig. 4.19 B).

Following the translocation to the protein, the glycostructures continue to be modified in the late ER and Golgi compartments by a trimming process. Beside the decreased level of *Man1a,* in line with the reduction of M5 species in PS1- and PS2KO MEFs, an altered level of the remaining enzymes in this pathway is observed in all the PS KO MEFs (Fig. 4.19 C). Expression level of *Mogs* and *Ganab*, ER enzymes inhibited by DNJ treatment, are not significantly modulated or rather increased in PS KO MEFs compared to the WT. Kifunensine is inhibiting two additional enzymes of this pathway, Man1b and Man1a.

While mRNA level of *Man1a* is reduced in PS KO MEFs, as mentioned before, *Man1b* level is not affected by lack of PS. Assuming that the decreased expression level corresponds to a reduced protein function, it is possible that the Kifunensine treatment only partially, regarding MAN1A activity, can mimic the PS KO condition. Additional inhibition of MAN1B can, therefore, be the reason why the Kifunensine treatment did not fully recapitulate the cholesterol phenotype observed upon PS deletion.

RNA levels of the majority of the genes encoding for Golgi-resident enzymes involved in the trimming of the N-glycan also appear affected in PS KO MEFs (Fig. 4.19 C).

The results obtained from this complex analysis prove that, at least at the mRNA level, all the stages of the N-glycosylation process are altered by lack of PS in MEFs. Up- or down-regulation of these genes does not necessarily result in changes of the protein level of the corresponding enzymes, but suggest complex transcriptional changes in genes that regulate protein N-glycosylation. Information about the expression level of certain enzymes can be relevant for future examination of the protein N-glycosylation impairment in PS KO MEFs.

In summary, in PS KO MEFs the protein N-glycosylation process starts to be affected in the ER and continues in the Golgi. Considering that the amount of M8 and M9 species, the first N-glycans attached to the nascent protein from the OST complex, is not decreased in PS KO MEFs compared with WT (Fig. 4.6), it is possible to assume that the number of modified sites on the membrane proteins is overall not affected by lack of PS. Impairment

of the maturation stages of the complex N-glycan in late ER and Golgi compartment, then, could be responsible for the observed increased mobility in SDS gels of the membrane protein bands in PS KO MEFs. In support of this hypothesis, inhibition of the initial enzymes involved in this pathway (Mogs, Ganab, Man1, Man2) by DNJ, Kifunensine and Swainsonine treatments, mimics, in WT MEFs, the faster migration of the membrane protein during electrophoresis observed in samples from PS KO MEFs. In WT cells disruption of protein N-glycosylation in the ER, instead, cause the same cholesterol phenotype observed in PS KO cells, probably as result from the enhanced degradation of NPC1 via ERAD (Gelsthorpe et al., 2008; Nakasone et al., 2014; Schultz et al., 2018). This hypothesis is supported by the observation that only after the Tunicamycin treatment, affecting the early glycosylation step in the ER, we could observe a significant reduction of NPC1 expression level, overexpression of CYP51 and endo-lysosomal cholesterol accumulation.

An altered protein glycosylation pattern, with increased level of bisecting GlcNAc N-glycans, generated in the Golgi, and the responsible enzyme encoded by *Mgat3*, have been found increased in AD patients (Akasaka-Manya et al., 2010; Wang et al., 2019). Also sialylation appears to be decreased in AD patients serum, CSF and brains (Maguire and Breen, 1995; Fodero et al., 2008). Several studies focused on understanding how aberrant glycosylation of the most common AD-related proteins could contribute to AD pathogenesis (Kizuka et al., 2015; Haukedal and Freude, 2021). Although PSs are not glycosylated themselves, they can influence the glycosylation of other proteins directly or by affecting their cellular localization (Schedin-Weiss et al., 2014). PS1 and PS2, in fact, are known to be involved in the glycosylation and sialylation of the adhesion molecule NCAM (Farquhar et al., 2003), as well as glycosylation, maturation and subcellular localization of TrkB (Naruse et al., 1998).

Glycan alterations were observed in patients with mild cognitive impairment that later progressed to AD, therefore, it is plausible that glycan impairment precedes the clinical onset of AD. Glycan alteration in patients has been proposed as a potential biomarker for early AD diagnosis (Palmigiano et al., 2016) and the restoration of the glycosylation homeostasis could be a possible interesting therapeutic strategy (Wang et al., 2019).

5.4 Altered membrane protein N-glycosylation in PS KO MEFs seems to be independent from γ-secretase activity, cellular calcium perturbation and lysosomal cholesterol sequestration.

Because PS proteins are the catalytic subunits of γ-secretase complexes, their deletion affects the activity of the enzymatic complex (De Strooper et al., 1998, 1999). The altered protein glycosylation described in PS KO MEFs could, therefore, depend on γ-secretase dysfunction.

In order to directly test whether impaired γ-secretase activity is causally related to the observed changes in protein N-glycosylation, MEFs were treated with the γ-secretase inhibitor DAPT. The results presented here clearly show that DAPT failed to reproduce the band mobility shift in SDS gels, in all membrane proteins examined (Fig. 10). Accordingly, no induction of CYP51 was observed and hence cholesterol synthesis remained unchanged.

These results suggest that the observed effects of PS deletion are related to non-proteolytic functions of PS. Among these functions, calcium signaling is one of the most studied. Several groups reported a PS-dependent modulation of cellular Ca^{2+} involving ER calcium channels (Leissring et al., 1999; Chan et al., 2000; Stutzmann, 2004; Green et al., 2008). Some studies even suggested that PS themselves act as ER calcium leak channels (Tu et al., 2006; Bandara et al., 2013).

Because the previous results showed an involvement of ER localized enzymes in altered N-glycosylation process upon PS deletion, a potential mechanism connecting PS to protein glycosylation could be altered calcium homeostasis. However, this hypothesis is not confirmed by the use of calcium modulators. Alteration of calcium levels in ER or lysosomes in WT MEFs, in fact, does not change the migration of NPC1 band or its expression level (Fig. 11), suggesting that the effect on protein glycosylation observed in PS KO MEFs might not be caused by impairment of calcium homeostasis. However, this conclusion is solely based on the expression level of NPC1 and its mobility in electrophoresis.

Although altered protein glycosylation by Tunicamycin treatment shows a lysosomal cholesterol accumulation in WT MEFs, the possibility that PS deficiency leads to cholesterol accumulation first and that this may then affect the ER functions was still

possible. This possibility is excluded by the observation that during lysosomal cholesterol sequestration in WT MEFs by U18666A does not alter NPC1 protein migration during electrophoresis or decrease its expression levels (Fig. 4.12). It is important to underline here the limitations of the pharmacological approach. The present experiments were performed using selected concentrations of the compounds, based on an initial toxicity test. The same experimental setting, regarding time frame and replenishment of the compounds in the medium, was applied for all the treatments. Nevertheless, it is not possible to exclude that the use of different concentrations or time of treatments would not translate in different results from what is here reported. In addition, the use of inhibitors always comes with a certain uncertainty about possible unknown side effects.

5.5 Reduced NPC1 expression leads to lysosomal cholesterol accumulation in PS1 and PS2KO MEFs.

If reduced expression of NPC1 in PS KO MEFs would be caused by enhanced degradation of the protein in the ER following the impaired N-glycosylation, one would expect that increasing NPC1 expression should ameliorate cholesterol accumulation. Arimoclomol maleate is a chemical chaperone which induces expression of HSPs (Heat shock proteins), in particular HSP70 family, that are considered critical for the correct folding of NPC1 protein (Kirkegaard et al., 2010; Nakasone et al., 2014). This treatment also normalized the lysosomal cholesterol storage in NPC patients, improved the neurological condition of NPC mouse model (Kirkegaard et al., 2016) and, currently, is used in clinical trials for NPC disease (clinicaltrials.gov/NCT02612129).

Our experiments followed the idea that Arimoclomol maleate treatment might induce the expression of chaperones, which would improve the folding of NPC1 and help NPC1 to escape ERAD, and consequently increase its protein level in PS KO MEFs. If NPC1 levels increase, cholesterol accumulation should be reduced in PS KO MEFs.

Indeed, upon Arimoclomol maleate treatment, it was possible to observe an increased NPC1 protein level associated with a reduction of the CYP51 level in PS1- and PS2KO MEFs (Fig. 4.13 A). Analysis of the cellular cholesterol distribution, by co-staining of Filipin with markers for the subcellular compartments, shows that the endo-lysosomal cholesterol accumulation is reduced in PS KO MEFs upon treatment (Fig. 4.13 B). Importantly, the treatment with Arimoclomol maleate does not reduce the lysosomal cholesterol

accumulation in a NPC1 KO model (Fig. 4.14), suggesting that the effect of the treatment on cholesterol distribution in PS KO cells involves stabilization of NPC1 function.
Additional support for the focal role of NPC1 transporter in the cholesterol accumulation observed in PS1 and PS2KO MEFs is obtained by transient overexpression of NPC1 in KO cells (Fig. 4.15), resulting in an evident reduction in Filipin signal in transfected cells, compared to non-transfected cells.
These results strongly suggest that the impaired cholesterol trafficking from lysosomes to ER compartment observed upon PS deletion is due to a reduction in NPC1 level.

Based on the present data it can be proposed that ablation of PS1 or PS2 in MEFs affects cellular cholesterol distribution leading to its sequestration in lysosomal compartments and enhances *de novo* synthesis through a common molecular mechanism that involved altered N-glycosylation. In particular, the primary alteration of the protein N-glycosylation machinery affects the general maturation of complex N-glycan on several membrane proteins involved in cellular cholesterol metabolism. The impaired glycosylation of the cholesterol transporter NPC1 appears to induce its degradation, probably due to improper folding. Reduction of NPC1 level, in turn, could lead to a cholesterol accumulation in lysosomal compartments. The block of cholesterol transport to the ER, then, enhance the expression of CYP51, an enzyme critically involved in the cholesterol *de novo* synthesis suggesting a further perturbation of the cellular cholesterol homeostasis.
The relevance of cholesterol in AD pathogenesis is demonstrated by several observations. High cholesterol level has been reported in AD patient´s brains (Gylys et al., 2007; Cutler et al., 2004) and studies showed how an increased cholesterol level can promote APP processing (Marquer et al., 2014), facilitate Aβ aggregation (Matsuzaki et al., 2010; Yanagisawa, 2015), and affect phospho-tau levels (van der Kant et al., 2019). Accumulation of cholesterol was observed, as well, in the presence of PS FAD mutations (Grimm et al., 2005; Tamboli et al., 2008; Area-Gomez et al., 2012) (Grimm et al., 2005; Tamboli et al., 2008; Gutierrez et al., 2020) (Cho et al., 2019) or genetic ablation of both PS in mouse fibroblast (Tamboli et al., 2008). The presence of increased cholesterol level upon PS FAD mutations could have an important role in accelerating and/or aggravating the course of the disease as observed in FAD cases.

Therefore, understanding the mechanism behind this cholesterol dyshomeostasis upon PS dysfunction can have a great impact for potential treatment strategies. In particular considering that studies on use of statins, drugs to lower cholesterol levels, have been associated with a risk reduction of AD and dementia with a decrement of the risk in a duration and dose-dependent manner (Jick et al., 2000; Lin et al., 2015; Zissimopoulos et al., 2017; Zhang et al., 2018).
The present data on the molecular mechanism leading to increased cellular cholesterol, therefore, could constitute the rationale behind these results using cholesterol lowering drugs.

5.6 Limitation of the study

While the data and conclusions presented above explain some of the key findings of this work on PS and cellular cholesterol accumulation, they could not sort out the mechanism underlying the glycosylation impairment observed in PS KO MEFs. The results obtained from the mass spectrometry on N-glycans show an altered glycosylation pattern upon PS deletion. Furthermore, the mRNA level of several enzymes involved in the glycosylation process was different in PS KO cells compared to WT. Impairment of the early ER stages of the process appears to affect NPC1 stability probably leading to its degradation. Use of Arimoclomol maleate helped to increase the NPC1 protein level, however, the glycosylation state of NPC1 in PS KO MEFs is not normalized by the treatment. This means that the impairment of the N-glycosylation machinery is not corrected by Arimoclomol. This conclusion is in line with the hypothesis, already mentioned, of an impaired complex N-glycan maturation occurring in the later stages of the glycosylation process, that is not involved in the lysosomal cholesterol phenotype. In fact, in WT cells the use of Swainsonine, inhibiting a Golgi stage of complex type N-glycan synthesis, induces a faster migration of the membrane proteins bands similarly to what observed in PS KO MEFs. This impairment of the N-glycan did not correspond to a cholesterol accumulation in lysosomal compartment so it did not recapitulate the PS KO phenotype.
Beside these observations, the obtained results were not conclusive and did not lead to a clear explanatory mechanism how protein glycosylation is impaired by lack of PS1 and PS2.

In an attempt to elucidate this molecular mechanism, the possibility that perturbation of calcium homeostasis was affecting N-glycosylation was explored. A large number of studies, in fact, showed a connection between PS activity and cellular calcium levels. The use of calcium modulators in WT MEFs, with the purpose of mimicking the PS KO phenotype, failed to reproduce the glycosylation impairment in NPC1 (Fig. 4.11), suggesting a different link between PS and N-glycosylation machinery.

An alternative explanation that we did not explore so far might be the involvement of ER stress mechanisms. In fact, several research groups reported evidence of ER stress mechanisms upon PS dysfunction (Hashimoto and Saido, 2018). The actual effect of lack or mutation of PS on ER stress response is still under debate. Contrasting results about the effect of PS1 dysfunction, showing an induction or not of ER stress response depending on the examined model, have been obtained by several studies (Katayama et al., 1999, 2001; Yukioka et al., 2008; Száraz et al., 2013). Studies with PS2 FAD mutations were inconclusive, since some studies showed enhanced expression of ER stress markers, while others found a down-regulation of UPR pathway(Sato et al., 2001; Kang et al., 2013). Remarkably, this ability to affect ER response to stress is reported for both, PS1 and PS2, suggesting a common mechanism through which they can influence ER functions.

It has to be considered here that the present results are obtained from PS knockout model, known to cause an acne inversa phenotype (Wang et al., 2010), therefore, a direct extrapolation of these results on AD pathogenesis is not possible. Nevertheless, the present observations could lay the base for future investigation using an AD-related model, such as cells expressing PS FAD mutations.

5.7 Summary

The present work shows that a potential link between PS and cholesterol can be found in the altered translocation of cholesterol. In particular the transport of cholesterol from lysosomes appears impaired due to a decreased level of the NPC1 transporter in PS KO cells. The cholesterol sequestration in lysosomes affects the level of CYP51, a key enzyme in *de novo* cholesterol synthesis, of which level was already reported to be altered upon PS deletion (Tamboli 2008). The finding of an involvement of NPC1 in the cholesterol phenotype observed in PS KO MEFs, is particularly intriguing considering that mutation in

this protein cause a neurodegenerative disease, Niemann-Pick type C disease, where Aβ cortical deposits, and hyperphosphorylation of tau protein have been observed (Malnar 2014).

In addition, the present data show an impairment of the N-glycosylation machinery, upon PS deletion in MEFs, affecting NPC1, among other membrane proteins. Considering that evidences of a degradation process via ERAD of dysfunctional NPC1 have been reported (Gelsthorpe et al., 2008; Nakasone et al., 2014; Schultz et al., 2018). It is possible to speculate that a similar degradation, causing the NPC1 level reduction, can happen also in PS KO MEFs following the impaired protein glycosylation.

The purpose of the present study is to obtain new insights about the basic molecular mechanism connecting PS function to cellular cholesterol mechanism. The obtained data, in fact, offer interesting and important observations on PS functions and their role on cellular lipid homeostasis through protein glycosylation.

The shown link between lysosomal cholesterol accumulation and NPC1 dysfunction upon PS deletion could open the possibility of a new target to modulate the cellular cholesterol level.

6. Abstract

Major genetic causes of familial Alzheimer disease are mutations in genes encoding presenilin (PS) 1 and 2. PS1 and PS2 are known to constitute the catalytic subunits of the γ-secretase complex, but also for being involved in cellular cholesterol metabolism which is connected to AD development via the genetic risk factor apolipoprotein E (*APOE*). However, the molecular mechanisms how PS affect cellular cholesterol metabolism are not understood. We observed increased cholesterol content in neurons from PS knockout (KO) mice in cortex and CA1 regions and characterize the cholesterol metabolism in PS1- or PS2 KO mouse embryonic fibroblasts (MEFs).

Cholesterol and sterols were measured in MEFs by mass spectrometry (MS) while filipin, a fluorescent cholesterol binding compound was used to visualize free cholesterol. Non-toxic concentrations of inhibitors or chaperone inducer were selected to treat the cells. Protein expression was analyzed by Western blotting (WB) while mRNA levels were measured by 3´mRNa sequencing.

Cellular levels of cholesterol as well as its precursors were high in PS1- and PS2KO MEFs, while filipin revealed intracellular cholesterol accumulation in endo-lysosomal compartments. The expression patterns of proteins involved in cholesterol metabolism were different in PS1- and PS2KO MEFs. Nevertheless, we detected a significant increase in SREBP-2 and CYP51 and a decrease in NPC1 expression level in PS KO MEFs. Deficiency of the cholesterol transporter NPC1 leads to lysosomal cholesterol storage and neurodegeneration in Niemann-Pick´s disease type C. Glycosylation of NPC1 and other membrane proteins, including LRP1, LAMP2 and N-cadherin was impaired in PS KO MEFs. To test whether inhibition of protein glycosylation affects cholesterol metabolism, WT MEFs were treated with inhibitors targeting different enzymes of the process. Inhibition of the early glycosylation step at ER alone was able to decrease NPC1 expression level, induce CYP51 expression and, at the same time, phenocopy the lysosomal cholesterol accumulation observed in PS KO MEFs.

Treatment with a chaperone inducer increasing NPC1 levels significantly attenuated lysosomal cholesterol accumulation and decrease CYP51 level in PS KO MEFs. Overexpression of NPC1 in PS KO MEFs also showed a reduction in lysosomal cholesterol content.

Our results suggest that lack of PS1 or PS2 affects cellular cholesterol metabolism toward upregulation of *de novo* cholesterol synthesis and lysosomal cholesterol accumulation via impaired protein glycosylation and reduced NPC1 level.

7. List of figures and tables

Figures

Tables

8. References

Aebi M (2001) Congenital disorders of glycosylation: genetic model systems lead the way. Trends Cell Biol 11:136–141.

Aebi M (2013) N-linked protein glycosylation in the ER. Biochim Biophys Acta BBA - Mol Cell Res 1833:2430–2437.

Aebi M, Gassenhuber J, Domdey H, Heesen S te (1996) Cloning and characterization of the ALG3 gene of Saccharomyces cerevisiae. Glycobiology 6:439–444.

Akasaka-Manya K, Manya H, Sakurai Y, Wojczyk BS, Kozutsumi Y, Saito Y, Taniguchi N, Murayama S, Spitalnik SL, Endo T (2010) Protective effect of N-glycan bisecting GlcNAc residues on -amyloid production in Alzheimer's disease. Glycobiology 20:99–106.

Alzheimer A, (1911) Über eigenartige Krankheitsfälle des späteren Alters. Zeitschrift für die gesamte Neurologie und Psychiatrie. 4:356-385.

Alzheimer A, Förstl H, Levy R (1991) On certain peculiar diseases of old age. Hist Psychiatry 2:71–73.

Alzheimer's Association (2019) 2019 Alzheimer's disease facts and figures. Alzheimers Dement 15:321–387.

Annaert W, De Strooper B (2002) A Cell Biological Perspective on Alzheimer's Disease. Annu Rev Cell Dev Biol 18:25–51.

Annaert WG, Esselens C, Baert V, Boeve C, Snellings G, Cupers P, Craessaerts K, De Strooper B (2001) Interaction with Telencephalin and the Amyloid Precursor Protein Predicts a Ring Structure for Presenilins. Neuron 32:579–589.

Area-Gomez E, del Carmen Lara Castillo M, Tambini MD, Guardia-Laguarta C, de Groof AJC, Madra M, Ikenouchi J, Umeda M, Bird TD, Sturley SL, Schon EA (2012) Upregulated function of mitochondria-associated ER membranes in Alzheimer disease: Upregulated function of MAM in AD. EMBO J 31:4106–4123.

Arendt T, Stieler JT, Holzer M (2016) Tau and tauopathies. Brain Res Bull 126:238–292.

Baas PW, Rao AN, Matamoros AJ, Leo L (2016) Stability properties of neuronal microtubules: Stability Properties of Neuronal Microtubules. Cytoskeleton 73:442–460.

Baki L, Neve RL, Shao Z, Shioi J, Georgakopoulos A, Robakis NK (2008) Wild-Type But Not FAD Mutant Presenilin-1 Prevents Neuronal Degeneration by Promoting Phosphatidylinositol 3-Kinase Neuroprotective Signaling. J Neurosci 28:483–490.

Baki L, Shioi J, Wen P, Shao Z, Schwarzman A, Gama-Sosa M, Neve R, Robakis NK (2004) PS1 activates PI3K thus inhibiting GSK-3 activity and tau overphosphorylation: effects of FAD mutations. EMBO J 23:2586–2596.

Bandara S, Malmersjö S, Meyer T (2013) Regulators of Calcium Homeostasis Identified by Inference of Kinetic Model Parameters from Live Single Cells Perturbed by siRNA. Sci Signal. 6(283):ra56.

Banerjee S, Vishwanath P, Cui J, Kelleher DJ, Gilmore R, Robbins PW, Samuelson J (2007) The evolution of N-glycan-dependent endoplasmic reticulum quality control factors for glycoprotein folding and degradation. Proc Natl Acad Sci 104:11676–11681.

Barrett PJ, Song Y, Van Horn WD, Hustedt EJ, Schafer JM, Hadziselimovic A, Beel AJ, Sanders CR (2012) The Amyloid Precursor Protein Has a Flexible Transmembrane Domain and Binds Cholesterol. Science 336:1168–1171.

Bastrup J, Hansen KH, Poulsen TBG, Kastaniegaard K, Asuni AA, Christensen S, Belling D, Helboe L, Stensballe A, Volbracht C (2021) Anti-Aβ Antibody Aducanumab Regulates the Proteome of Senile Plaques and Closely Surrounding Tissue in a Transgenic Mouse Model of Alzheimer's Disease. J Alzheimers Dis 79:249–265.

Bause E (1983) Structural requirements of N -glycosylation of proteins. Studies with proline peptides as conformational probes. Biochem J 209:331–336.

Beel AJ, Mobley CK, Kim HJ, Tian F, Hadziselimovic A, Jap B, Prestegard JH, Sanders CR (2008) Structural Studies of the Transmembrane C-Terminal Domain of the Amyloid Precursor Protein (APP): Does APP Function as a Cholesterol Sensor? Biochemistry 47:9428–9446.

Bieberich E (2014) Synthesis, Processing, and Function of N-glycans in N-glycoproteins. In: Glycobiology of the Nervous System (Yu RK, Schengrund C-L, eds), pp 47–70 Advances in Neurobiology. New York, NY: Springer New York.

Bonifacino JS (2014) Adaptor proteins involved in polarized sorting. J Cell Biol 204:7–17.

Borchelt DR et al. (1996) Familial Alzheimer's Disease–Linked Presenilin 1 Variants Elevate Aβ1–42/1–40 Ratio In Vitro and In Vivo. Neuron 17:1005–1013.

Borchelt DR, Ratovitski T, van Lare J, Lee MK, Gonzales V, Jenkins NA, Copeland NG, Price DL, Sisodia SS (1997) Accelerated Amyloid Deposition in the Brains of Transgenic Mice Coexpressing Mutant Presenilin 1 and Amyloid Precursor Proteins. Neuron 19:939–945.

Braak H, Alafuzoff I, Arzberger T, Kretzschmar H, Del Tredici K (2006) Staging of Alzheimer disease-associated neurofibrillary pathology using paraffin sections and immunocytochemistry. Acta Neuropathol (Berl) 112:389–404.

Braak H, Braak E (1991) Neuropathological stageing of Alzheimer-related changes. Acta Neuropathol (Berl) 82:239–259.

Braak H, Braak E (1995) Staging of alzheimer's disease-related neurofibrillary changes. Neurobiol Aging 16:271–278.

Brady RO, Filling-Katz MR, Barton NW, Pentchev PG (1989) Niemann-Pick disease types C and D. Neurol Clin 7:75–88.

Breitling J, Aebi M (2013) N-Linked Protein Glycosylation in the Endoplasmic Reticulum. Cold Spring Harb Perspect Biol 5:a013359–a013359.

Brown J, Theisler C, Silberman S, Magnuson D, Gottardi-Littell N, Lee JM, Yager D, Crowley J, Sambamurti K, Rahman MM, Reiss AB, Eckman CB, Wolozin B (2004) Differential Expression of Cholesterol Hydroxylases in Alzheimer's Disease. J Biol Chem 279:34674–34681.

Brown MS, Radhakrishnan A, Goldstein JL (2018) Retrospective on Cholesterol Homeostasis: The Central Role of Scap. Annu Rev Biochem 87:783–807.

Burns M, Gaynor K, Olm V, Mercken M, LaFrancois J, Wang L, Mathews PM, Noble W, Matsuoka Y, Duff K (2003) Presenilin Redistribution Associated with Aberrant Cholesterol Transport Enhances β-Amyloid Production In Vivo. J Neurosci 23:5645–5649.

Cai D, Leem JY, Greenfield JP, Wang P, Kim BS, Wang R, Lopes KO, Kim S-H, Zheng H, Greengard P, Sisodia SS, Thinakaran G, Xu H (2003) Presenilin-1 Regulates Intracellular Trafficking and Cell Surface Delivery of β-Amyloid Precursor Protein. J Biol Chem 278:3446–3454.

Cataldo AM, Peterhoff CM, Schmidt SD, Terio NB, Duff K, Beard M, Mathews PM, Nixon RA (2004) Presenilin Mutations in Familial Alzheimer Disease and Transgenic Mouse Models Accelerate Neuronal Lysosomal Pathology. J Neuropathol Exp Neurol 63:821–830.

Chan SL, Mayne M, Holden CP, Geiger JD, Mattson MP (2000) Presenilin-1 Mutations Increase Levels of Ryanodine Receptors and Calcium Release in PC12 Cells and Cortical Neurons. J Biol Chem 275:18195–18200.

Chang IJ, He M, Lam CT (2018) Congenital disorders of glycosylation. Ann Transl Med 6:477–477.

Chang TY, Chang CC, Cheng D (1997) Acyl-coenzyme A:cholesterol acyltransferase. Annu Rev Biochem 66:613–638.

Cheung K-H, Shineman D, Müller M, Cárdenas C, Mei L, Yang J, Tomita T, Iwatsubo T, Lee VM-Y, Foskett JK (2008) Mechanism of Ca2+ disruption in Alzheimer's disease by presenilin regulation of InsP3 receptor channel gating. Neuron 58:871–883.

Cho YY, Kwon O-H, Chung S (2020) Preferred Endocytosis of Amyloid Precursor Protein from Cholesterol-Enriched Lipid Raft Microdomains. Molecules 25:5490.

Cho YY, Kwon O-H, Park MK, Kim T-W, Chung S (2019a) Elevated cellular cholesterol in Familial Alzheimer's presenilin 1 mutation is associated with lipid raft localization of β-amyloid precursor protein. PloS One 14:e0210535.

Cho YY, Kwon O-H, Park MK, Kim T-W, Chung S (2019b) Elevated cellular cholesterol in Familial Alzheimer's presenilin 1 mutation is associated with lipid raft localization of β-amyloid precursor protein Lakshmana MK, ed. PLOS ONE 14:e0210535.

Chung DC, Roemer S, Petrucelli L, Dickson DW (2021) Cellular and pathological heterogeneity of primary tauopathies. Mol Neurodegener 16:57.

Citron M et al. (1997) Mutant presenilins of Alzheimer's disease increase production of 42-residue amyloid β-protein in both transfected cells and transgenic mice. Nat Med 3:67–72.

Coen K, Flannagan RS, Baron S, Carraro-Lacroix LR, Wang D, Vermeire W, Michiels C, Munck S, Baert V, Sugita S, Wuytack F, Hiesinger PR, Grinstein S, Annaert W (2012) Lysosomal calcium homeostasis defects, not proton pump defects, cause endo-lysosomal dysfunction in PSEN-deficient cells. J Cell Biol 198:23–35.

Corder EH, Saunders AM, Strittmatter WJ, Schmechel DE, Gaskell PC, Small GW, Roses AD, Haines JL, Pericak-Vance MA (1993) Gene Dose of Apolipoprotein E Type 4 Allele and the Risk of Alzheimer's Disease in Late Onset Families. Science 261:921–923.

Cossec J-C, Simon A, Marquer C, Moldrich RX, Leterrier C, Rossier J, Duyckaerts C, Lenkei Z, Potier M-C (2010) Clathrin-dependent APP endocytosis and Aβ secretion are highly sensitive to the level of plasma membrane cholesterol. Biochim Biophys Acta BBA - Mol Cell Biol Lipids 1801:846–852.

Costa R, Drew C, Silva A (2005) Notch to remember. Trends Neurosci 28:429–435.

Costa RM, Honjo T, Silva AJ (2003) Learning and Memory Deficits in Notch Mutant Mice. Curr Biol 13:1348–1354.

Cummings J, Lee G, Ritter A, Sabbagh M, Zhong K (2020) Alzheimer's disease drug development pipeline: 2020. Alzheimers Dement (N Y) 6(1):e12050.

Cutler RG, Kelly J, Storie K, Pedersen WA, Tammara A, Hatanpaa K, Troncoso JC, Mattson MP (2004) Involvement of oxidative stress-induced abnormalities in ceramide and cholesterol metabolism in brain aging and Alzheimer's disease. Proc Natl Acad Sci 101:2070–2075.

D'Alessio C, Caramelo JJ, Parodi AJ (2010) UDP-GlC:glycoprotein glucosyltransferase-glucosidase II, the ying-yang of the ER quality control. Semin Cell Dev Biol 21:491–499.

De Strooper B, Annaert W (2010) Novel Research Horizons for Presenilins and γ-Secretases in Cell Biology and Disease. Annu Rev Cell Dev Biol 26:235–260.

De Strooper B, Annaert W, Cupers P, Saftig P, Craessaerts K, Mumm JS, Schroeter EH, Schrijvers V, Wolfe MS, Ray WJ, Goate A, Kopan R (1999) A presenilin-1-dependent γ-secretase-like protease mediates release of Notch intracellular domain. Nature 398:518–522.

De Strooper B, Saftig P, Craessaerts K, Vanderstichele H, Guhde G, Annaert W, Von Figura K, Van Leuven F (1998) Deficiency of presenilin-1 inhibits the normal cleavage of amyloid precursor protein. Nature 391:387–390.

Deprez P, Gautschi M, Helenius A (2005) More Than One Glycan Is Needed for ER Glucosidase II to Allow Entry of Glycoproteins into the Calnexin/Calreticulin Cycle. Mol Cell 19:183–195.

Dercksen M, Crutchley AC, Honey EM, Lippert MM, Matthijs G, Mienie LJ, Schuman HC, Vorster BC, Jaeken J (2012) ALG6-CDG in South Africa: Genotype-Phenotype Description of Five Novel Patients. JIMD Reports 8:17-23.

Dhaliwal J, Kannangara TS, Vaculik M, Xue Y, Kumar KL, Maione A, Béïque J-C, Shen J, Lagace DC (2018) Adult hippocampal neurogenesis occurs in the absence of Presenilin 1 and Presenilin 2. Sci Rep 8:17931.

Dietschy JM, Turley SD (2001) Cholesterol metabolism in the brain: Curr Opin Lipidol 12:105–112.

Dobin A, Davis CA, Schlesinger F, Drenkow J, Zaleski C, Jha S, Batut P, Chaisson M & Gingeras T (2013) STAR: ultrafast universal RNA-seq aligner. Bioinformatics 29 15–21.

Dobrowolski R, Vick P, Ploper D, Gumper I, Snitkin H, Sabatini DD, De Robertis EM (2012) Presenilin Deficiency or Lysosomal Inhibition Enhances Wnt Signaling through Relocalization of GSK3 to the Late-Endosomal Compartment. Cell Rep 2:1316–1328.

Donoviel DB, Hadjantonakis A-K, Ikeda M, Zheng H, Hyslop PSG, Bernstein A (1999) Mice lacking both presenilin genes exhibitearlyembryonic patterningdefects. Genes Dev 13:2801–2810.

Duff K, Eckman C, Zehr C, Yu X, Prada C-M, Perez-tur J, Hutton M, Buee L, Harigaya Y, Yager D, Morgan D, Gordon MN, Holcomb L, Refolo L, Zenk B, Hardy J, Younkin S (1996) Increased amyloid-β42(43) in brains of mice expressing mutant presenilin 1. Nature 383:710–713.

Dulac O, Lassonde M, Sarnat HB eds. (2013) Pediatric neurology. Edinburgh; New York: Elsevier.

Dunphy WG, Fries E, Urbani LJ, Rothman JE (1981) Early and late functions associated with the Golgi apparatus reside in distinct compartments. Proc Natl Acad Sci 78:7453–7457.

Elbein AD, Heath EC (1984) Inhibitors of the Biosynthesis and Processing of N-Linked Oligosaccharide. Crit Rev Biochem 16:21–49.

Elgner F, Ren H, Medvedev R, Ploen D, Himmelsbach K, Boller K, Hildt E (2016) The Intracellular Cholesterol Transport Inhibitor U18666A Inhibits the Exosome-Dependent Release of Mature Hepatitis C Virus Ou J-HJ, ed. J Virol 90:11181–11196.

Erondu N, Kennedy M (1985) Regional distribution of type II Ca2+/calmodulin-dependent protein kinase in rat brain. J Neurosci 5:3270–3277.

Esparza TJ, Zhao H, Cirrito JR, Cairns NJ, Bateman RJ, Holtzman DM, Brody DL (2013) Amyloid-beta oligomerization in Alzheimer dementia versus high-pathology controls. Ann Neurol 73:104–119.

Esselens C, Oorschot V, Baert V, Raemaekers T, Spittaels K, Serneels L, Zheng H, Saftig P, De Strooper B, Klumperman J, Annaert W (2004) Presenilin 1 mediates the turnover of telencephalin in hippocampal neurons via an autophagic degradative pathway. J Cell Biol 166:1041–1054.

Farquhar MJ, Gray CW, Breen KC (2003) The over-expression of the wild type or mutant forms of the presenilin-1 protein alters glycoprotein processing in a human neuroblastoma cell line. Neurosci Lett 346:53–56.

Fedeli C, Filadi R, Rossi A, Mammucari C, Pizzo P (2019) PSEN2 (presenilin 2) mutants linked to familial Alzheimer disease impair autophagy by altering Ca 2+ homeostasis. Autophagy 15:2044–2062.

Feng R, Rampon C, Tang Y-P, Shrom D, Jin J, Kyin M, Sopher B, Martin GM, Kim S-H, Langdon RB, Sisodia SS, Tsien JZ (2001) Deficient Neurogenesis in Forebrain-Specific Presenilin-1 Knockout Mice Is Associated with Reduced Clearance of Hippocampal Memory Traces. Neuron 32:911–926.

Fodero LR, Sáez-Valero J, Barquero M-S, Marcos A, McLean CA, Small DH (2008) Wheat germ agglutinin-binding glycoproteins are decreased in Alzheimer's disease cerebrospinal fluid: WGA glycoproteins in Alzheimer's CSF. J Neurochem 79:1022–1026.

Foley P (2010) Lipids in Alzheimer's disease: A century-old story. Biochim Biophys Acta BBA - Mol Cell Biol Lipids 1801:750–753.

Frank CG, Aebi M (2005) ALG9 mannosyltransferase is involved in two different steps of lipid-linked oligosaccharide biosynthesis. Glycobiology 15:1156–1163.

Freeze HH, Aebi M (2005) Altered glycan structures: the molecular basis of congenital disorders of glycosylation. Curr Opin Struct Biol 15:490–498.

Freeze HH, Chong JX, Bamshad MJ, Ng BG (2014) Solving Glycosylation Disorders: Fundamental Approaches Reveal Complicated Pathways. Am J Hum Genet 94:161–175.

Gelsthorpe ME, Baumann N, Millard E, Gale SE, Langmade SJ, Schaffer JE, Ory DS (2008) Niemann-Pick Type C1 I1061T Mutant Encodes a Functional Protein That Is Selected for Endoplasmic Reticulum-associated Degradation Due to Protein Misfolding. J Biol Chem 283:8229–8236.

Glöckner F, Meske V, Lütjohann D, Ohm TG (2011) Dietary Cholesterol and Its Effect on Tau Protein: A Study in Apolipoprotein E-Deficient and P301L Human Tau Mice. J Neuropathol Exp Neurol 70:292–301.

Goldstein JL, Brown MS (2009) The LDL receptor. Arterioscler Thromb Vasc Biol 29:431–438.

Gong X, Qian H, Zhou X, Wu J, Wan T, Cao P, Huang W, Zhao X, Wang X, Wang P, Shi Y, Gao GF, Zhou Q, Yan N (2016) Structural Insights into the Niemann-Pick C1 (NPC1)-Mediated Cholesterol Transfer and Ebola Infection. Cell 165:1467–1478.

Gorath M, Stahnke T, Mronga T, Goldbaum O, Richter-Landsberg C (2001) Developmental changes of tau protein and mRNA in cultured rat brain oligodendrocytes. Glia 36:89–101.

Green KN, Demuro A, Akbari Y, Hitt BD, Smith IF, Parker I, LaFerla FM (2008) SERCA pump activity is physiologically regulated by presenilin and regulates amyloid beta production. J Cell Biol 181:1107–1116.

Grimm MOW, Grimm HS, Pätzold AJ, Zinser EG, Halonen R, Duering M, Tschäpe J-A, Strooper BD, Müller U, Shen J, Hartmann T (2005) Regulation of cholesterol and sphingomyelin metabolism by amyloid-β and presenilin. Nat Cell Biol 7:1118–1123.

Grimm MOW, Grimm HS, Tomic I, Beyreuther K, Hartmann T, Bergmann C (2008) Independent Inhibition of Alzheimer Disease β- and γ-Secretase Cleavage by Lowered Cholesterol Levels. J Biol Chem 283:11302–11311.

Grothe MJ, Villeneuve S, Dyrba M, Bartrés-Faz D, Wirth M, For the Alzheimer's Disease Neuroimaging Initiative (2017) Multimodal characterization of older APOE2 carriers reveals selective reduction of amyloid load. Neurology 88:569–576.

Güner G, Lichtenthaler SF (2020) The substrate repertoire of γ-secretase/presenilin. Semin Cell Dev Biol 105:27–42.

Gutierrez E, Lütjohann D, Kerksiek A, Fabiano M, Oikawa N, Kuerschner L, Thiele C, Walter J (2020) Importance of γ-secretase in the regulation of liver X receptor and cellular lipid metabolism. Life Sci Alliance 3:e201900521.

Gylys KH, Fein JA, Yang F, Miller CA, Cole GM (2007) Increased cholesterol in Aβ-positive nerve terminals from Alzheimer's disease cortex. Neurobiol Aging 28:8–17.

Haass C, Kaether C, Thinakaran G, Sisodia S (2012) Trafficking and Proteolytic Processing of APP. Cold Spring Harb Perspect Med 2:a006270–a006270.

Habchi J, Chia S, Galvagnion C, Michaels TCT, Bellaiche MMJ, Ruggeri FS, Sanguanini M, Idini I, Kumita JR, Sparr E, Linse S, Dobson CM, Knowles TPJ, Vendruscolo M (2018) Cholesterol catalyses Aβ42 aggregation through a heterogeneous nucleation pathway in the presence of lipid membranes. Nat Chem 10:673–683.

Haeberlein SB, Aisen PS, Barkhof F, Chalkias S, Chen T, Cohen S, Dent G, Hansson O, Harrison K, von Hehn C, Iwatsubo T, Mallinckrodt C, Mummery CJ, Muralidharan KK, Nestorov I, Nisenbaum L, Rajagovindan R, Skordos L, Tian Y, van Dyck CH, Vellas B, Wu S, Zhu Y, Sandrock A. Two Randomized Phase 3 Studies of Aducanumab in Early Alzheimer's Disease. *J Prev Alzheimers Dis* 9, 197–210 (2022).

Haeberlein SB, von Hehn C, Tian Y, Chalkias S, Muralidharan KK, Chen T, Wu S, Skordos L, Nisenbaum L, Rajagovindan R, Dent G, Harrison K, Nestorov I, Zhu Y, Mallinckrodt C, Sandrock A (2020) Emerge and Engage topline results: Phase 3 studies of aducanumab in early Alzheimer's disease: Developments in clinical trials and cognitive assessment. Alzheimers Dement 16.

Halder SK, Fink M, Waterman MR, Rozman D (2002) A cAMP-Responsive Element Binding Site Is Essential for Sterol Regulation of the Human Lanosterol 14α-Demethylase Gene (CYP51). Mol Endocrinol 16:1853–1863.

Hammond C, Helenius A (1994) Quality control in the secretory pathway: retention of a misfolded viral membrane glycoprotein involves cycling between the ER, intermediate compartment, and Golgi apparatus. J Cell Biol 126:41–52.

Handler M, Yang X, Shen J (2000) Presenilin-1 regulates neuronal differentiation during neurogenesis. Dev Camb Engl 127:2593–2606.

Hardy JA, Higgins GA (1992) Alzheimer's Disease: The Amyloid Cascade Hypothesis. Science 256:184–185.

Hartmann D, Strooper BD, Saftig P (1999) Presenilin-1 deficiency leads to loss of Cajal–Retzius neurons and cortical dysplasia similar to human type 2 lissencephaly. Curr Biol 9:719–727.

Hashimoto S, Saido TC (2018) Critical review: involvement of endoplasmic reticulum stress in the aetiology of Alzheimer's disease. Open Biol 8:180024.

Haukedal H, Freude KK (2021) Implications of Glycosylation in Alzheimer's Disease. Front Neurosci 14:625348.

Hayrapetyan V, Rybalchenko V, Rybalchenko N, Koulen P (2008) The N-terminus of presenilin-2 increases single channel activity of brain ryanodine receptors through direct protein-protein interaction. Cell Calcium 44:507–518.

Hébert SS, Serneels L, Dejaegere T, Horré K, Dabrowski M, Baert V, Annaert W, Hartmann D, De Strooper B (2004) Coordinated and widespread expression of γ-secretase in vivo: evidence for size and molecular heterogeneity. Neurobiol Dis 17:260–272.

Helenius A, Aebi M (2004) Roles of N-Linked Glycans in the Endoplasmic Reticulum. Annu Rev Biochem 73:1019–1049.

Hensley K, Carney JM, Mattson MP, Aksenova M, Harris M, Wu JF, Floyd RA, Butterfield DA (1994) A model for beta-amyloid aggregation and neurotoxicity based on free radical generation by the peptide: relevance to Alzheimer disease. Proc Natl Acad Sci 91:3270–3274.

Herreman A, Van Gassen G, Bentahir M, Nyabi O, Craessaerts K, Mueller U, Annaert W, De Strooper B (2003) γ-Secretase activity requires the presenilin-dependent trafficking of nicastrin through the Golgi apparatus but not its complex glycosylation. J Cell Sci 116:1127–1136.

Hong S, Ostaszewski BL, Yang T, O'Malley TT, Jin M, Yanagisawa K, Li S, Bartels T, Selkoe DJ (2014) Soluble Aβ Oligomers Are Rapidly Sequestered from Brain ISF In Vivo and Bind GM1 Ganglioside on Cellular Membranes. Neuron 82:308–319.

Hughes AB, Rudge AJ (1994) Deoxynojirimycin: synthesis and biological activity. Nat Prod Rep 11:135.

Hur J-Y, Welander H, Behbahani H, Aoki M, Frånberg J, Winblad B, Frykman S, Tjernberg LO (2008) Active γ-secretase is localized to detergent-resistant membranes in human brain: Human brain γ-secretase in DRMs. FEBS J 275:1174–1187.

Infante RE, Wang ML, Radhakrishnan A, Kwon HJ, Brown MS, Goldstein JL (2008) NPC2 facilitates bidirectional transfer of cholesterol between NPC1 and lipid bilayers, a step in cholesterol egress from lysosomes. Proc Natl Acad Sci 105:15287–15292.

Iqbal K, Grundke-Iqbal I (1991) Ubiquitination and abnormal phosphorylation of paired helical filaments in Alzheimer's disease. Mol Neurobiol 5:399–410.

Iqbal K, Liu F, Gong C-X (2016) Tau and neurodegenerative disease: the story so far. Nat Rev Neurol 12:15–27.

Jaeken J, Péanne R (2017) What is new in CDG? J Inherit Metab Dis 40:569–586.

Jayadev S, Case A, Eastman AJ, Nguyen H, Pollak J, Wiley JC, Möller T, Morrison RS, Garden GA (2010) Presenilin 2 Is the Predominant γ-Secretase in Microglia and Modulates Cytokine Release Ikezu T, ed. PLoS ONE 5:e15743.

Jick H, Zornberg G, Jick S, Seshadri S, Drachman D (2000) Statins and the risk of dementia. The Lancet 356:1627–1631.

Jin L-W, Maezawa I, Vincent I, Bird T (2004) Intracellular Accumulation of Amyloidogenic Fragments of Amyloid-β Precursor Protein in Neurons with Niemann-Pick Type C Defects Is Associated with Endosomal Abnormalities. Am J Pathol 164:975–985.

Kadavath H, Hofele RV, Biernat J, Kumar S, Tepper K, Urlaub H, Mandelkow E, Zweckstetter M (2015) Tau stabilizes microtubules by binding at the interface between tubulin heterodimers. Proc Natl Acad Sci 112:7501–7506.

Kaether C, Lammich S, Edbauer D, Ertl M, Rietdorf J, Capell A, Steiner H, Haass C (2002) Presenilin-1 affects trafficking and processing of βAPP and is targeted in a complex with nicastrin to the plasma membrane. J Cell Biol 158:551–561.

Kang DE, Soriano S, Xia X, Eberhart CG, De Strooper B, Zheng H, Koo EH (2002) Presenilin Couples the Paired Phosphorylation of β-Catenin Independent of Axin. Cell 110:751–762.

Kang E-B, Kwon I-S, Koo J-H, Kim E-J, Kim C-H, Lee J, Yang C-H, Lee Y-I, Cho I-H, Cho J-Y (2013) Treadmill exercise represses neuronal cell death and inflammation during Aβ-induced ER stress by regulating unfolded protein response in aged presenilin 2 mutant mice. Apoptosis 18:1332–1347.

Kapoor A, Nation DA (2021) Role of Notch signaling in neurovascular aging and Alzheimer's disease. Semin Cell Dev Biol 116:90–97.

Karran E, Mercken M, Strooper BD (2011) The amyloid cascade hypothesis for Alzheimer's disease: an appraisal for the development of therapeutics. Nat Rev Drug Discov 10:698–712.

Kasri NN, Kocks SL, Verbert L, Hébert SS, Callewaert G, Parys JB, Missiaen L, De Smedt H (2006) Up-regulation of inositol 1,4,5-trisphosphate receptor type 1 is responsible for a decreased endoplasmic-reticulum Ca2+ content in presenilin double knock-out cells. Cell Calcium 40:41–51.

Katayama T, Imaizumi K, Honda A, Yoneda T, Kudo T, Takeda M, Mori K, Rozmahel R, Fraser P, George-Hyslop PSt, Tohyama M (2001) Disturbed Activation of Endoplasmic Reticulum Stress Transducers by Familial Alzheimer's Disease-linked Presenilin-1 Mutations. J Biol Chem 276:43446–43454.

Katayama T, Imaizumi K, Sato N, Miyoshi K, Kudo T, Hitomi J, Morihara T, Yoneda T, Gomi F, Mori Y, Nakano Y, Takeda J, Tsuda T, Itoyama Y, Murayama O, Takashima A, St George-Hyslop P, Takeda M, Tohyama M (1999) Presenilin-1 mutations downregulate the signalling pathway of the unfolded-protein response. Nat Cell Biol 1:479–485.

Kimberly WT, Xia W, Rahmati T, Wolfe MS, Selkoe DJ (2000) The Transmembrane Aspartates in Presenilin 1 and 2 Are Obligatory for γ-Secretase Activity and Amyloid β-Protein Generation. J Biol Chem 275:3173–3178.

Kirkegaard T, Gray J, Priestman DA, Wallom K, Atkins J, Olsen OD, Klein A, Drndarski S, Petersen NHT, Ingemann L, Smith DA, Morris L, Bornaes C, Jørgensen SH, Williams I, Hinsby A, Arenz C, Begley D, Jäättela M, Platt FM (2016) Heat shock protein–based therapy as a potential candidate for treating the sphingolipidoses. Sci Transl Med 8 (355):355ra118.

Kirkegaard T, Roth AG, Petersen NHT, Mahalka AK, Olsen OD, Moilanen I, Zylicz A, Knudsen J, Sandhoff K, Arenz C, Kinnunen PKJ, Nylandsted J, Jäättelä M (2010) Hsp70 stabilizes lysosomes and reverts Niemann–Pick disease-associated lysosomal pathology. Nature 463:549–553.

Kizuka Y, Kitazume S, Fujinawa R, Saito T, Iwata N, Saido TC, Nakano M, Yamaguchi Y, Hashimoto Y, Staufenbiel M, Hatsuta H, Murayama S, Manya H, Endo T, Taniguchi N (2015) An aberrant sugar modification of BACE 1 blocks its lysosomal targeting in A lzheimer's disease. EMBO Mol Med 7:175–189.

Knopman DS, Jones DT, Greicius MD (2021) Failure to demonstrate efficacy of aducanumab: An analysis of the EMERGE and ENGAGE trials as reported by Biogen, December 2019. Alzheimers Dement 17:696–701.

Kovacs GG (2015) Invited review: Neuropathology of tauopathies: principles and practice: Neuropathology of tauopathies. Neuropathol Appl Neurobiol 41:3–23.

LaFerla FM (2002) Calcium dyshomeostasis and intracellular signalling in alzheimer's disease. Nat Rev Neurosci 3:862–872.

Lai M-T, Chen E, Crouthamel M-C, DiMuzio-Mower J, Xu M, Huang Q, Price E, Register RB, Shi X-P, Donoviel DB, Bernstein A, Hazuda D, Gardell SJ, Li Y-M (2003) Presenilin-1 and Presenilin-2 Exhibit Distinct yet Overlapping γ-Secretase Activities. J Biol Chem 278:22475–22481.

Langness VF, van der Kant R, Das U, Wang L, Chaves R dos S, Goldstein LSB (2021) Cholesterol-lowering drugs reduce APP processing to Aβ by inducing APP dimerization Olzmann J, ed. Mol Biol Cell 32:247–259.

Laudon H, Hansson EM, Melén K, Bergman A, Farmery MR, Winblad B, Lendahl U, von Heijne G, Näslund J (2005) A Nine-transmembrane Domain Topology for Presenilin 1. J Biol Chem 280:35352–35360.

Ledreux A, Wang X, Schultzberg M, Granholm A-C, Freeman LR (2016) Detrimental effects of a high fat/high cholesterol diet on memory and hippocampal markers in aged rats. Behav Brain Res 312:294–304.

Lee J, Song L, Terracina G, Bara T, Josien H, Asberom T, Sasikumar TK, Burnett DA, Clader J, Parker EM, Zhang L (2011) Identification of Presenilin 1-Selective γ-Secretase Inhibitors with Reconstituted γ-Secretase Complexes. Biochemistry 50:4973–4980.

Lee J-H, Yu WH, Kumar A, Lee S, Mohan PS, Peterhoff CM, Wolfe DM, Martinez-Vicente M, Massey AC, Sovak G, Uchiyama Y, Westaway D, Cuervo AM, Nixon RA (2010) Lysosomal Proteolysis and Autophagy Require Presenilin 1 and Are Disrupted by Alzheimer-Related PS1 Mutations. Cell 141:1146–1158.

Lee VM-Y, Goedert M, Trojanowski JQ (2001) Neurodegenerative Tauopathies. Annu Rev Neurosci 24:1121–1159.

Leissring MA, Parker I, LaFerla FM (1999) Presenilin-2 mutations modulate amplitude and kinetics of inositol 1, 4,5-trisphosphate-mediated calcium signals. J Biol Chem 274:32535–32538.

Leroy JG (2006) Congenital Disorders of N-Glycosylation Including Diseases Associated With O- as Well as N-Glycosylation Defects. Pediatr Res 60:643–656.

Levy-Lahad E, Wasco W, Poorkaj P, Romano DM, Oshima J, Pettingell WH, Yu C, Jondro PD, Schmidt SD, Wang K, Crowley AC, Fu Y-H, Guenette SY, Galas D, Nemens E, Wijsman EM, Bird TD, Schellenberg GD, Tanzi RE (1995) Candidate Gene for the Chromosome 1 Familial Alzheimer's Disease Locus. Science 269:973–977.

Li L, Zeng F, Liu Y-H, Li H-Y, Dong S-Y, Peng Z-Y, Wang Y-J, Zhou H-D (2018) CYP46A1 and the APOEε4 Allele Polymorphisms Correlate with the Risk of Alzheimer's Disease. Mol Neurobiol 55:8179–8187.

Li Z, Shue F, Zhao N, Shinohara M, Bu G (2020) APOE2: protective mechanism and therapeutic implications for Alzheimer's disease. Mol Neurodegener 15:63.

Lin F-C, Chuang Y-S, Hsieh H-M, Lee T-C, Chiu K-F, Liu C-K, Wu M-T (2015) Early Statin Use and the Progression of Alzheimer Disease: A Total Population-Based Case-Control Study. Medicine (Baltimore) 94:e2143.

Liou H-L, Dixit SS, Xu S, Tint GS, Stock AM, Lobel P (2006) NPC2, the Protein Deficient in Niemann-Pick C2 Disease, Consists of Multiple Glycoforms That Bind a Variety of Sterols. J Biol Chem 281:36710–36723.

Lloyd-Evans E, Morgan AJ, He X, Smith DA, Elliot-Smith E, Sillence DJ, Churchill GC, Schuchman EH, Galione A, Platt FM (2008) Niemann-Pick disease type C1 is a sphingosine storage disease that causes deregulation of lysosomal calcium. Nat Med 14:1247–1255.

Love MI, Huber W & Anders S (2014) Moderated estimation of fold change and dispersion for RNA-seq data with DESeq2. Genome Biology 15 550.

Loving BA, Bruce KD (2020) Lipid and Lipoprotein Metabolism in Microglia. Front Physiol 11:393.

Lund EG, Guileyardo JM, Russell DW (1999) cDNA cloning of cholesterol 24-hydroxylase, a mediator of cholesterol homeostasis in the brain. Proc Natl Acad Sci 96:7238–7243.

Lund EG, Xie C, Kotti T, Turley SD, Dietschy JM, Russell DW (2003) Knockout of the Cholesterol 24-Hydroxylase Gene in Mice Reveals a Brain-specific Mechanism of Cholesterol Turnover. J Biol Chem 278:22980–22988.

Luo J, Jiang L-Y, Yang H, Song B-L (2019) Intracellular Cholesterol Transport by Sterol Transfer Proteins at Membrane Contact Sites. Trends Biochem Sci 44:273–292.

Lutjohann D, Breuer O, Ahlborg G, Nennesmo I, Siden A, Diczfalusy U, Bjorkhem I (1996) Cholesterol homeostasis in human brain: evidence for an age-dependent flux of 24S-hydroxycholesterol from the brain into the circulation. Proc Natl Acad Sci 93:9799–9804.

Lütjohann D, Papassotiropoulos A, Björkhem I, Locatelli S, Bagli M, Oehring RD, Schlegel U, Jessen F, Rao ML, von Bergmann K, Heun R (2000) Plasma 24S-hydroxycholesterol (cerebrosterol) is increased in Alzheimer and vascular demented patients. J Lipid Res 41:195–198.

Madison BB (2016) Srebp2: A master regulator of sterol and fatty acid synthesis. J Lipid Res 57:333–335.

Maguire TM, Breen KC (1995) A Decrease in Neural Sialyltransferase Activity in Alzheimer's Disease. Dement Geriatr Cogn Disord 6:185–190.

Malnar M, Hecimovic S, Mattsson N, Zetterberg H (2014) Bidirectional links between Alzheimer's disease and Niemann–Pick type C disease. Neurobiol Dis 72:37–47.

Malnar M, Kosicek M, Lisica A, Posavec M, Krolo A, Njavro J, Omerbasic D, Tahirovic S, Hecimovic S (2012) Cholesterol-depletion corrects APP and BACE1 misstrafficking in NPC1-deficient cells. Biochim Biophys Acta BBA - Mol Basis Dis 1822:1270–1283.

Malnar M, Kosicek M, Mitterreiter S, Omerbasic D, Lichtenthaler SF, Goate A, Hecimovic S (2010) Niemann–Pick type C cells show cholesterol dependent decrease of APP expression at the cell surface and its increased processing through the β-secretase pathway. Biochim Biophys Acta BBA - Mol Basis Dis 1802:682–691.

Marek KW, Vijay IK, Marth JD (1999) A recessive deletion in the GlcNAc-1-phosphotransferase gene results in peri-implantation embryonic lethality. Glycobiology 9:1263–1271.

Marquer C, Devauges V, Cossec J, Liot G, Lécart S, Saudou F, Duyckaerts C, Léveque-Fort S, Potier M (2011) Local cholesterol increase triggers amyloid precursor protein-Bacel clustering in lipid rafts and rapid endocytosis. FASEB J 25:1295–1305.

Marquer C, Laine J, Dauphinot L, Hanbouch L, Lemercier-Neuillet C, Pierrot N, Bossers K, Le M, Corlier F, Benstaali C, Saudou F, Thinakaran G, Cartier N, Octave J-N, Duyckaerts C, Potier M-C (2014) Increasing membrane cholesterol of neurons in culture recapitulates Alzheimer's disease early phenotypes. Mol Neurodegener 9:60.

Matsuzaki K, Kato K, Yanagisawa K (2010) Aβ polymerization through interaction with membrane gangliosides. Biochim Biophys Acta BBA - Mol Cell Biol Lipids 1801:868–877.

Matthijs G, Schollen E, Pardon E, Veiga-Da-Cunha M, Jaeken J, Cassiman J-J, Schaftingen EV (1997) Mutations in PMM2, a phosphomannomutase gene on chromosome 16p13 in carbohydrate-deficient glycoprotein type I syndrome (Jaeken syndrome). Nat Genet 16:88–92.

Mattsson N, Zetterberg H, Bianconi S, Yanjanin NM, Fu R, Mansson J-E, Porter FD, Blennow K (2011) -Secretase-dependent amyloid- is increased in Niemann-Pick type C: A cross-sectional study. Neurology 76:366–372.

McGowan E et al. (2005) Aβ42 Is Essential for Parenchymal and Vascular Amyloid Deposition in Mice. Neuron 47:191–199.

Meckler X, Checler F (2016) Presenilin 1 and Presenilin 2 Target γ-Secretase Complexes to Distinct Cellular Compartments. J Biol Chem 291:12821–12837.

Medoro A, Bartollino S, Mignogna D, Passarella D, Porcile C, Pagano A, Florio T, Nizzari M, Guerra G, Di Marco R, Intrieri M, Raimo G, Russo C (2018) Complexity and Selectivity of γ-Secretase Cleavage on Multiple Substrates: Consequences in Alzheimer's Disease and Cancer. J Alzheimers Dis JAD 61:1–15.

Mohorko E, Glockshuber R, Aebi M (2011) Oligosaccharyltransferase: the central enzyme of N-linked protein glycosylation. J Inherit Metab Dis 34:869–878.

Montesinos J, Pera M, Larrea D, Guardia-Laguarta C, Agrawal RR, Velasco KR, Yun TD, Stavrovskaya IG, Xu Y, Koo SY, Snead AM, Sproul AA, Area-Gomez E (2020) The Alzheimer's disease-associated C99 fragment of APP regulates cellular cholesterol trafficking. EMBO J 39(20):e103791.

Moremen KW (2002) Golgi α-mannosidase II deficiency in vertebrate systems: implications for asparagine-linked oligosaccharide processing in mammals. Biochim Biophys Acta BBA - Gen Subj 1573:225–235.

Moremen KW, Robbins PW (1991) Isolation, characterization, and expression of cDNAs encoding murine alpha-mannosidase II, a Golgi enzyme that controls conversion of high mannose to complex N-glycans. J Cell Biol 115:1521–1534.

Nakasone N, Nakamura YS, Higaki K, Oumi N, Ohno K, Ninomiya H (2014) Endoplasmic Reticulum-associated Degradation of Niemann-Pick C1. J Biol Chem 289:19714–19725.

Naruse S, Thinakaran G, Luo JJ, Kusiak JW, Tomita T, Iwatsubo T, Qian X, Ginty DD, Price DL, Borchelt DR, Wong PC, Sisodia SS (1998) Effects of PS1 deficiency on membrane protein trafficking in neurons. Neuron 21:1213–1221.

Neely KM, Green KN, LaFerla FM (2011) Presenilin Is Necessary for Efficient Proteolysis through the Autophagy-Lysosome System in a -Secretase-Independent Manner. J Neurosci 31:2781–2791.

Nieweg K, Schaller H, Pfrieger FW (2009) Marked differences in cholesterol synthesis between neurons and glial cells from postnatal rats. J Neurochem 109:125–134.

Nixon RA, Wegiel J, Kumar A, Yu WH, Peterhoff C, Cataldo A, Cuervo AM (2005) Extensive Involvement of Autophagy in Alzheimer Disease: An Immuno-Electron Microscopy Study. J Neuropathol Exp Neurol 64:113–122.

Nixon RA, Yang D-S (2011) Autophagy failure in Alzheimer's disease—locating the primary defect. Neurobiol Dis 43:38–45.

Noble W, Hanger DP, Miller CCJ, Lovestone S (2013) The Importance of Tau Phosphorylation for Neurodegenerative Diseases. Front Neurol 4:83.

Oikawa N, Hatsuta H, Murayama S, Suzuki A, Yanagisawa K (2014) Influence of APOE genotype and the presence of Alzheimer's pathology on synaptic membrane lipids of human brains: APOE Genotype and Synaptic Membrane Cholesterol. J Neurosci Res 92:641–650.

Osenkowski P, Ye W, Wang R, Wolfe MS, Selkoe DJ (2008) Direct and Potent Regulation of γ-Secretase by Its Lipid Microenvironment. J Biol Chem 283:22529–22540.

Palmigiano A, Barone R, Sturiale L, Sanfilippo C, Bua RO, Romeo DA, Messina A, Capuana ML, Maci T, Le Pira F, Zappia M, Garozzo D (2016) CSF N-glycoproteomics for early diagnosis in Alzheimer's disease. J Proteomics 131:29–37.

Panahi A, Bandara A, Pantelopulos GA, Dominguez L, Straub JE (2016) Specific Binding of Cholesterol to C99 Domain of Amyloid Precursor Protein Depends Critically on Charge State of Protein. J Phys Chem Lett 7:3535–3541.

Papassotiropoulos A, Lütjohann D, Bagli M, Locatelli S, Jessen F, Buschfort R, Ptok U, Björkhem I, von Bergmann K, Heun R (2002) 24S-hydroxycholesterol in cerebrospinal fluid is elevated in early stages of dementia. J Psychiatr Res 36:27–32.

Payne et all. (2015) Regulation of ryanodine receptor-mediated calcium signaling by presenilins. Recept Clin Investig 2(1): e449.

Pendin D, Fasolato C, Basso E, Filadi R, Greotti E, Galla L, Gomiero C, Leparulo A, Redolfi N, Scremin E, Vajente N, Pozzan T, Pizzo P (2021) Familial Alzheimer's disease presenilin-2 mutants affect Ca2+ homeostasis and brain network excitability. Aging Clin Exp Res 33:1705–1708.

Pintchovski A. S, B. Schenk D, S. Basi G (2013) Evidence that Enzyme Processivity Mediates Differential Aβ Production by PS1 and PS2. Curr Alzheimer Res 10:4–10.

Raemaekers T, Peric A, Baatsen P, Sannerud R, Declerck I, Baert V, Michiels C, Annaert W (2012) ARF6-mediated endosomal transport of Telencephalin affects dendritic filopodia-to-spine maturation: ARF6-mediated trafficking of Telencephalin affects spine maturation. EMBO J 31:3252–3269.

Rahman A, Akterin S, Flores-Morales A, Crisby M, Kivipelto M, Schultzberg M, Cedazo-Mínguez A (2005) High cholesterol diet induces tau hyperphosphorylation in apolipoprotein E deficient mice. FEBS Lett 579:6411–6416.

Ramirez DMO, Andersson S, Russell DW (2008) Neuronal expression and subcellular localization of cholesterol 24-hydroxylase in the mouse brain. J Comp Neurol 507:1676–1693.

Refolo LM, Pappolla MA, Malester B, LaFrancois J, Bryant-Thomas T, Wang R, Tint GS, Sambamurti K, Duff K (2000) Hypercholesterolemia Accelerates the Alzheimer's Amyloid Pathology in a Transgenic Mouse Model. Neurobiol Dis 7:321–331.

Reiss G, Heesen S te, Zimmerman J, Robbins P, Aebi M (1996) Isolation of the ALG6 locus of Saccharomyces cerevisiae required for glucosylation in the N-linked glycosylation pathway. Glycobiology 6:493–498.

Repetto E, Yoon I-S, Zheng H, Kang DE (2007) Presenilin 1 Regulates Epidermal Growth Factor Receptor Turnover and Signaling in the Endosomal-Lysosomal Pathway. J Biol Chem 282:31504–31516.

Rizk A, Paul G, Incardona P, Bugarski M, Mansouri M, Niemann A, Ziegler U, Berger P, Sbalzarini IF (2014) Segmentation and quantification of subcellular structures in fluorescence microscopy images using Squassh. Nat Protoc 9:586–596.

Rogaev EI et al. (1995) Familial Alzheimer's disease in kindreds with missense mutations in a gene on chromosome 1 related to the Alzheimer's disease type 3 gene. Nature 376:775–778.

Ruiz-Canada C, Kelleher DJ, Gilmore R (2009) Cotranslational and Posttranslational N-Glycosylation of Polypeptides by Distinct Mammalian OST Isoforms. Cell 136:272–283.

Runz H, Rietdorf J, Tomic I, de Bernard M, Beyreuther K, Pepperkok R, Hartmann T (2002) Inhibition of Intracellular Cholesterol Transport Alters Presenilin Localization and Amyloid Precursor Protein Processing in Neuronal Cells. J Neurosci 22:1679–1689.

Rush JS (2015) Role of Flippases in Protein Glycosylation in the Endoplasmic Reticulum. Lipid Insights 8s1:LPI.S31784.

Sakai J, Nohturfft A, Cheng D, Ho YK, Brown MS, Goldstein JL (1997) Identification of complexes between the COOH-terminal domains of sterol regulatory element-binding proteins (SREBPs) and SREBP cleavage-activating protein. J Biol Chem 272:20213–20221.

Salloway S, Chalkias S, Barkhof F, Burkett P, Barakos J, Purcell D, Suhy J, Forrestal F, Tian Y, Umans K, Wang G, Singhal P, Budd Haeberlein S, Smirnakis K (2021) Amyloid-Related Imaging Abnormalities in 2 Phase 3 Studies Evaluating Aducanumab in Patients With Early Alzheimer Disease. JAMA Neurol 79(1):13-21.

Sannerud R et al. (2016) Restricted Location of PSEN2/γ-Secretase Determines Substrate Specificity and Generates an Intracellular Aβ Pool. Cell 166:193–208.

Sato N, Imaizumi K, Manabe T, Taniguchi M, Hitomi J, Katayama T, Yoneda T, Morihara T, Yasuda Y, Takagi T, Kudo T, Tsuda T, Itoyama Y, Makifuchi T, Fraser PE, St George-Hyslop P, Tohyama M (2001) Increased Production of β-Amyloid and Vulnerability to Endoplasmic Reticulum Stress by an Aberrant Spliced Form of Presenilin 2. J Biol Chem 276:2108–2114.

Saunders AM, Strittmatter WJ, Schmechel D, St. George-Hyslop PH, Pericak-Vance MA, Joo SH, Rosi BL, Gusella JF, Crapper-MacLachlan DR, Alberts MJ, Hulette C, Crain B, Goldgaber D, Roses AD (1993) Association of apolipoprotein E allele 4 with late-onset familial and sporadic Alzheimer's disease. Neurology 43:1467–1467.

Saura CA, Choi S-Y, Beglopoulos V, Malkani S, Zhang D, Rao BSS, Chattarji S, Kelleher RJ, Kandel ER, Duff K, Kirkwood A, Shen J (2004) Loss of Presenilin Function Causes Impairments of Memory and Synaptic Plasticity Followed by Age-Dependent Neurodegeneration. Neuron 42:23–36.

Sawamura N, Gong J-S, Garver WS, Heidenreich RA, Ninomiya H, Ohno K, Yanagisawa K, Michikawa M (2001) Site-specific Phosphorylation of Tau Accompanied by Activation of Mitogen-activated Protein Kinase (MAPK) in Brains of Niemann-Pick Type C Mice. J Biol Chem 276:10314–10319.

Schedin-Weiss S, Winblad B, Tjernberg LO (2014) The role of protein glycosylation in Alzheimer disease. FEBS J 281:46–62.

Scheuner D et al. (1996) Secreted amyloid β–protein similar to that in the senile plaques of Alzheimer's disease is increased in vivo by the presenilin 1 and 2 and APP mutations linked to familial Alzheimer's disease. Nat Med 2:864–870.

Schneider A, Schulz-Schaeffer W, Hartmann T, Schulz JB, Simons M (2006) Cholesterol depletion reduces aggregation of amyloid-beta peptide in hippocampal neurons. Neurobiol Dis 23:573–577.

Schönknecht P, Lütjohann D, Pantel J, Bardenheuer H, Hartmann T, von Bergmann K, Beyreuther K, Schröder J (2002) Cerebrospinal fluid 24S-hydroxycholesterol is increased in patients with Alzheimer's disease compared to healthy controls. Neurosci Lett 324:83–85.

Schultz ML, Krus KL, Kaushik S, Dang D, Chopra R, Qi L, Shakkottai VG, Cuervo AM, Lieberman AP (2018) Coordinate regulation of mutant NPC1 degradation by selective ER autophagy and MARCH6-dependent ERAD. Nat Commun 9:3671.

Serge Gauthier, Pedro Rosa-Neto, José A. Morais, Claire Webster (2021) World-Alzheimer-Report-2021. Available at: https://www.alzint.org/u/World-Alzheimer-Report-2021.pdf.

Serneels L, Biervliet J, Craessaerts K, Dejaegere T, Horré K, Houtvin T, Esselmann H, Paul S, Schäfer MK, Berezovska O, Hyman BT, Sprangers B, Moons L, Jucker M, Yang Z, May PC, Karran E, Wiltfang J, D´Hooge R, De Strooper B (2009) γ-Secretase Heterogeneity in the Aph1 Subunit: Relevance for Alzheimer's Disease. Science 324:639–642.

Serrano-Pozo A, Qian J, Monsell SE, Betensky RA, Hyman BT (2015) APOE ε2 is associated with milder clinical and pathological Alzheimer disease: Effects of APOE Alleles in AD. Ann Neurol 77:917–929.

Shen J, Bronson RT, Chen DF, Xia W, Selkoe DJ, Tonegawa S (1997) Skeletal and CNS Defects in Presenilin-1-Deficient Mice. Cell 89:629–639.

Shen J, Kelleher RJ (2007) The presenilin hypothesis of Alzheimer's disease: Evidence for a loss-of-function pathogenic mechanism. Proc Natl Acad Sci 104:403–409.

Sherrington R et al. (1995) Cloning of a gene bearing missense mutations in early-onset familial Alzheimer's disease. Nature 375:754–760.

Shirotani K, Edbauer D, Capell A, Schmitz J, Steiner H, Haass C (2003) γ-Secretase Activity Is Associated with a Conformational Change of Nicastrin. J Biol Chem 278:16474–16477.

Shirotani K, Edbauer D, Prokop S, Haass C, Steiner H (2004) Identification of Distinct γ-Secretase Complexes with Different APH-1 Variants. J Biol Chem 279:41340–41345.

Simons M, Keller P, De Strooper B, Beyreuther K, Dotti CG, Simons K (1998) Cholesterol depletion inhibits the generation of -amyloid in hippocampal neurons. Proc Natl Acad Sci 95:6460–6464.

Smith LM, Strittmatter SM (2017) Binding Sites for Amyloid-β Oligomers and Synaptic Toxicity. Cold Spring Harb Perspect Med 7:a024075.

Sodero AO (2021) 24S-hydroxycholesterol: Cellular effects and variations in brain diseases. J Neurochem 157:899–918.

Song W, Nadeau P, Yuan M, Yang X, Shen J, Yankner BA (1999) Proteolytic release and nuclear translocation of Notch-1 are induced by presenilin-1 and impaired by pathogenic presenilin-1 mutations. Proc Natl Acad Sci 96:6959–6963.

Song Y, Hustedt EJ, Brandon S, Sanders CR (2013) Competition Between Homodimerization and Cholesterol Binding to the C99 Domain of the Amyloid Precursor Protein. Biochemistry 52:5051–5064.

Spasic D, Annaert W (2008) Building γ-secretase – the bits and pieces. J Cell Sci 121:413–420.

Spasic D, Tolia A, Dillen K, Baert V, De Strooper B, Vrijens S, Annaert W (2006) Presenilin-1 Maintains a Nine-Transmembrane Topology throughout the Secretory Pathway. J Biol Chem 281:26569–26577.

Stagljar I, te Heesen S, Aebi M (1994) New phenotype of mutations deficient in glucosylation of the lipid-linked oligosaccharide: cloning of the ALG8 locus. Proc Natl Acad Sci 91:5977–5981.

Stange AD, Hsu JP-C, Ravnkilde LK, Berglund N, Schiøtt B (2021) Effect of cholesterol on the dimerization of C99—A molecular modeling perspective. Biointerphases 16:031002.

Stanley P (2011) Golgi Glycosylation. Cold Spring Harb Perspect Biol 3:a005199–a005199.

Stelzmann RA, Norman Schnitzlein H, Reed Murtagh F (1995) An english translation of alzheimer's 1907 paper, "Uber eine eigenartige Erkankung der Hirnrinde." Clin Anat 8:429–431.

Strittmatter WJ, Saunders AM, Schmechel D, Pericak-Vance M, Enghild J, Salvesen GS, Roses AD (1993) Apolipoprotein E: high-avidity binding to beta-amyloid and increased frequency of type 4 allele in late-onset familial Alzheimer disease. Proc Natl Acad Sci 90:1977–1981.

Stutzmann GE (2004) Dysregulated IP3 Signaling in Cortical Neurons of Knock-In Mice Expressing an Alzheimer's-Linked Mutation in Presenilin1 Results in Exaggerated Ca2+ Signals and Altered Membrane Excitability. J Neurosci 24:508–513.

Sun L, Zhou R, Yang G, Shi Y (2017) Analysis of 138 pathogenic mutations in presenilin-1 on the in vitro production of Aβ42 and Aβ40 peptides by γ-secretase. Proc Natl Acad Sci 114:E476–E485.

Száraz P, Bánhegyi G, Marcolongo P, Benedetti A (2013) Transient knockdown of presenilin-1 provokes endoplasmic reticulum stress related formation of autophagosomes in HepG2 cells. Arch Biochem Biophys 538:57–63.

T. G. Ohm, S. Treiber-Held, R. Distl, F. Glöckner, Schönheit, M. Tamanai, V. Meske (2003) Cholesterol and Tau Protein - Findings in Alzheimer's and Niemann Pick C's Disease. Pharmacopsychiatry 36:120–126.

Takahashi Y, Koizumi K, Takagi A, Kitajima S, Inoue T, Koseki H, Saga Y (2000) Mesp2 initiates somite segmentation through the Notch signalling pathway. Nat Genet 25:390–396.

Tamboli IY, Prager K, Thal DR, Thelen KM, Dewachter I, Pietrzik CU, St. George-Hyslop P, Sisodia SS, De Strooper B, Heneka MT, Filippov MA, Muller U, van Leuven F, Lutjohann D, Walter J (2008) Loss of -Secretase Function Impairs Endocytosis of Lipoprotein Particles and Membrane Cholesterol Homeostasis. J Neurosci 28:12097–12106.

Tan J, Evin G (2012) β-Site APP-cleaving enzyme 1 trafficking and Alzheimer's disease pathogenesis: BACE1 trafficking and Alzheimer's disease. J Neurochem:no-no.

Tang N, Kepp KP (2018) Aβ42/Aβ40 Ratios of Presenilin 1 Mutations Correlate with Clinical Onset of Alzheimer's Disease. J Alzheimers Dis 66:939–945.

Toh WH, Gleeson PA (2016) Dysregulation of intracellular trafficking and endosomal sorting in Alzheimer's disease: controversies and unanswered questions. Biochem J 473:1977–1993.

Tu H, Nelson O, Bezprozvanny A, Wang Z, Lee S-F, Hao Y-H, Serneels L, De Strooper B, Yu G, Bezprozvanny I (2006) Presenilins Form ER Ca2+ Leak Channels, a Function Disrupted by Familial Alzheimer's Disease-Linked Mutations. Cell 126:981–993.

van der Kant R, Langness VF, Herrera CM, Williams DA, Fong LK, Leestemaker Y, Steenvoorden E, Rynearson KD, Brouwers JF, Helms JB, Ovaa H, Giera M, Wagner SL, Bang AG, Goldstein LSB (2019) Cholesterol Metabolism Is a Druggable Axis that Independently Regulates Tau and Amyloid-β in iPSC-Derived Alzheimer's Disease Neurons. Cell Stem Cell 24:363-375.e9.

Vance JE, Hayashi H (2010) Formation and function of apolipoprotein E-containing lipoproteins in the nervous system. Biochim Biophys Acta BBA - Mol Cell Biol Lipids 1801:806–818.

Vance JE, Hayashi H, Karten B (2005) Cholesterol homeostasis in neurons and glial cells. Semin Cell Dev Biol 16:193–212.

Vanier M, Millat G (2003) Niemann-Pick disease type C: Niemann-Pick disease type C. Clin Genet 64:269–281.

Vanmierlo T, Bloks VW, van Vark-van der Zee LC, Rutten K, Kerksiek A, Friedrichs S, Sijbrands E, Steinbusch HW, Kuipers F, Lütjohann D, Mulder M (2010) Alterations in brain cholesterol metabolism in the APPSLxPS1mut mouse, a model for Alzheimer's disease. J Alzheimers Dis 19:117–127.

Varki A (2017) Biological roles of glycans. Glycobiology 27:3–49.

Varki A, Cummings RD, Esko JD, Freeze HH, Stanley P, Bertozzi CR, Hart GW, Etzler ME eds. (2009) Essentials of Glycobiology, 2nd ed. Cold Spring Harbor (NY): Cold Spring Harbor Laboratory Press. Available at: http://www.ncbi.nlm.nih.gov/books/NBK1908/ [Accessed December 9, 2021].

Vetrivel KS, Cheng H, Kim S-H, Chen Y, Barnes NY, Parent AT, Sisodia SS, Thinakaran G (2005) Spatial Segregation of γ-Secretase and Substrates in DistinctMembraneDomains. J Biol Chem 280:25892–25900.

Vetrivel KS, Cheng H, Lin W, Sakurai T, Li T, Nukina N, Wong PC, Xu H, Thinakaran G (2004) Association of γ-Secretase with Lipid Rafts in Post-Golgi and Endosome Membranes. J Biol Chem 279:44945–44954.

Walter J, Kaether C, Steiner H, Haass C (2001) The cell biology of Alzheimer's disease: uncovering the secrets of secretases. Curr Opin Neurobiol 11:585–590.

Wang H, Kulas JA, Wang C, Holtzman DM, Ferris HA, Hansen SB (2021a) Regulation of beta-amyloid production in neurons by astrocyte-derived cholesterol. Proc Natl Acad Sci 118:e2102191118.

Wang H, Shen Y, Zhao L, Ye Y (2021b) 1-Deoxynojirimycin and its Derivatives: A Mini Review of the Literature. Curr Med Chem 28:628–643.

Wang W, Gopal S, Pocock R, Xiao Z (2019) Glycan Mimetics from Natural Products: New Therapeutic Opportunities for Neurodegenerative Disease. Molecules 24:4604.

Wang Y, Chan SL, Miele L, Yao PJ, Mackes J, Ingram DK, Mattson MP, Furukawa K (2004) Involvement of Notch signaling in hippocampal synaptic plasticity. Proc Natl Acad Sci 101:9458–9462.

Wilson CA, Murphy DD, Giasson BI, Zhang B, Trojanowski JQ, Lee VM-Y (2004) Degradative organelles containing mislocalized α- and β-synuclein proliferate in presenilin-1 null neurons. J Cell Biol 165:335–346.

Wolfe MS, Xia W, Ostaszewski BL, Diehl TS, Kimberly WT, Selkoe DJ (1999) Two transmembrane aspartates in presenilin-1 required for presenilin endoproteolysis and γ-secretase activity. Nature 398:513–517.

Woo H-N, Park J-S, Gwon A-R, Arumugam TV, Jo D-G (2009) Alzheimer's disease and Notch signaling. Biochem Biophys Res Commun 390:1093–1097.

Xia D, Watanabe H, Wu B, Lee SH, Li Y, Tsvetkov E, Bolshakov VY, Shen J, Kelleher RJ (2015) Presenilin-1 Knockin Mice Reveal Loss-of-Function Mechanism for Familial Alzheimer's Disease. Neuron 85:967–981.

Xie C, Lund EG, Turley SD, Russell DW, Dietschy JM (2003) Quantitation of two pathways for cholesterol excretion from the brain in normal mice and mice with neurodegeneration. J Lipid Res 44:1780–1789.

Xiong H, Callaghan D, Jones A, Walker DG, Lue L-F, Beach TG, Sue LI, Woulfe J, Xu H, Stanimirovic DB, Zhang W (2008) Cholesterol retention in Alzheimer's brain is responsible for high β- and γ-secretase activities and Aβ production. Neurobiol Dis 29:422–437.

Yanagisawa K (2015) GM1 ganglioside and Alzheimer's disease. Glycoconj J 32:87–91.

Yang D-S, Tandon A, Chen F, Yu G, Yu H, Arawaka S, Hasegawa H, Duthie M, Schmidt SD, Ramabhadran TV, Nixon RA, Mathews PM, Gandy SE, Mount HTJ, St George-Hyslop P, Fraser PE (2002) Mature Glycosylation and Trafficking of Nicastrin Modulate Its Binding to Presenilins. J Biol Chem 277:28135–28142.

Yoo AS, Cheng I, Chung S, Grenfell TZ, Lee H, Pack-Chung E, Handler M, Shen J, Xia W, Tesco G, Saunders AJ, Ding K, Frosch MP, Tanzi RE, Kim T-W (2000) Presenilin-Mediated Modulation of Capacitative Calcium Entry. Neuron 27:561–572.

Younkin SG (1998) The role of Aβ42 in Alzheimer's disease. J Physiol-Paris 92:289–292.

Yu H, Saura CA, Choi S-Y, Sun LD, Yang X, Handler M, Kawarabayashi T, Younkin L, Fedeles B, Wilson MA, Younkin S, Kandel ER, Kirkwood A, Shen J (2001) APP Processing and Synaptic Plasticity in Presenilin-1 Conditional Knockout Mice. Neuron 31:713–726.

Yukioka F, Matsuzaki S, Kawamoto K, Koyama Y, Hitomi J, Katayama T, Tohyama M (2008) Presenilin-1 mutation activates the signaling pathway of caspase-4 in endoplasmic reticulum stress-induced apoptosis. Neurochem Int 52:683–687.

Zatti G, Burgo A, Giacomello M, Barbiero L, Ghidoni R, Sinigaglia G, Florean C, Bagnoli S, Binetti G, Sorbi S, Pizzo P, Fasolato C (2006) Presenilin mutations linked to familial Alzheimer's disease reduce endoplasmic reticulum and Golgi apparatus calcium levels. Cell Calcium 39:539–550.

Zatti G, Ghidoni R, Barbiero L, Binetti G, Pozzan T, Fasolato C, Pizzo P (2004) The presenilin 2 M239I mutation associated with familial Alzheimer's disease reduces Ca2+ release from intracellular stores. Neurobiol Dis 15:269–278.

Zhang C, Liu P (2017) The lipid droplet: A conserved cellular organelle. Protein Cell 8:796–800.

Zhang J, Liu Q (2015) Cholesterol metabolism and homeostasis in the brain. Protein Cell 6:254–264.

Zhang X, Garbett K, Veeraraghavalu K, Wilburn B, Gilmore R, Mirnics K, Sisodia SS (2012) A Role for Presenilins in Autophagy Revisited: Normal Acidification of Lysosomes in Cells Lacking PSEN1 and PSEN2. J Neurosci 32:8633–8648.

Zhang X, Wen J, Zhang Z (2018) Statins use and risk of dementia: A dose–response meta analysis. Medicine (Baltimore) 97:e11304.

Zhang Y, Wang R, Liu Q, Zhang H, Liao F-F, Xu H (2007) Presenilin/γ-secretase-dependent processing of β-amyloid precursor protein regulates EGF receptor expression. Proc Natl Acad Sci 104:10613–10618.

Zhou Q, Xie Y, Lam M, Lebrilla CB (2021) N-Glycomic Analysis of the Cell Shows Specific Effects of Glycosyl Transferase Inhibitors. Cells 10:2318.

Zissimopoulos JM, Barthold D, Brinton RD, Joyce G (2017) Sex and Race Differences in the Association Between Statin Use and the Incidence of Alzheimer Disease. JAMA Neurol 74:225.

9. Acknowledgments

I would like to express my sincere gratitude to my supervisors, Prof. Jochen Walter and Dr. Naoto Oikawa, for giving me the opportunity to pursue my PhD degree. Their supervision, support and invaluable advice guided me during the course of my research experience. Their teachings were instrumental in shaping and improving my experimental methods and in learning to criticize my results. Their dedication to science and research has been a source of inspiration for me and pushed me to try to give my best throughout all my PhD experience.

I would like to thank my second supervisor Prof. Jörg Höhfeld for his kind willingness to follow the development of my project over the years. His questions and feedbacks helped me to sharpen my thinking and improve my work.

I am really grateful to all the colleagues who have supported me along this journey. In particular Akshay, without whose help and friendship I would not have been able to overcome the difficulties of the research life.

I am deeply grateful to Uli for his presence, his support, his love and his encouragement. He helped me cope with the stress, realize my potential and give perspective to situations. I don't know how I would have done without him next to me. TP

I would like to thank my parents for their support. They are my inexhaustible source of strength, courage and love even miles away. I wouldn't have been able to go any further without them.

10. Publications

Marko HL, Hornig NC, Betz R, Holterhuus P, Altmüller J, Thiele H, **Fabiano M**, Schweikert H, Braun D, Schweizer U. Genomic variants reducing expression of two endocytic receptors in 46,XY differences of sex development. Hum Mutat. 2022 Mar; 43(3):420-433. doi:10.1002/humu.24325. Epub 2022 Jan 15.

Oikawa N, **Fabiano M**, Müller UC, Walter J. Carboxy-terminal fragment of amyloid precursor protein mediates lipid droplet accumulation upon γ- secretase inhibition. Biochem Biophys Res Commun. 2021 Sep 17;570:137-142. doi: 10.1016/j.bbrc.2021.07.021.Epub 2021 Jul17.

Brandi R*, **Fabiano M***, Giorgi C, Arisi I, La Regina F,Malerba F, Turturro S, Storti AE, Ricevuti F, Amadio S, Volontè C, Capsoni S, Scardigli R, D'Onofrio M, Cattaneo A. Nerve Growth Factor Neutralization Promotes Oligodendrogenesis by increasing miR-219a-5p Levels. Cells. 2021 Feb 16;10(2):405. doi: 10.3390/cells10020405.
***first name co-authorship**

Gutierrez E, Lütjohann D, Kerksiek A, **Fabiano M**, Oikawa N, Kuerschner L, Thiele C, Walter J. Importance of γ-secretase in the regulation of liver X receptor and cellular lipid metabolism. Life Sci Alliance 2020 Apr 30; 3(6):e201900521. doi: 10.26508/lsa.201900521.